DMD Fast Forward. Published on November 8, 2006 as doi:10.1124/dmd.106.012633

MECHANISM BASED INACTIVATION OF HUMAN CYTOCHROME P450 ENZYMES AND THE PREDICTION OF DRUG-DRUG INTERACTIONS

R. Scott Obach, Robert L. Walsky, and Karthik Venkatakrishnan

Pharmacokinetics, Dynamics, and Drug Metabolism (RSO, RLW)

and Clinical Pharmacology (KV)

Pfizer, Inc.

Groton, CT, 06340

DMD Fast Forward. Published on November 8, 2006 as DOI: 10.1124/dmd.106.012633
This article has not been copyedited and formatted. The final version may differ from this version.

Running Title: Inactivation of Cytochrome P450 Enzymes

Address Correspondence to:

R. Scott Obach

Pfizer Global Research and Development

Groton Labs

Groton, CT 06340

Ph. 860-441-6122

Fax 860-715-3239

E-mail: r.scott.obach@pfizer.com

Number of Text Pages: 17

Number of Tables: 6

Number of Figures: 5

Number of References: 50

Number of Words in:

Abstract: 261

Introduction: 555

Discussion: 1705

Abbreviations: CYP: cytochrome P450; DDI: drug-drug interaction; GMFE: geometric mean fold error; PPP: 1-(1-methyl-1-phenyl-ethyl)-piperidine; RMSE: root mean squared error; thioTEPA: N,N',N"-triethylenethiophosphoramide.

DMD Fast Forward. Published on November 8, 2006 as DOI: 10.1124/dmd.106.012633
This article has not been copyedited and formatted. The final version may differ from this version.

ABSTRACT

The ability to use vitro inactivation kinetic parameters in scaling to in vivo drug-drug interactions (DDI) for mechanism based inactivators of human cytochrome P450 enzymes was examined using eight human P450 selective marker activities in pooled human liver microsomes. These data were combined with other parameters (systemic C_{max}, estimated hepatic inlet C_{max}, fraction unbound, in vivo P450 enzyme degradation rate constants estimated from clinical pharmacokinetic data, and fraction of the affected drug cleared by the inhibited enzyme) to predict increases in exposure to drugs, and the predictions were compared to in vivo DDI gathered from clinical studies reported in the scientific literature. In general, the use of unbound systemic C_{max} as the inactivator concentration in vivo yielded the most accurate predictions of DDI with a mean fold error of 1.64. Abbreviated in vitro approaches to identifying mechanism based inactivators were developed. Testing potential inactivators at a single concentration (IC_{25}) in a 30 min preincubation with human liver microsomes in the absence and presence of NADPH followed by assessment of P450 marker activities readily identified those compounds known to be mechanism-based inactivators, and represents an approach that can be employed with greater throughput. Measurement of decreases in IC_{50} occurring with a 30 min preincubation with liver microsomes and NADPH were also useful in identifying mechanism-based inactivators, and the IC_{50} measured after such a preincubation was highly correlated with the k_{inact}/K_I ratio measured after a full characterization of inactivation. Overall, these findings support the conclusion that P450 in vitro inactivation data are valuable in predicting clinical DDI that can occur via this mechanism.

INTRODUCTION

The prediction of drug-drug interactions (DDI) using in vitro enzyme kinetic data has been an area of increasing advances and sophistication. This has proven to be a valuable endeavor because DDI remain an important issue in clinical practice and the discovery and development of new drugs. The earlier that the potential for DDI can be identified in new compounds being studied as potential drugs, the greater the likelihood that this deleterious property can be removed through improved design of the molecule. Also, for those compounds already undergoing clinical trials, in vitro DDI data can be leveraged in the design of adequate and appropriate clinical DDI studies. With our increased understanding of drug metabolizing enzymes and their roles in the metabolism of specific drugs, a mechanistic approach to assessing DDI can be taken. The results of clinical DDI studies with one drug can be extrapolated to other drugs that are cleared by the same enzyme.

The alteration of drug metabolizing enzyme activities can occur by three main mechanisms: reversible inhibition, mechanism-based inactivation, and induction. Confidence in quantitatively extrapolating in vitro results to in vivo varies with these mechanisms. For reversible inhibition mechanisms, recent advances in our ability to predict the magnitude of DDI from in vitro inhibition data have been made such that for cytochrome P450 enzymes, increases in exposure can be predicted within 2-fold (Obach, et al., 2006; Brown, et al., 2005; Ito, et al., 2005). Through the use of human hepatocytes in culture, enzyme inducers can be readily identified (Silva and Nicholl-Griffith, 2002). However the magnitude of predicted DDI for inducers varies with the source of individual hepatocytes. Recently, in vitro induction data from an immortalized human hepatocyte line, which gives a robust and reliable response, has been demonstrated to yield quantitative predictions of CYP3A induction-based DDI in vivo (Ripp, et al, 2006).

For mechanism-based inactivators, there have been some reports describing the prediction of in vivo DDI, particularly for CYP3A (Galetin, et al., 2006; Wang, et al., 2004; Ito,

et al., 2003; Yamano, et al., 2001; Mayhew, et al., 2000; Kanamitsu, et al., 2000) as well as one analysis for CYP2D6 (Venkatakrishnan and Obach, 2005). Compared to reversible inhibition, there are some added complexities regarding the prediction of DDI from inactivation data. The design and conduct of in vitro inactivation studies are more complex than reversible inhibition studies, in that experiments require two-steps (preincubation with inactivator followed by dilution and incubation to measure the standard marker activity) and several incubation times are needed to generate inactivation rate constants (k_{inact}). For extrapolation to in vivo, knowledge of the in vivo rate of degradation of the target enzyme in human is needed. Such a value cannot be measured directly, forcing the use of in vitro data in human hepatocytes, animal data (Mayhew, et al., 2000), or data modeled from human pharmacokinetic studies of de-induction or recovery following inactivation (Faber and Fuhr, 2004; Venkatakrishnan and Obach, 2005; Takanaga, et al., 2000; Greenblatt, et al., 2003), and thus greater uncertainty is introduced.

The primary objectives of this work are two fold: (1) to devise a simplified in vitro approach whereby mechanism-based inactivators of P450 enzymes can be identified, and (2) to determine if there is a reliable method that can be used to predict the magnitude of DDI from in vitro inactivation data across multiple P450 enzymes.

METHODS

Materials. P450 substrates, internal standards, and pooled liver microsomes were the same as those described earlier (Walsky and Obach, 2004). NADPH was from ICN (Aurora, OH). The compounds examined as inactivators were obtained from one of the following sources: Aldrich Chemical Co. (Milwaukee, WI), Sequoia Research Products (Oxford, UK), or Sigma Chemical Co. (St. Louis, MO) with the exception of desethylamiodarone (Synfine, Richmond Hill, Ontario, Canada) and tienilic acid (Cerilliant, Austin, TX). PPP was synthesized at Pfizer by Dr. James Eggler. Other reagents were obtained from common commercial suppliers.

Single Point Inactivation and IC_{50} Shift Experiments. Pooled human liver microsomes (0.3 to 2 mg/ml, depending on which enzyme was assessed) were incubated with inactivators, and $MgCl_2$ (3.3 mM) in potassium phosphate buffer (100 mM, pH 7.4) in the absence and presence of NADPH (1.3 mM). In single point inactivation experiments, the concentration of the inactivator used was 10-fold that which gave 25% inhibition when tested under reversible inhibition conditions. (Thus, after dilution of 10X into the subsequent activity assay, the concentration in the minus NADPH control will be at IC_{25}.) In IC_{50} shift experiments, multiple concentrations of inactivators were used such that the range included the concentration that was 10-times the IC_{50} measured for reversible inhibition. (Thus, after dilution of 10X into the subsequent activity assay, the concentrations in the minus NADPH controls will span IC_{50}.) The inactivators were delivered in solvent such that the final solvent concentration was less than 1% (v/v). These preincubations (i.e. the "Inactivation Incubation") were carried out for 30 min at 37^{o}C. For highly efficient inactivators, a 30 min preincubation time will exceed the time over which the inactivation is first order (i.e. log-linear). However, the selection of a 30 min preincubation period was made to ensure that even weak inactivators could be identified (i.e. to avoid false negatives). Vehicle controls were run to account for any decrease in enzyme activity caused by incubation under these conditions. After the inactivation incubation, a portion of the inactivation mixture (0.02 ml) was added to a mixture containing a standard cytochrome P450 substrate in

DMD Fast Forward. Published on November 8, 2006 as DOI: 10.1124/dmd.106.012633
This article has not been copyedited and formatted. The final version may differ from this version.

0.18 ml potassium phosphate buffer (100 mM, pH 7.4) containing $MgCl_2$ (3.3 mM) and NADPH (1.3 mM) for measurement of P450 activities (i.e. the "Activity Incubation"). The substrates used and their concentrations are listed in Table 1. Substrate concentrations used were proximal to K_M values. Incubations were carried out and samples analyzed by HPLC-MS using previously described methods (Walsky and Obach, 2004).

Single point inactivation data were analyzed by comparing the % inhibition measured when the inactivator was preincubated for 30 min in the presence of NADPH vs that in the absence of NADPH:

$$\%\ \text{decrease in activity} = 100 \cdot \left(\left(\frac{\text{activity with inactivator}}{\text{activity with vehicle}} \right)_{\text{no NADPH}} - \left(\frac{\text{activity with inactivator}}{\text{activity with vehicle}} \right)_{\text{+ NADPH}} \right) \quad \text{(Eq 1)}$$

Inactivation Kinetic Experiments to Determine K_I and k_{inact}. Inactivation kinetic experiments were conducted in a manner similar to that described above. In the inactivation preincubation, various concentrations of inactivator were incubated at 37°C with pooled human liver microsomes (0.3 to 2 mg/ml, depending on which enzyme was assessed), $MgCl_2$ (3.3 mM), NADPH (1.3 mM), in potassium phosphate buffer (100 mM, pH 7.4). At six timepoints, aliquots of the inactivation preincubation mixture (0.02 ml) were removed and added to a mixture containing a standard cytochrome P450 substrate, $MgCl_2$ (3.3 mM), NADPH (1.3 mM), in potassium phosphate buffer (100 mM, pH 7.4) at 37°C. The substrates used were those described above at concentrations approximately 10-times the K_M (Table 1). To determine k_{obs} values, the decrease in natural logarithm of the activity over time was plotted for each inactivator concentration, and k_{obs} values were described as the negative slopes of the lines. Inactivation kinetic parameters were determined using non-linear regression of the data to the following expression:

$$k_{obs} = k_{obs[I]=0} + \frac{k_{inact} \bullet [I]}{K_I + [I]} \quad \text{(Eq. 2)}$$

in which [I] are the concentrations of inactivators in the inactivation preincubations, k_{obs} are the negative values of the slopes of the natural logrithm of the percent activity remaining vs inactivation incubation time at various [I], $k_{obs[I]=0}$ is the apparent inactivation rate constant measured in the absence of inactivator, k_{inact} is the limit maximum inactivation rate constant as $[I]\rightarrow\infty$, and K_I is the inactivator concentration yielding k_{obs} at the sum of $k_{obs[I]=0}$ and 0.5 times k_{inact}.

Predictions of Drug Interactions. The potential for an inactivator to cause an increase in exposure to a drug due to inactivation of hepatic enzymes was assessed using the following equation (Mayhew, et al., 2000):

$$\frac{AUC_i}{AUC} = \frac{1}{\left(\frac{f_{m(CYP)}}{1+\left(\frac{k_{inact} \bullet [I]_{in\ vivo}}{K_I \bullet k_{deg}}\right)}\right) + \left(1 - f_{m(CYP)}\right)} \quad \text{(Eq. 3)}$$

The terms are defined as follows: AUC_i/AUC is the predicted ratio of in vivo exposure of a CYP cleared drug with coadministration of the inactivator vs that in control state, $f_{m(CYP)}$ is the fraction of total clearance of the drug to which the affected CYP enzyme contributes, k_{deg} is the first-order rate constant of in vivo degradation of the affected CYP enzyme, k_{inact} is the theoretical maximum inactivation rate constant at infinite inactivator concentration as assessed in vitro, K_I is the inactivator concentration yielding a measured inactivation rate at half of k_{inact}, and $[I]_{in\ vivo}$ is the in vivo concentration of the inactivator. For CYP3A, the impact on extraction by the intestine also needs to be accounted for, by including a term for the effect on CYP3A in the intestine (Wang, et al., 2004):

DMD Fast Forward. Published on November 8, 2006 as DOI: 10.1124/dmd.106.012633
This article has not been copyedited and formatted. The final version may differ from this version.

$$\frac{AUC_i}{AUC} = \frac{1}{F_g + \left((1 - F_g) \bullet \frac{1}{1 + \left(\frac{k_{inact} \bullet [I]_g}{k_{deg,CYP3A,gut} \bullet ([I]_g + K_I)}\right)}\right)} \bullet \frac{1}{\left(\frac{f_{m(CYP3A)}}{1 + \left(\frac{k_{inact} \bullet [I]_{in\ vivo}}{K_I \bullet k_{deg,CYP3A,hep}}\right)}\right) + (1 - f_{m(CYP3A)})} \quad \text{(Eq 4)}$$

The parameters are as described above, with the addition of the following: F_g is the fraction of the dose of the affected drug that passes through the intestine unchanged after oral administration in the control state, $[I]_g$ is the concentration of the inactivator in the intestine, $f_{m(CYP3A)}$ is the fraction of the affected drug cleared by hepatic CYP3A, and $k_{deg,CYP3A,gut}$ and $k_{deg,CYP3A,hep}$ represent in vivo degradation rate constants for CYP3A in the intestine and liver, respectively.

The following values were used for the parameters needed for equations 3 and 4:

Fraction of the Affected Drug Metabolized by Cytochrome P450s ($f_{m(CYP)}$): Values for the fraction of the affected drug metabolized by the CYP enzyme that is inactivated were previously reported (Obach, et al., 2006) and had been derived from various sources. These are: theophylline $f_{m(CYP1A2)}$ = 0.8; S-warfarin $f_{m(CYP2C9)}$ = 0.91; omeprazole $f_{m(CYP2C19)}$ = 0.87; desipramine $f_{m(CY2D6)}$ = 0.9; midazolam and buspirone $f_{m(CYP3A)}$ = 0.93. For bupropion hydroxylation a value of $f_{m(CYP2B6)}$ = 0.95 was used based on estimates from in vitro data (Hesse, et al., 2000) and for caffeine a value of $f_{m(CYP1A2)}$ = 0.95 was made using a combination of quantitative human metabolism data reported from control subjects receiving radiolabelled drug (Rodopoulos, et al., 1995) and in vitro data describing P450 enzymes involved in metabolic pathways (Ha, et al., 1996).

Concentration of the Inactivator In Vivo ([I]). For the term [I], described as the concentration of inactivator available to the enzyme, the systemic steady-state C_{max}, the systemic steady-state unbound C_{max} (defined as $f_u \bullet C_{max}$), and the estimated unbound steady-state C_{max} at the inlet to the liver (i.e. $C_{max,u,inlet}$; Kanamitsu, et al., 2000) as:

$$C_{max,u,inlet} = f_u \bullet \left(C_{max} + \frac{D \bullet k_a \bullet F_a}{Q_h}\right) \quad \text{(Eq. 5)}$$

in which D is the dose of the inactivator, k_a is the oral absorption rate constant of the inactivator, F_a is the fraction of the inactivator absorbed following oral administration, C_{max} is the systemic steady-state maximum concentration of the inactivator, f_u is the unbound fraction of inactivator in plasma, and Q_h is hepatic blood flow (1450 ml/min).

For CYP3A, the concentration of the inactivator in the enterocyte during absorption ($[I]_g$) was also considered, and defined as (Rostami-Hodjegan and Tucker, 2004):

$$[I]_g = \frac{D \bullet k_a \bullet F_a}{Q_g} \quad \text{(Eq. 6)}$$

Parameters are the same as described above, with Q_g representing enterocytic blood flow (248 ml/min).

In Vivo CYP Degradation Rate Constants (k_{deg}). Under normal conditions, the rate of de novo biosynthesis of cytochrome P450 enzymes should equal the rate of degradation. Experimentally measured values for such a parameter in humans are not obtainable, therefore these values must be estimated. In this analysis, where available, k_{deg} values for each CYP enzyme were estimated by modeling the time course of de-induction or recovery following inactivation of oral clearance of substrates specific for various CYPs. This was accomplished using data from well-designed studies in the clinical pharmacokinetic literature for CYPs 1A2 (Faber and Fuhr, 2004), 2D6 (Liston et al., 2002, Venkatakrishnan and Obach, 2005) and intestinal CYP3A (Greenblatt et al., 2003) based on the time course of de-induction following smoking cessation, recovery following paroxetine inactivation, and recovery following inactivation by grapefruit juice, respectively. The resulting k_{deg} estimates (min^{-1}) were: 0.000296, 0.000226 and 0.000481, for CYP1A2, CYP2D6 and intestinal CYP3A, respectively. For hepatic CYP3A, an initial estimate of 0.000321 min^{-1} was used based on the kinetics of de-induction of the oral clearance of verapamil (Fromm et al., 1996), general clinical pharmacologic understanding of the kinetics of induction and de-induction of CYP3A (Lin, 2006; Thummel, et al., 2000) additionally supported by in vitro estimates of CYP3A turnover in primary human hepatocytes using pulse-chase methods (Pichard et al., 1992).

DMD Fast Forward. Published on November 8, 2006 as DOI: 10.1124/dmd.106.012633
This article has not been copyedited and formatted. The final version may differ from this version.

For the other enzymes (CYPs 2B6, 2C9, 2C19), a mean value of the above described estimates for hepatic CYPs (0.00026 min^{-1}) was used since clinical pharmacokinetic data to support similar calculations were not available.

In addition, empirical predictions of the magnitude of DDI were explored using IC_{50} values measured following a 30 min preincubation of inactivator, human liver microsomes, and NADPH. Equations used for these predictions were those previously described (Obach, et al., 2006):

$$\frac{AUC_i}{AUC} = \frac{1}{\left(\frac{f_{m(CYP)}}{1+\left(\frac{[I]_{in\ vivo}}{0.5 \bullet IC_{50}}\right)}\right) + \left(1 - f_{m(CYP)}\right)} \quad \text{(Eq. 7)}$$

and for CYP3A:

$$\frac{AUC_i}{AUC} = \frac{1}{F_g + \left(\left(1 - F_g\right) \bullet \frac{1}{1+\left(\frac{[I]_g}{0.5 \bullet IC_{50}}\right)}\right)} \bullet \frac{1}{\left(\frac{f_{m(CYP3A)}}{1+\left(\frac{[I]_{in\ vivo}}{0.5 \bullet IC_{50}}\right)}\right) + \left(1 - f_{m(CYP3A)}\right)} \quad \text{(Eq. 8)}$$

in which IC_{50} is the value measured in an activity assay after the inactivator had been preincubated for 30 min with microsomes and NADPH.

Accuracies of prediction methods were assessed using the geometric mean fold error:

$$GMFE = 10^{\frac{\sum\left|\log\frac{\text{predicted DDI}}{\text{actual DDI}}\right|}{N}} \quad \text{(Eq. 9)}$$

and the root mean squared error:

$$RMSE = \sqrt{\frac{\left(\text{predicted DDI} - \text{actual DDI}\right)^2}{N}} \quad \text{(Eq. 10)}$$

in which N is the total number of predictions.

RESULTS

Characterization of Single Point Inactivation. Compounds known to be inactivators for various human CYP enzymes were incubated in an inactivation preincubation at a single concentration representing 10-fold of the concentration known to cause 25% inhibition in the activity incubation. These same compounds were also tested for the other CYP enzymes for which it had not been demonstrated to cause inactivation. This concentration was selected because, in theory, it should be at the most sensitive point for detecting a mechanism-based inactivator (refer to Figure 1). The data showing the percent decrease in activity caused by a 30 min incubation of inactivators in the presence of NADPH, vs that in the absence of NADPH are shown in Table 2. With the exception of ticlopidine/CYP2C19 and rotonavir/CYP3A, for those combinations where inactivation was expected the percent decrease in activity was at least 30%. These include furafylline and zileuton (CYP1A2, Racha, et al., 1998; Lu, et al., 2003), ticlopidine, methyl phenethyl piperidine (a.k.a. PPP), and thioTEPA (CYP2B6; Richter, et al., 2004; 2005; Chun, et al., 2000), desethylamiodarone (CYP2C8; Polasek, et al., 2004), tienilic acid (CYP2C9; Melet, et al., 2003), methylenedioxymethamphetamine (MDMA) and paroxetine (CYP2D6; Bertelsen, et al., 2003; Heydari, et al., 2004), and diltiazem, erythromycin, and verapamil (CYP3A; Wang, et al., 2004; Mayhew, et al., 2000; McConn, et al., 2004; Ernest, et al., 2005). With a few exceptions (e.g. desethylamiodarone, thioTEPA), these compounds did not show appreciable inactivation for other CYP enzymes. As a negative control, montelukast, which potently inhibits several P450 enzymes (Walsky, et al., 2005), did not demonstrate inactivation for any of the enzymes. Ticlopidine showed only an 11% decrease in CYP2C19 activity when incubated in the presence of NADPH. This could be partially due to the fact that the incubation time for assessing CYP2C19 S-mephenytoin hydroxylase activity (40 min) is longer than the 30 min inactivation incubation time, which would be expected to blunt any observable difference. Thus, a decrease in activity of 15% was identified as a cutoff value for identifying inactivators for CYP enzymes, except for CYP2C19 for which a cutoff value of 10% was identified.

DMD Fast Forward. Published on November 8, 2006 as DOI: 10.1124/dmd.106.012633
This article has not been copyedited and formatted. The final version may differ from this version.

IC_{50} Shift Results. For those agents that demonstrated a 15% (or 10% for CYP2C19) decrease in activity when incubated for 30 min at 10-fold the IC_{25}, a determination of the decrease in the IC_{50} was measured. Inactivators were incubated at several concentrations spanning the value of 10 times the reversible inhibition IC_{50} for 30 min in the presence or absence of NADPH, followed by a 10-fold dilution into an activity assay incubation. A list of the IC_{50} values generated with and without NADPH in the inactivation incubation is in Table 3 and an example is shown in Figure 2 (panel A). The range of IC_{50} shifts spanned from a >800-fold decrease (inactivation of testosterone 6β-hydroxylase by erythromycin) to 1.6-fold (inactivation of midazolam 1'-hydroxylase by ritonavir).

Inactivation Kinetics. Values for k_{inact} and K_I were measured for those compounds demonstrating IC_{50} shifts, and these are listed in Table 4, with an example shown in Figure 2. (Refer to the Supplemental Information for plots for all of the inactivators.) A practical limit for measuring k_{inact} values appears to be about 0.005/min, and depends to some extent on the enzyme being studied. Based on k_{inact} values alone, the compounds with the greatest capacity to inactivate various CYP enzymes were ritonavir (CYP3A), MDMA (CYP2D6), ticlopidine (CYP2B6), and tienilic acid (CYP2C9). When the potency is also included to generate k_{inact}/K_I ratios, the compounds with the greatest capability to inactivate CYP enzymes are ritonavir (CYP3A), ticlopidine (CYP2B6), tienilic acid (CYP2C9), paroxetine (CYP2D6), and furafylline (CYP1A2). Comparing values for k_{inact}/K_I and the IC_{50}, the shifted IC_{50}, and the fold shift in IC_{50} revealed that the greatest correlation existed with the shifted IC_{50} (Figure 3). A correlation also existed between the shifted IC_{50} and K_I, which may indicate that the shifted IC_{50} contains elements of the inactivator potency. This indicates that the fold change in IC_{50} alone is not the most important predictor of the efficiency of an inactivator, but rather what the potency is after conducting a 30 min incubation with the inactivator prior to measurement of activity. Some compounds exhibited substantial fold changes in IC_{50} yet the overall potency was not high (e.g. MDMA and CYP1A2; thioTEPA and CYP2C8, etc).

DMD Fast Forward. Published on November 8, 2006 as DOI: 10.1124/dmd.106.012633
This article has not been copyedited and formatted. The final version may differ from this version.

Prediction of Drug-Drug Interactions: Utilizing Shifted IC_{50} Values. The generation of IC_{50} values after a 30 min preincubation of the inactivator, liver microsomes, and NADPH may represent a scaled-down empirical surrogate of a full determination of inactivation kinetic parameters, considering the excellent correlation to the k_{inact}/K_I ratio, an established measure of inactivation efficiency (Ernest, et al., 2005). In a previous report it had been demonstrated that the magnitude of DDI could be reliably predicted for reversible inhibitors when the estimated unbound portal vein C_{max} was used, along with reversible inhibition constants (Obach, et al., 2005). However, it was observed that this approach was not generally accurate for compounds known to be mechanism based inactivators. Thus, IC_{50} values generated after an inactivation preincubation (i.e. "shifted" IC_{50} values) were used in equations 7 and 8 which had been previously demonstrated to yield accurate predictions of DDI for reversible inhibitors when combined with estimates of unbound portal vein C_{max} values. Results are listed in Table 5, and a plot of predicted DDI vs actual values from clinical studies is shown in Figure 4 (panel A). A comparison of the shifted and non-shifted IC_{50} values yields mixed results. For some compounds, the shifted IC_{50} values yielded more accurate predictions (e.g. paroxetine, ritonavir), while for others the prediction was less accurate (e.g. tienilic acid, erythromycin). Preincubation led to the identification of diltiazem, paroxetine, and verapamil as perpetrators of DDI while no preincubation would have misidentified these drugs as non-inactivators. In almost every case, the actual DDI magnitude was in between the values predicted from shifted and non-shifted IC_{50} values.

Prediction of Drug-Drug Interactions: Utilizing Inactivation Kinetic Parameters. In Table 6, predictions of the magnitude of DDIs are listed using three different values for in vivo concentration of the inactivator ($[I]_{in\ vivo}$): total systemic C_{max}, unbound systemic C_{max}, and estimated unbound C_{max} at the inlet to the liver. In almost all cases, predictions yielded greater values than the actual DDI values. Total systemic C_{max} yielded over-predictions; in some cases these were very inaccurate (e.g. erythromycin, tienilic acid, verapamil) and in others, predictions

of DDI greater than 2-fold would be made but the actual value was less than 2-fold (e.g. ticlopidine/theophylline and zileuton). Similar observations were made when the estimated unbound portal vein C_{max} was used for [I]. Unbound systemic C_{max} values generally provided the most accurate predictions. Geometric mean fold errors for predictions using total systemic C_{max}, unbound systemic C_{max}, and estimated unbound portal vein C_{max} were 2.50, 1.64, and 2.63, respectively.

DISCUSSION

Among scientists studying drug metabolism it has been a longstanding goal to develop methods whereby in vitro data can be used for making reliable predictions of various pharmacokinetic phenomena such as clearance and DDI. An increased understanding of the enzymes and transporters involved in drug metabolism and disposition has led to an increasing ability to make such predictions. Drugs that are known to cause increases in exposure to other drugs commonly cause these by reversible inhibition or irreversible inactivation of metabolizing enzymes. In previous reports, demonstrate an ability to predict DDI for those compounds that reversibly inhibit human CYP enzymes was demonstrated (Obach, et al., 2005, 2006). However, in these reports, underpredictions of DDI for several drugs using reversible inhibition data were made, due to these compounds actually being irreversible inactivators of drug metabolizing enzymes. For individual drugs, others have shown that DDI caused by irreversible inactivation of CYP enzymes can be predicted (Galetin, et al., 2006; Venkatakrishnan and Obach, 2005, Wang, et al., 2004; Ito, et al., 2003; Yamano, et al., 2001; Mayhew, et al., 2000; Kanamitsu, et al., 2000). In these reports, the investigators have used various values for the input parameters such as enzyme degradation rate constants derived from animal or hepatocyte data. However, to date, the prediction of DDI caused by CYP inactivators for a comprehensive set of drugs has not been reported. In the present work, attempts to make DDI predictions for inactivators using a set of drugs that spans multiple CYP enzymes were made, albeit the number of drugs for which this can be done (particularly for non-CYP3A enzymes) is still limited compared to the set used to predict DDI for reversible inhibitors (Obach, et al., 2005).

In the present report, a hierarchy of in vitro inactivation approaches was presented. It was demonstrated that a simple experiment that employs a single concentration of inactivator that is preincubated with human liver microsomes in the presence and absence of NADPH for 30 min prior to measurement of a CYP marker activity can distinguish irreversible inactivators from non-inactivators (Table 2). Such an experimental design can be employed in early stages of drug

DMD Fast Forward. Published on November 8, 2006 as DOI: 10.1124/dmd.106.012633
This article has not been copyedited and formatted. The final version may differ from this version.

research in which hundreds of compounds are being considered in order to select those compounds devoid of an ability to inactivate CYP enzymes. A more complex experimental design, which is still simpler than a full determination of inactivation kinetics, is the determination of IC_{50} after a 30 min preincubation in the presence and absence of NADPH. Inactivators show a lower IC_{50} when preincubated with NADPH, and the resulting "shifted" IC_{50} could be useful for predicting the magnitude of a DDI when combined with the estimated unbound portal C_{max} of the inactivator and inserted into equations used for predicting DDI for reversible inhibitors (Obach, et al., 2006). While this approach is empirical, and the shifted IC_{50} values measured would depend on elements of the experimental design (e.g. preincubation time, dilution factor, etc), it does appear to be a reasonable approach to making initial predictions of the magnitude of DDI when conducted in the manner described in this report. Furthermore, use of this approach can be rationalized by the excellent correlation observed between the "shifted" IC_{50} and the k_{inact}/K_I value, the latter being an established measure of inactivator efficiency.

The use of k_{inact} and K_I in predicting DDI for inactivators has been the most frequently reported approach. In the present study, application of this approach was attempted across multiple known inactivators and seven human CYP enzymes. The complexity underlying predicting DDI for inactivators must be appreciated; there are multiple parameters that need to be considered, each with their own sources of uncertainty. Also, there are aspects of in vitro experimental design that can yield variability and inaccuracy. These have been discussed in a recent paper by Ghanbari, et al. (2006). The four parameters that are most important to making accurate predictions of DDI caused by inactivators are (1) the in vivo rate of enzyme degradation, k_{deg}, (2) the relevant in vivo concentration of the inactivator, [I], available to the target enzyme, (3) the in vitro inactivation kinetic parameters (K_I and k_{inact}), and (4) the fraction of the clearance of the affected drug that is mediated by the inactivated enzyme. The first three input parameters are discussed below, while the importance of the fourth has been previously discussed (Ito, et al., 2005; Obach, et al., 2006). Furthermore, it must be kept in mind that the clinical drug interaction

data used to test the accuracy of predictions from in vitro inactivation data is derived from reports that employed a variety of study designs each of which have influence on the magnitude of the interaction (e.g. timing of the dosing, etc.).

In previous reports, the value used for k_{deg} for CYP enzymes frequently was a value derived from rat ($k_{deg} \approx 0.0008$/min; Mayhew, et al., 2000). In the present work, values for k_{deg} were utilized that were derived from modeling of the time course of reversal of DDI caused by induction or inactivation of CYP enzymes in human study subjects. The values obtained were substantially lower than the rat value, were within values reported in Ghanbari, et al. (2006), and when used generally led to over-prediction of the magnitude of DDI (i.e. lower k_{deg} leads to greater DDI). Actual measurements of CYP enzyme k_{deg} values in humans in vivo are not obtainable with technology presently available, leaving this parameter as one important source of potential error in DDI predictions for inactivators.

The use of estimated unbound hepatic inlet concentrations of inhibitors occurring during the absorption phase, as surrogates for free concentrations in the liver, proved to be a reliable value for in vivo inhibitor concentration in prediction of DDI magnitude for reversible inhibition (Obach, et al., 2006). Such a value has face validity as the target enzymes are in the liver (and for CYP3A in the gut as well), thus it is expected that this tissue, and hence the target CYP enzyme, would be exposed to considerably greater concentrations of inhibitor than those reflected by systemic concentrations. However, when employed for the prediction of DDI caused by inactivators, estimated free portal concentrations generally led to over-predictions of the magnitude of DDI (Table 6). Rather, use of the free systemic C_{max} of the inactivator yielded the most accurate predictions of DDI when combined with inactivation data (Table 6). Although this was observed for the compounds examined in this report, continued testing of the use of free systemic C_{max} for predicting DDI for CYP inactivators is warranted. An explanation for the discrepancy between the value for [I] that is most useful for DDI prediction for reversible inhibitors vs irreversible inactivators is not readily apparent and merits further exploration.

DMD Fast Forward. Published on November 8, 2006 as DOI: 10.1124/dmd.106.012633
This article has not been copyedited and formatted. The final version may differ from this version.

The experimental design employed in inactivation experiments can have an impact on the measured parameters (Yang et al., 2005; Ghanbari, et al., 2006). In the present studies, an approach was used wherein the inactivator was incubated with enzyme and cofactor for periods of time prior to dilution of the mixture into incubations in which the marker activity was measured. A major advantage of such an approach includes limiting reversible competitive inhibition, due to dilution of the inactivator in the incubation where marker activity is measured and the use of saturating index substrate concentrations in the activity assay. Comparison of activities to incubations that were preincubated with NADPH in the absence of inactivator is important for CYP enzymes since reactive oxygen species that can inactivate the enzyme can be generated in the presence of NADPH and absence of inactivator or substrate. This phenomenon can be accounted for by including the k_{obs} at [I] = 0 in the non-linear fitting of the k_{obs} vs [I] relationship (e.g. Figure 2c), as was done in this report. Use of linearized data to estimate inactivation kinetic parameters can undervalue this important factor. A disadvantage of using the dilution approach resides in the potential for inactivators to non-specifically bind to microsomal protein in the inactivation incubation since greater protein concentrations (i.e. >0.1 mg/ml) are needed. This factor was not accounted for in the present study, however correction for any non-specific binding would only cause the K_I to decrease and lead to even greater over-predictions of DDI. With the exception of CYP2C19, the protein concentrations used in inactivation incubations were still relatively low ($\leq$0.3 mg/ml; Table 1) compared to other reports.

Contour plots tracking combinations of the ratio of k_{inact} and k_{deg} and the ratio of [I] and K_I that would yield identical magnitudes of DDI are shown in Figure 5. Inactivators with high k_{inact} can cause DDI even at low concentrations relative to K_I (upper left side of the plot), while weaker inactivators (low k_{inact}) that are highly potent (low K_I) can also cause DDI (right side of the plot) and approach the behavior of reversible inhibitors rather than inactivators. By plotting the coordinates for each inactivator, a clustering can be observed for these compounds. In the region bounded by lower and upper limits of reliable in vitro measurements of k_{inact}, inactivators

that cause marked DDI tend to reside toward the upper right while those that do not cause DDI reside in the lower left. Predictions of DDI could be made for those drugs for which inactivation kinetic data have been measured in this report but for which there are no in vivo DDI data, by judging whether they reside on the plot near the cluster of known perpetrators of DDI or known non-perpetrators of DDI. Thus, it would be expected that MDMA should cause DDIs of concern for CYP2D6 cleared drugs (point 6b on the plot) and thioTEPA should cause DDIs of concern for CYP2B6 cleared drugs (point 3a), whereas ticlopidine, thioTEPA, and MDMA should not cause interactions with drugs cleared by CYP3A, CYP2C19, or CYP1A2, respectively (points 5d, 3c, and 6a). Continued testing of the application of this contour plot is required to determine whether it is broadly applicable to aid inactivation DDI risk assessment for new molecular entities based on where they fall on the contour map relative to known clinically established DDI perpetrators and non-perpetrators.

In summary, the data presented in this report demonstrate that in vitro inactivation kinetic data for human CYP enzymes can be useful in predicting in vivo DDI, when combined with the systemic unbound concentration of inactivator, the fraction of the affected drug metabolized by the inactivated CYP, and estimates of in vivo degradation rates of enzyme. Uncertainty in the multiple parameters needed for these predictions must be appreciated. Additionally, some abbreviated experimental approaches that can identify mechanism-based inactivators were presented. These can be employed in early drug discovery research when the number of new compounds requiring investigation for this undesired property can exceed the capacity for conducting complete characterizations of inactivation kinetics.

References:

Alderman J, Preskorn SH, Greenblatt DJ, Harrison W, Penenberg D, Allison J, Chung M. (1997) Desipramine pharmacokinetics when coadministered with paroxetine or sertraline in extensive metabolizers. J Clin Psychopharmacol. 17: 284-291.

Backman JT, Olkkola KT, Aranko K, Himberg JJ, Neuvonen PJ. (1994) Dose of midazolam should be reduced during diltiazem and verapamil treatments. Br J Clin Pharmacol 37: 221-225.

Bertelsen KM, Venkatakrishnan K, Von Moltke LL, Obach RS, and Greenblatt DJ. (2003) Apparent mechanism-based inhibition of human CYP2D6 in vitro by paroxetine : Comparison with fluoxetine and quinidine. Drug Metab. Dispos. 31: 289-293.

Brown HS, Ito K, Galetin A, and Houston JB. (2005) Prediction of in vivo drug-drug interactions from in vitro data: impact of incorporating parallel pathways of drug elimination and inhibitor absorption rate constant. Br. J. Clin. Pharmacol. 60: 508-518.

Calvo G, Garcia-Gea C, Luque A, Morte A, Dal-Re R, Barbanoj M. (2004) Lack of pharmacologic interaction between paroxetine and alprazolam at steady state in healthy volunteers. J Clin Psychopharmacol. 24: 268-276.

Chun J, Kent UM, Moss RM, Sayre LM, and Hollenberg PF. (2000) Mechanism-based inactivation of cytochromes P450 2B1 and P450 2B6 by 2-phenyl-2-(1-piperidinyl)propane. Drug Metab. Dispos. 28: 905-911.

Colli A, Buccino G, Cocciolo M, Parravicini R, Elli GM, Scaltrini G. (1987) Ticlopidine-theophylline interaction. Clin Pharmacol Ther. 41: 358-362.

Ernest CS, Hall SD, and Jones DR. (2005) Mechanism-based inactivation of CYP3A by HIV protease inhibitors. J. Pharmacol. Exp. Ther. 312: 583-591.

Faber MS and Fuhr U. (2004) Time response of cytochrome P450 1A2 activity on cessation of heavy smoking. Clin. Pharmacol. Ther. 76: 178-184.

Fromm MF, Busse D, Kroemer HK, and Eichelbaum M. (1996) Differential induction of prehepatic and hepatic metabolism of verapamil by rifampin Hepatology 24: 796-801.

Galetin A, Burt H, Gibbons L, and Houston JB. (2006) Prediction of time-dependent CYP3A4 drug-drug interactions: Impact of enzyme degradation, parallel elimination pathways, and intestinal inhibition. Drug Metab. Dispos. 34: 166-175.

Ghanbari F, Rowland-Yeo K, Bloomer JC, Clarke SE, Lennard MS, Tucker GT, and Rostami-Hodjegan A. (2006) A critical evaluation of the experimental design of studies of mechanism based enzyme inhibition, with implications for in vitro-in vivo extrapolation. Curr. Drug Metab. 7: 315-334.

Granneman GR, Braeckman RA, Locke CS, Cavanaugh JH, Dube LM, and Awni WM. (1995) Effect of zileuton on theophylline pharmacokinetics. Clin. Pharmacokinet. 29(Suppl. 2): 77-83.

Greenblatt DJ, von Moltke LL, Harmatz JS, Durol AL, Daily JP, Graf JA, et al. (2000) Differential impairment of triazolam and zolpidem clearance by ritonavir. J Acquir Immune Defic Syndr 24:129-136.

Greenblatt DJ, von Moltke LL, Harmatz JS, Chen G, Weemhoff JL, Jen C, Kelley CJ, LeDuc BW, and Zinny MA. (2003) Time course of recovery of cytochrome p450 3A function after single doses of grapefruit juice. Clin. Pharmacol. Ther. 74: 121-129.

Ha HR, Chen J, Krahenbuhl S, and Follath F. (1996) Biotransformation of caffeine by cDMA expressed human cytochromes P-450. Eur. J. Clin. Pharmacol. 49: 309-315.

Hesse LM, Venkatakrishnan K, Court MH, Von Moltke LL, Duan SX, Shader RI, Greenblatt DJ. (2000) CYP2B6 mediates the in vitro hydroxylation of bupropion: potential drug interactions with other antidepressants. Drug Metab. Dispos. 28: 1176-1183.

Heydari A, Rowland-Yeo K, Lennard MS, Ellis SW, Tucker GT, Rostami-Hodjegan A. (2004) Mechanism-based inactivation of CYP2D6 by methylenedioxymethamphetamine. Drug Metab. Dispos. 32: 1213-1217.

Ito K, Ogihara K, Kanamitsu SI, and Itoh T. (2003) Prediction of the in vivo interaction between midazolam and macrolides based on in vitro studies using human liver microsomes. Drug Metab. Dispos. 31: 945-954.

Ito K, Hallifax D, Obach RS, and Houston JB. (2005) Impact of parallel pathways of drug elimination and multiple cytochrome P450 involvement on drug-drug interactions: CYP2D6 paradigm. Drug Metab. Dispos. 33: 837-844.

Kanamitsu SI, Ito K, Green CE, Tyson CA, Shimada N, Sugiyama Y. (2000) Prediction of in vivo interaction between triazolam and erythromycin based on in vitro studies using human liver microsomes and recombinant human CYP3A4. Pharm. Res. 17: 419-426

Kanamitsu SI, Ito K, Sugiyama Y. (2000) Quantitative prediction of in vivo drug-drug interactions from in vitro data based on physiological pharmacokinetics: use of maximum unbound concentration of inhibitor at the inlet to the liver. Pharm Res 17: 336-343.

Kivisto KT, Lamberg TS, Kantola T, Neuvonen PJ. (1997) Plasma buspirone concentrations are greatly increased by erythromycin and itraconazole. Clin Pharmacol Ther. 62: 348-354.

Lamberg TS, Kivisto KT, Neuvonen PJ. (1998) of verapamil and diltiazem on the pharmacokinetics and pharmacodynamics of buspirone. Clin Pharmacol Ther. 63: 640-645.

Lin JH. (2006). CYP Induction-Mediated Drug Interactions: in Vitro Assessment and Clinical Implications. Pharm Res 23: 1089-1116

Liston HL, DeVane CL, Boulton DW, Risch SC, Markowitz JS, Goldman J. Differential time course of cytochrome P450 2D6 enzyme inhibition by fluoxetine, sertraline, and paroxetine in healthy volunteers. J Clin Psychopharmacol. 22: 169-173.

Lu P, Schrag ML, Slaughter DE, Raab CE, Shou M, and Rodrigues AD. (2003) Mechanism-based inhibition of human liver microsomal cytochrome P450 1A2 by zileuton , a 5-

lipoxygenase inhibitor. Drug Metab. Dispos. 31: 1352-1360.

Mayhew BS, Jones DR, Hall SD. (2000) An in vitro model for predicting in vivo inhibition of cytochrome P450 3A4 by metabolic intermediate complex formation. Drug Metab Dispos 28: 1031-1037.

McConn DJ, Lin YS, Allen K, Kunze KL, and Thummel KE. (2004) Differences in the inhibition of cytochromes P450 3A4 and 3A5 by metabolite-inhibitor complex-forming drugs. Drug Metab. Dispos. 32: 1083-1091.

Melet A, Assrir N, Jean P, Pilar Lopez-Garcia M, Marques-Soares C, Jaouen M, Dansette PM, Sari MA, and Mansuy D. (2003) Substrate selectivity of human cytochrome P450 2C9: importance of residues 476, 365, and 114 in recognition of diclofenac and sulfaphenazole and in mechanism-based inactivation by tienilic acid. Arch. Biochem. Biophys. 409: 80-91.

Obach RS, Walsky RL, Venkatakrishnan K, Houston BJ, and Tremaine LM. (2006) In vitro cytochrome P450 inhibition data and the prediction of drug-drug interactions: qualitative relationships, quantitative predictions, and the rank-order approach. Clin. Pharmacol. Ther. 78: 582-592.

Obach RS, Walsky RL, Venkatakrishnan K, Gaman EA, Houston BJ, and Tremaine LM. (2006) The utility of in vitro cytochrome P450 inhibition data in the prediction of drug-drug interactions. J. Pharmacol. Exp. Ther. 316: 336-348.

O'Reilly RA. (1982) Ticrynafen-racemic warfarin interaction: hepatotoxic or stereoselective? Clin. Pharmacol. Ther. 32: 356-361.

Pichard L, Fabre I, Daujat M, Domergue J, Joyeux H, and Maurel P (1992) Effect of corticosteroids on the expression of cytochromes P450 and on cyclosporin A oxidase activity in primary cultures of human hepatocytes. Mol Pharmacol 41: 1047-1055.

Polasek TM, Elliot DJ, Lewis BC, and Miners JO. (2004) Mechanism-based inactivation of human cytochrome P4502C8 by drugs in vitro. J. Pharmacol. Exp. Ther. 311: 996-1007.

Racha JK, Rettie AE, and Kunze KL. (1998) Mechanism-Based Inactivation of Human Cytochrome P450 1A2 by Furafylline : Detection of a 1:1 Adduct to Protein and Evidence for the Formation of a Novel Imidazomethide Intermediate. Biochemistry 37: 7407-7419.

Richter T, Muerdter TE, Heinkele G, Pleiss J, Tatzel S, Schwab M, Eichelbaum M, and Zanger UM. (2004) Potent mechanism-based inhibition of human CYP2B6 by clopidogrel and ticlopidine. J. Pharmacol. Exp. Ther. 308: 189-197.

Richter T, Schwab M, Eichelbaum M, and Zanger UM. (2005) Inhibition of human CYP2B6 by N,N',N"-triethylenethiophosphoramide is irreversible and mechanism-based. Biochem. Pharmacol. 69: 517-524.

Ripp SL, Mills JB, Fahmi OA, Trevena KA, Liras JL, Maurer TS, and de Morais SM (2006) Use of immortalized human hepatocytes to predict the magnitude of clinical drug-drug interactions caused by CYP3A4 1nduction. Drug Metab. Dispos. In press.

Rodopoulos N, Wisen O, and Norman A. (1995) Caffeine metabolism in patients with chronic

liver disease. Scand. J. Clin. Lab. Invest. 55: 229-242.

Rostami-Hodjegan A and Tucker GT (2004) 'In silico' simulations to assess the 'in vivo' consequences of 'in vitro' metabolic drug-drug interactions. Drug Disc. Today Tech. 1: 441-448.

Silva JM and Nicholl-Griffith DA (2002) In vitro models for studying induction of cytochrome P450 enzymes. In: Drug-Drug Interactions (ed. Rodrigues AD) Marcel Dekker, Inc. New York, pp. 189-216.

Takanaga H, Ohnishi A, Matsuo H, Murakami H, Sata H, Kuroda K, Urae A, Higuchi S, Sawada Y. (2000) Pharmacokinetic analysis of felodipine-grapefruit juice interaction based on an irreversible enzyme inhibition model. Br. J. Clin. Pharmacol. 49: 49-58.

Tarrus E, Cami J, Roberts DJ, Spickett RGW, Celdran E, and Segura J. (1987) Accumulation of caffeine in healthy volunteers treated with furafylline. Br. J. Clin. Pharmacol. 23: 9-18.

Tateishi T, Kumai T, Watanabe M, Nakura H, Tanaka M, Kobayashi S. (1999) Ticlopidine decreases the in vivo activity of CYP2C19 as measured by omeprazole metabolism. Br J Clin Pharmacol. 47: 454-457.

Thummel KE, Kunze KL, and Shen DD. (2000). Metabolically Based Drug-Drug Interactions: Principles and Mechanisms. In: Metabolic Drug Interactions (Ed. Levy RH et al.) Lippincott Williams and Wilkins**,** Philadelphia, PA, pp. 3-19.

Turpeinen M, Tolonen A, Uusitalo J, Jalonen J, Pelkonen O, Laine K. (2005) Effect of clopidogrel and ticlopidine on cytochrome P450 2B6 activity as measured by bupropion hydroxylation. Clin. Pharmacol. Ther. 77: 553-559.

Venkatakrishnan K, and Obach RS. (2005) In vitro-in vivo extrapolation of CYP2D6 inactivation by paroxetine: Prediction of nonstationary pharmacokinetics and drug interaction magnitude. Drug Metab. Dispos. 33: 845-852.

Walsky RL and Obach RS. (2004) Validated assays for human cytochrome P450 activities. Drug Metab Dispos 32: 647-660.

Walsky RL, Obach RS, Gaman EA, Gleeson JPR, and Proctor WR. (2005) Selective inhibition of human cytochrome P4502C8 by montelukast. Drug Metab. Dispos. 33: 413-418.

Wang YH, Jones DR, Hall SD. (2004) Prediction of cytochrome P450 3A inhibition by verapamil enantiomers and their metabolites. Drug Metab Dispos 32: 259-266.

Yamano K, Yamamoto K, Katashima M, Kotaki H, Takedomi S, Matsuo H, Ohtani H, Sawada Y, and Iga T. (2001) Prediction of midazolam-CYP3A inhibitors interaction in the human liver from in vivo/in vitro absorption, distribution, and metabolism data. Drug Metab. Dispos. 29: 443-452.

Yang J, Jamei M, Yeo KR, Tucker GT, and Rostami-Hodjegan A (2005) Kinetic values for mechanism-based enzyme inhibition: assessing the bias introduced by the conventional experimental protocol. Eur J Pharm Sci 26: 334-340.

DMD Fast Forward. Published on November 8, 2006 as DOI: 10.1124/dmd.106.012633
This article has not been copyedited and formatted. The final version may differ from this version.

Figure Legends

Figure 1. Illustration of the Single Point Inactivation and IC_{50} Shift Experiments. The two theoretical curves represent IC_{50} determinations after prior 30 min incubation of enzyme and CYP inactivator in the absence and presence of NADPH. In the IC_{50} shift, the horizontal dashed arrow shows a ten-fold decrease in IC_{50} (in this case from 1.0 to 0.1 μM) when the inactivation incubation is done in the presence of NADPH. In the single point approach, the vertical dashed arrow represents the change in the % of control activity when the enzyme is incubated with inactivator at 10 times the IC_{25} for 30 min in the presence of NADPH, prior to assessment of activity. In this case, IC_{25} in the absence of NADPH is approximately 0.3 μM. When the enzyme is incubated with inactivator at 0.3 μM in the presence of NADPH, followed by assessment of CYP activity, there is a 50% decrease in activity (75% to 25%).

Figure 2. Example of Mechanism-Based Inactivation Data. In this example, the inactivation of CYP2B6 by thioTEPA is shown. Panel A: An IC_{50} shift plot. The IC_{50} values in this example are 0.099 and 3.8 μM for preincubation with and without NADPH, respectively. Panel B: Inactivation plots. The values for k_{obs} are determined as the negative slopes of the natural logarithm of the % of control vs time. Panel C: Non-linear regression to determine K_I and k_{inact} for the inactivation of CYP2B6 by thioTEPA. Values determined in this example were 5.3 μM and 0.17 min^{-1}, respectively. The value for $k_{obs[I]=0}$ was 0.0039 min^{-1}.

Figure 3. Comparison of the Relationships Between k_{inact}/K_I and IC_{50} (Panel A) , Shifted IC_{50} (Panel B), and Fold Shift in IC_{50} (Panel C), as well as Between Shifted IC_{50} and K_I.. The term "shifted IC_{50}" refers to the value measured after the inactivator has been preincubated with liver microsomes and NADPH for 30 min.

Figure 4. Comparison of Predicted vs Actual DDI for Mechanism-Based Inactivators. In panel A, the predictions were made using shifted IC_{50} values and the equation for reversible inhibition (equations 7 and 8). In panel B, predictions were made using inactivation kinetic parameters and

equations 3 and 4, using unbound systemic concentrations of the inactivator in the prediction. Note that the predicted value for erythromycin (57-fold) is off-scale in Panel A.

Figure 5. The relationship between DDI magnitude, [I]/K_I, and k_{deg}/k_{inac}.for CYP enzymes. The magnitude of the DDI will be dependent not only on the concentration of the inactivator in vivo relative to its inhibitory potency ([I]/K_i), as is the case for reversible inhibitors, but also on the relationship between the inactivation rate and the rate of degradation of enzyme (k_{inact}/k_{deg}). The colored contours represent the magnitude increases in exposure of an affected drug (AUC_i/AUC) ranging from 1.1-fold increases (violet line) to 50-fold increases (red line) assuming that oral clearance is entirely mediated via hepatic metabolism by the affected enzyme (i.e. $f_{m(CYP)} = 1$). The individual inactivators are indicated by number: 1: furafylline with CYP1A2; 2: zileuton with CYP1A2; 3a: thioTEPA with CYP2B6; 3b: thioTEPA with CYP2C8; 3c: thioTEPA with CYP2C19; 3d: thioTEPA with CYP3A; 4: tienilic acid with CYP2C9; 5a: ticlopidine with CYP1A2; 5b: ticlopidine with CYP2B6; 5c: ticlopidine with CYP2C19; 5d: ticlopidine with CYP3A; 6a: MDMA with CYP1A2; 6b: MDMA with CYP2D6; 7a: paroxetine with CYP2D6; 7b: paroxetine with CYP3A; 8: diltiazem with CYP3A; 9: erythromycin with CYP3A; 10: ritonavir with CYP3A; 11: verapamil with CYP3A. The color of the number indicates the magnitude of DDI caused by the inactivator: red text: DDI>5X; blue text: 2X<DDI< 5X; violet text: DDI<2X, black text: no clinical DDI data available. The horizontal dashed lines represent practical upper and lower limits for detecting inactivation in vitro (2/min > k_{inact} > 0.005/min; k_{deg} ≈ 0.00032/min).

TABLE 1. Concentrations of cytochrome P450 substrates used in single point, IC_{50} shift, and k_{inact}/K_I experiments.

			Single Point and IC_{50} Shift Experiments		k_{inact}/K_I Experiments	
Enzyme	Substrate	Protein Concentration (mg/ml)[a]	Incubation Time (min)	[S] (μM)	Incubation Time (min)	[S] (μM)
CYP1A2	Phenacetin	0.3 → 0.03	30	50	20	500
CYP2B6	Bupropion	0.5 → 0.05	20	80	12	800
CYP2C8	Amodiaquine	0.25 → 0.025	10	1.9	6	19
CYP2C9	Diclofenac	0.3 → 0.03	10	4	6	40
CYP2C19	S-Mephenytoin	2 → 0.2	40	60	30	600
CYP2D6	Dextromethorphan	0.3 → 0.03	10	5	6	50
CYP3A	Midazolam	0.3 → 0.03	4	2.5	6	25
CYP3A	Testosterone	0.3 → 0.03	10	50	6	500

[a]Denotes protein concentrations used in the inactivation preincubations diluted into the activity incubations.

TABLE 2. Percent change in inhibition of human cytochrome P450 enzymes with a 30 min incubation of inactivator, human liver microsomes, and NADPH.

Inactivator	Enzyme Known to be Inactivated	% Decrease in Activity at IC_{25}[b]							
		CYP1A2	CYP2B6	CYP2C8	CYP2C9	CYP2C19	CYP2D6	CYP3A(M)[a]	CYP3A(T)[a]
Furafylline	CYP1A2	55	-	-	-	25	28	-	-
Zileuton	CYP1A2	41	-	-	-	-	-	-	-
PPP	CYP2B6	-	54	-	-	-	-	-	-
ThioTEPA	CYP2B6	-	46	38	16	13	-	50	32
Desethylamiodarone	CYP2C8	-	21	30	36	-	21	29	25
Tienilic Acid	CYP2C9	-	-	-	59	-	-	-	-
Ticlopidine	CYP2C19	21	43	-	-	11	-	35	19
MDMA	CYP2D6	25	25	-	-	-	59	-	-
Paroxetine	CYP2D6	-	-	-	-	-	62	24	29
Diltiazem	CYP3A	-	-	-	-	-	-	37	43
Erythromycin	CYP3A	-	-	-	-	-	-	43	67
Ritonavir[c]	CYP3A	-	-	-	-	-	-	-	-
Verapamil	CYP3A	-	-	-	-	-	-	49	63
Montelukast	none	-	-	-	-	-	-	-	-

[a]CYP3A(M) and CYP3A(T) refer to midazolam and testosterone hydroxylase activities, respectively. [b]A dash indicates that the decrease in activity was less than 15%, except for CYP2C19 which was <10%. [c]It should be noted that ritonavir demonstrates less than a 15% in activity with preincubation. This is likely due to the extremely potent reversible inhibition caused by this compound.

DMD Fast Forward. Published on November 8, 2006 as DOI: 10.1124/dmd.106.012633
This article has not been copyedited and formatted. The final version may differ from this version.

TABLE 3. IC_{50} values for mechanism-based inactivators of human cytochrome P450 enzymes following a 30 min incubation with human liver microsomes in the absence and presence of NADPH.

Inactivator	CYP	IC_{50} (μM) Without NADPH	IC_{50} (μM) With NADPH	IC_{50} Shift Fold Difference
Furafylline[a]	CYP1A2	1.5	0.027	56
Zileuton	CYP1A2	41	2.9	14
PPP	CYP2B6	4.8	0.12	40
ThioTEPA	CYP2B6	3.8	0.099	38
	CYP2C8	>1000	21	>48
	CYP2C19	>600	75	>8
	CYP3A(midazolam)	2.7	7.1	3.8
	CYP3A(testosterone)	42	12	3.5
Desethylamiodarone	CYP2B6	2.2	0.67	3.3
	CYP2C8	2.0	0.68	2.9
	CYP2C9	2.6	0.47	5.5
	CYP2D6	3.1	0.64	4.8
	CYP3A(midazolam)	4.8	1.6	3.0
	CYP3A(testosterone)	1.8	0.76	2.4
Tienilic Acid	CYP2C9	0.43	0.027	16
Ticlopidine	CYP1A2	12	0.75	16
	CYP2B6	0.13	0.031	4.2
	CYP2C19	0.63	0.33	1.9
	CYP3A(testosterone)	48	18	2.7
MDMA	CYP1A2	>600	23	>26
	CYP2B6	>900	56	>16
	CYP2D6	4.2	0.046	91
Paroxetine	CYP2D6	0.23	0.012	19
	CYP3A(midazolam)	15	4.8	3.1
	CYP3A(testosterone)	19	6.5	2.9
Diltiazem	CYP3A(midazolam)	54	3.7	15
	CYP3A(testosterone)	55	1.8	31
Erythromycin	CYP3A(midazolam)	18	1.2	15
	CYP3A(testosterone)	>600	0.72	>830
Ritonavir	CYP3A(midazolam)	0.0044	0.0028	1.6
	CYP3A(testosterone)	0.0083	0.0040	2.1
Verapamil	CYP3A(midazolam)	12	0.12	100
	CYP3A(testosterone)	8.2	0.15	55

[a]Furafylline also demonstrated inactivation of CYP2C19 and CYP2D6 however solubility limitations prohibited the further examination of furafylline as an inactivator of these enzyme activities.

DMD Fast Forward. Published on November 8, 2006 as DOI: 10.1124/dmd.106.012633
This article has not been copyedited and formatted. The final version may differ from this version.

TABLE 4. Inactivation kinetic values for mechanism-based inactivators of human cytochrome P450 enzymes.

Inactivator	CYP	k_{inact} (min^{-1})	K_I (μM)	k_{inact}/K_I (ml/min/μmol)
Furafylline	CYP1A2	0.19	1.6	120
Zileuton	CYP1A2	0.11	89	1.2
PPP	CYP2B6	0.10	5.3	19
ThioTEPA	CYP2B6	0.17	5.3	32
	CYP2C8	0.026	88	0.30
	CYP2C19	0.029	1100	0.026
	CYP3A(midazolam)	0.035	300	0.12
	CYP3A(testosterone)	0.033	220	0.15
Desethylamiodarone	CYP2B6	0.026	14	1.9
	CYP2C8	0.009	4.4	2.1
	CYP2C9	0.053	38	1.4
	CYP2D6	0.029	24	1.2
	CYP3A(midazolam)	0.012	2.8	4.3
	CYP3A(testosterone)	0.018	4.0	4.5
Tienilic Acid	CYP2C9	0.28	1.0	280
Ticlopidine	CYP1A2	0.011	5.2	2.1
	CYP2B6	0.30	0.57	530
	CYP2C19	0.097	4.3	23
	CYP3A(midazolam)	0.039	77	0.51
	CYP3A(testosterone)	0.019	210	0.090
MDMA	CYP1A2	0.014	180	0.078
	CYP2D6	0.38	6.3	60
Paroxetine	CYP2D6	0.17	0.81	210
	CYP3A(midazolam)	0.011	13	0.85
	CYP3A(testosterone)	0.014	23	0.64
Diltiazem	CYP3A(midazolam)	0.012	4.5	2.7
	CYP3A(testosterone)	0.015	2.4	6.3
Erythromycin	CYP3A(midazolam)	0.036	10	3.6
	CYP3A(testosterone)	0.039	9.8	4.0
Ritonavir	CYP3A(midazolam)	0.45	0.38	1200
	CYP3A(testosterone)	0.28	0.18	1500
Verapamil	CYP3A(midazolam)	0.043	1.8	24
	CYP3A(testosterone)	0.043	1.7	25

TABLE 5. Predictions of Drug Interactions for Mechanism Based Inactivators Using IC_{50} Values Gathered After a 30 min Incubation With or Without NADPH and the Prediction Method Applicable for Reversible Inhibition.

			Predicted DDI[c]			
Inactivator	Enzyme	Affected Drug	-NADPH	+NADPH	Actual DDI[d]	Reference
Diltiazem	CYP3A	Buspirone	1.5	23	5.3	Lamberg, et al., 1998
Erythromycin	CYP3A	Buspirone	4.6	57	5.9	Kivisto, et al., 1997
Furafylline[b]	CYP1A2	Caffeine	5.5	19	~10	Tarrus, et al., 1987
Paroxetine	CYP2D6	Desipramine	1.7	5.1	5.2	Alderman, et al., 1997
	CYP3A	Alprazolam	1.0	1.2	0.99	Calvo, et al., 2004
Ritonavir	CYP3A	Triazolam	11	22	20	Greenblatt, et al., 2000
Ticlopidine	CYP1A2	Theophylline	1.1	2.3	1.6	Colli, et al., 1987
	CYP2B6	Bupropion[a]	5.8	12	14	Turpeinen, et al., 2005
	CYP2C19	Omeprazole	2.2	3.0	2.4	Tateishi, et al., 1999
Tienilic Acid	CYP2C9	S-Warfarin	2.7	8.7	2.9	O'Reilly, 1982
Verapamil	CYP3A	Midazolam	1.3	6.4	2.9	Backman, et al., 1994
Zileuton	CYP1A2	Theophylline	1.4	3.5	1.9	Granneman, et al., 1995

[a]This represents the effect on hydroxybupropion:bupropion AUC ratio, not parent exposure.
[b]The free fraction of furafylline in human plasma was unavailable in the scientific literature. A value of 0.39 was measured experimentally using ultrafiltration.
[c]The value for $[I]_{in\ vivo}$ used in the predictions was the unbound estimated portal vein C_{max} as described in Obach, et al. (2006).
[d]Clinical interaction data used in this analysis represents the largest reported interaction for each inactivator.

TABLE 6. Predictions of Drug Interactions for Mechanism Based Inactivators Using In Vitro Inactivation Parameters

Inactivator	Enzyme	Affected Drug	Predicted DDI Systemic $C_{max,}$	Predicted DDI Systemic $C_{max,u}$	Predicted DDI Portal $C_{max,u}$	Actual DDI[c]	Reference
Diltiazem	CYP3A	Buspirone	18	8.0	36	5.3	Lamberg, et al., 1998
Erythromycin	CYP3A	Buspirone	52	26	48	5.9	Kivisto, et al., 1997
Furafylline[b]	CYP1A2	Caffeine	20	20	20	~10	Tarrus, et al., 1987
Paroxetine	CYP2D6	Desipramine	6.4	4.1	6.3	5.2	Alderman, et al., 1997
	CYP3A	Alprazolam	1.3	1.0	1.2	0.99	Calvo, et al., 2004
Ritonavir	CYP3A	Triazolam	22	22	22	20	Greenblatt, et al., 2000
Ticlopidine	CYP1A2	Theophylline	4.2	1.3	2.7	1.6	Colli, et al., 1987
	CYP2B6	Bupropion[a]	20	17	20	14	Turpeinen, et al., 2005
	CYP2C19	Omeprazole	7.4	3.6	6.3	2.4	Tateishi, et al., 1999
Tienilic Acid	CYP2C9	S-Warfarin	11	11	11	2.9	O'Reilly, 1982
Verapamil	CYP3A	Midazolam	19	6.6	22	2.9	Backman, et al., 1994
Zileuton	CYP1A2	Theophylline	4.3	2.1	4.6	1.9	Granneman, et al., 1995
GMFE			2.50	1.64	2.63		
RMSE			15.1	7.1	19.3		

[a]This represents the effect on hydroxybupropion:bupropion AUC ratio, not parent exposure.
[b]The free fraction of furafylline in human plasma was unavailable in the scientific literature. A value of 0.39 was measured experimentally using ultrafiltration.
[c] Clinical interaction data used in this analysis represents the largest reported interaction for each inactivator.

Figure 1

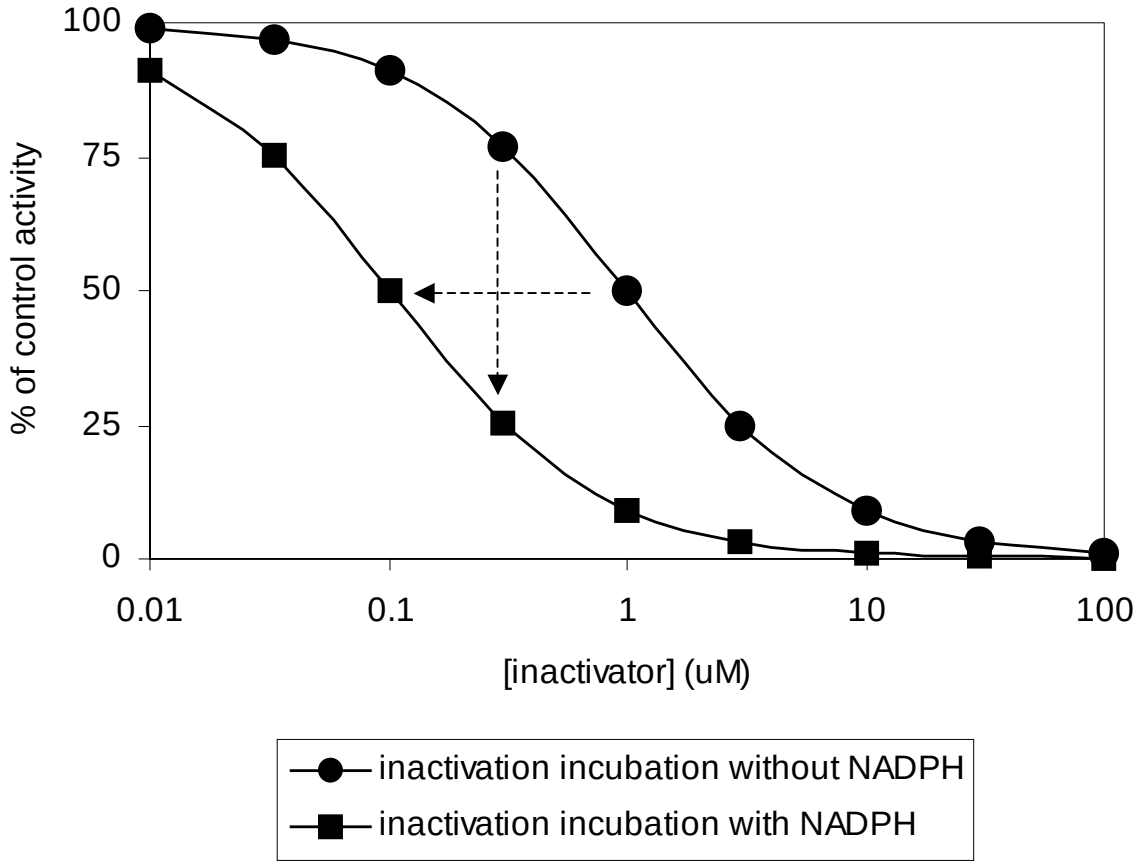

Figure 2

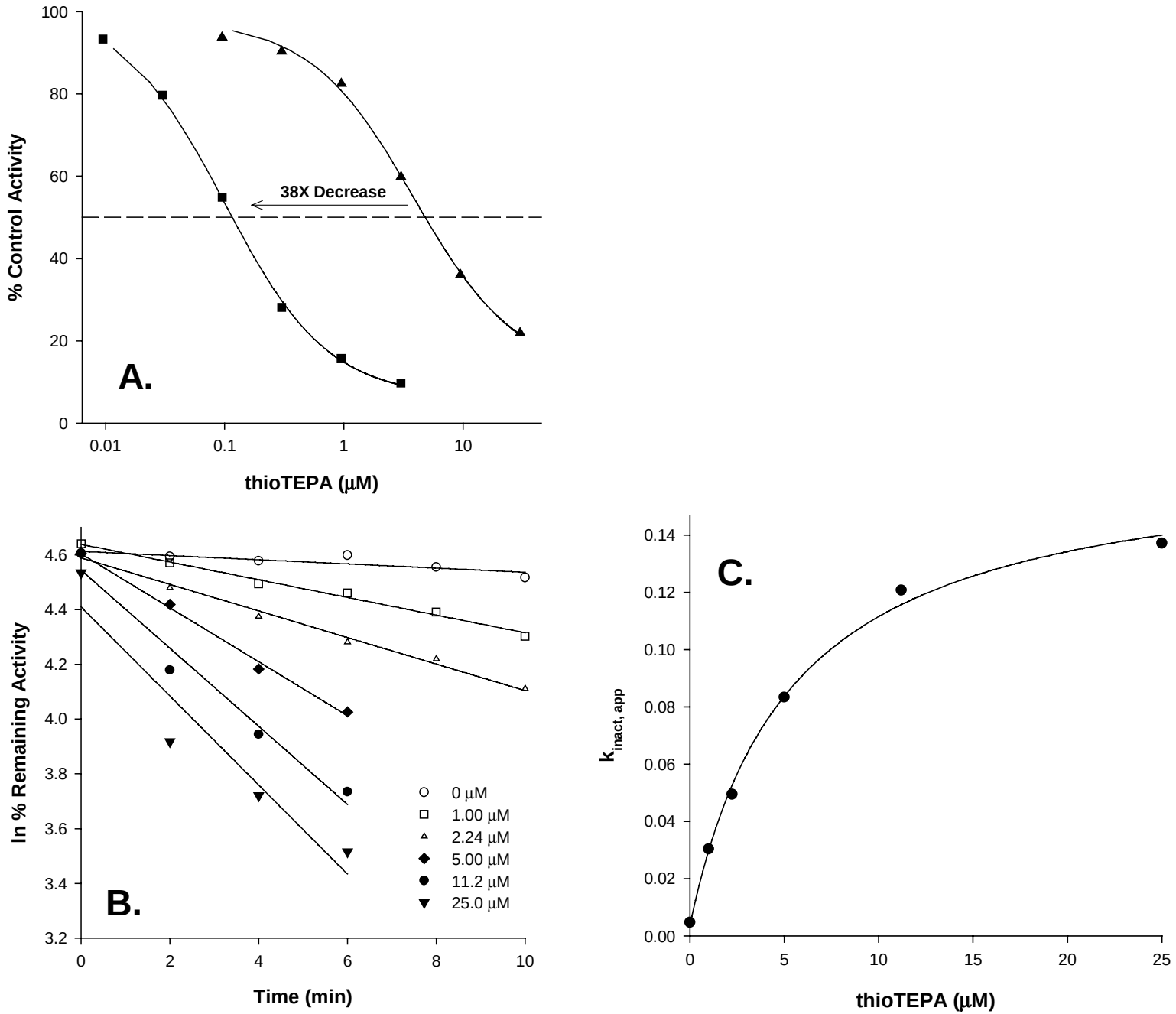

DMD Fast Forward. Published on November 8, 2006 as DOI: 10.1124/dmd.106.012633
This article has not been copyedited and formatted. The final version may differ from this version.

Figure 3

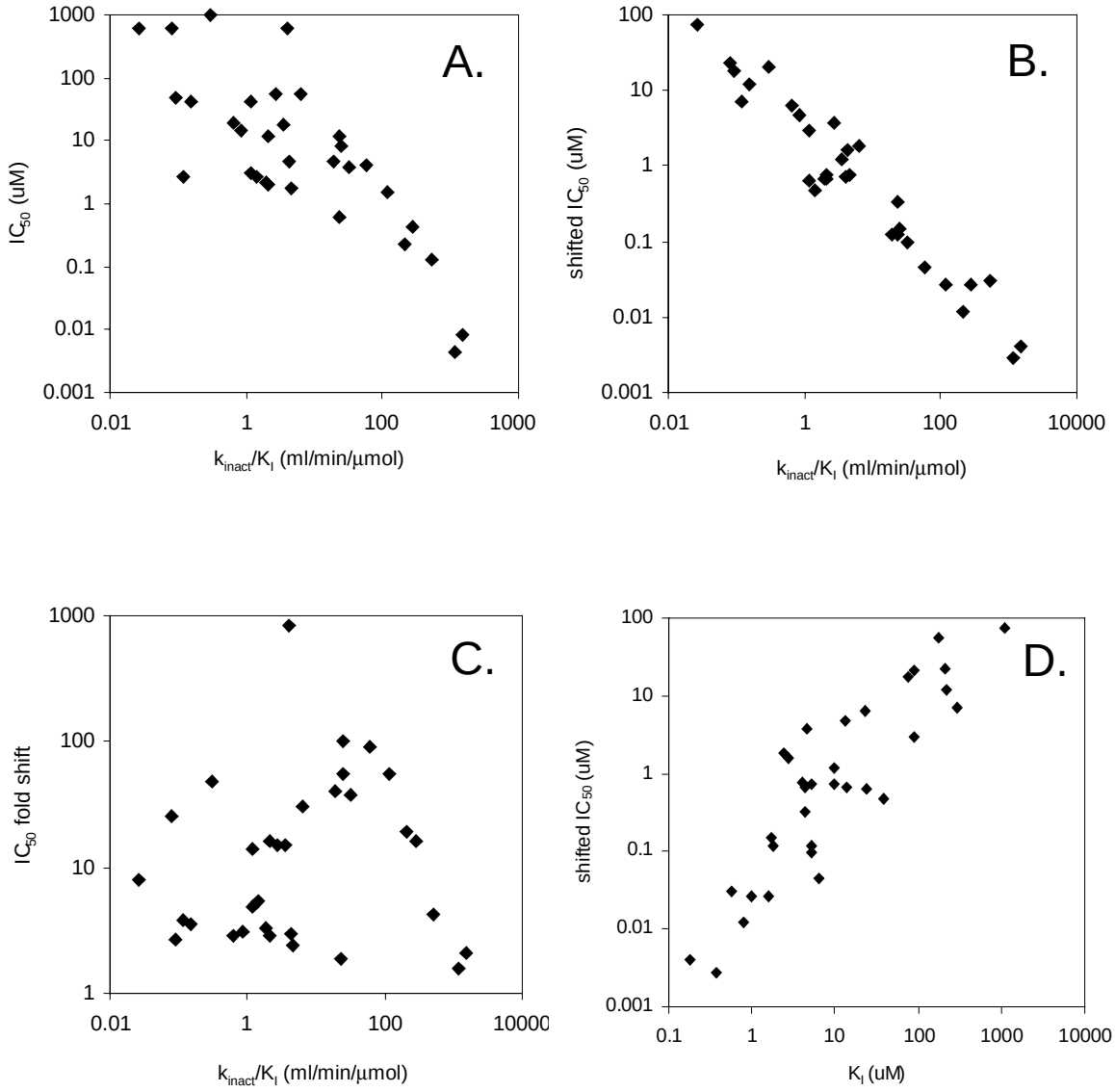

Figure 4

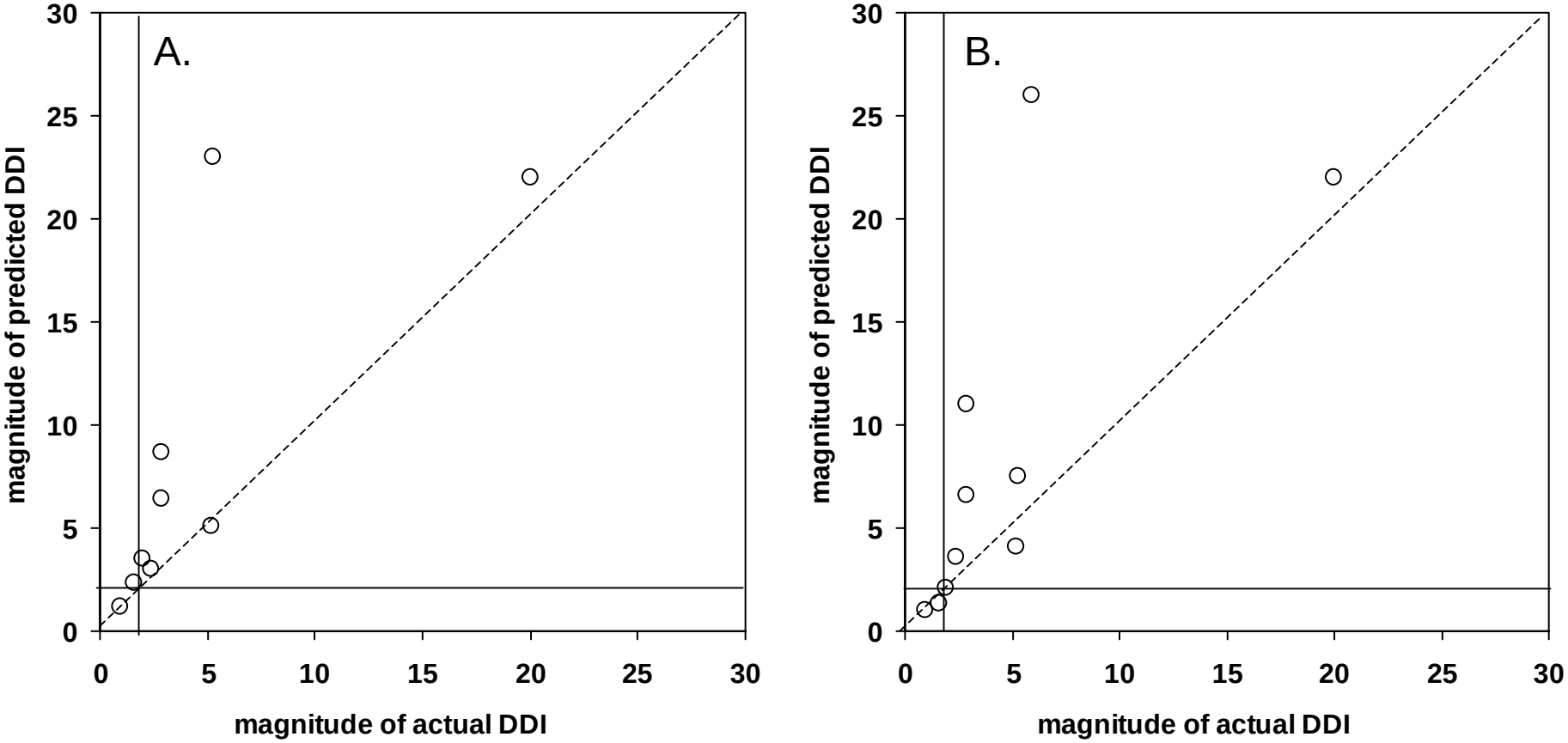

Figure 5

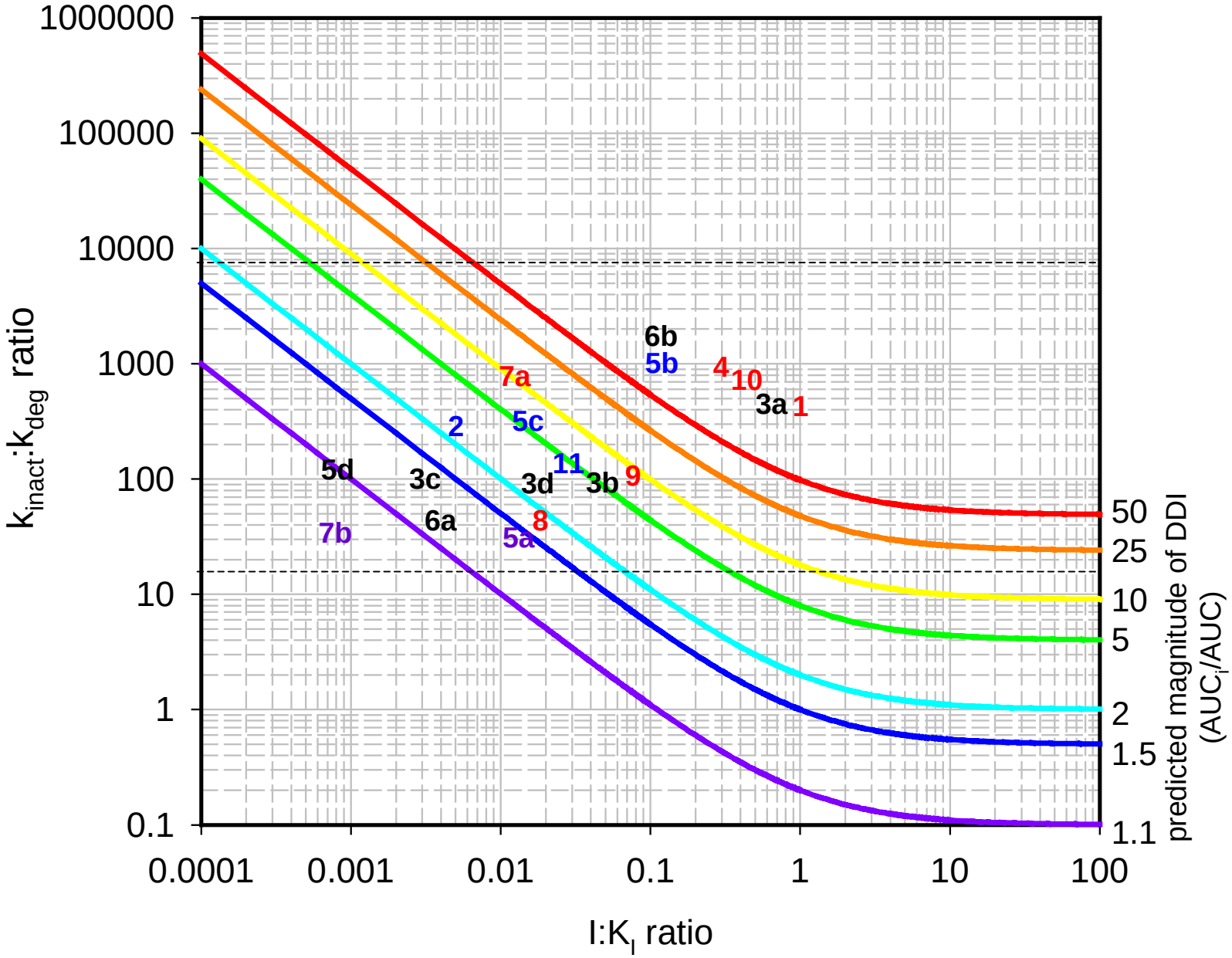

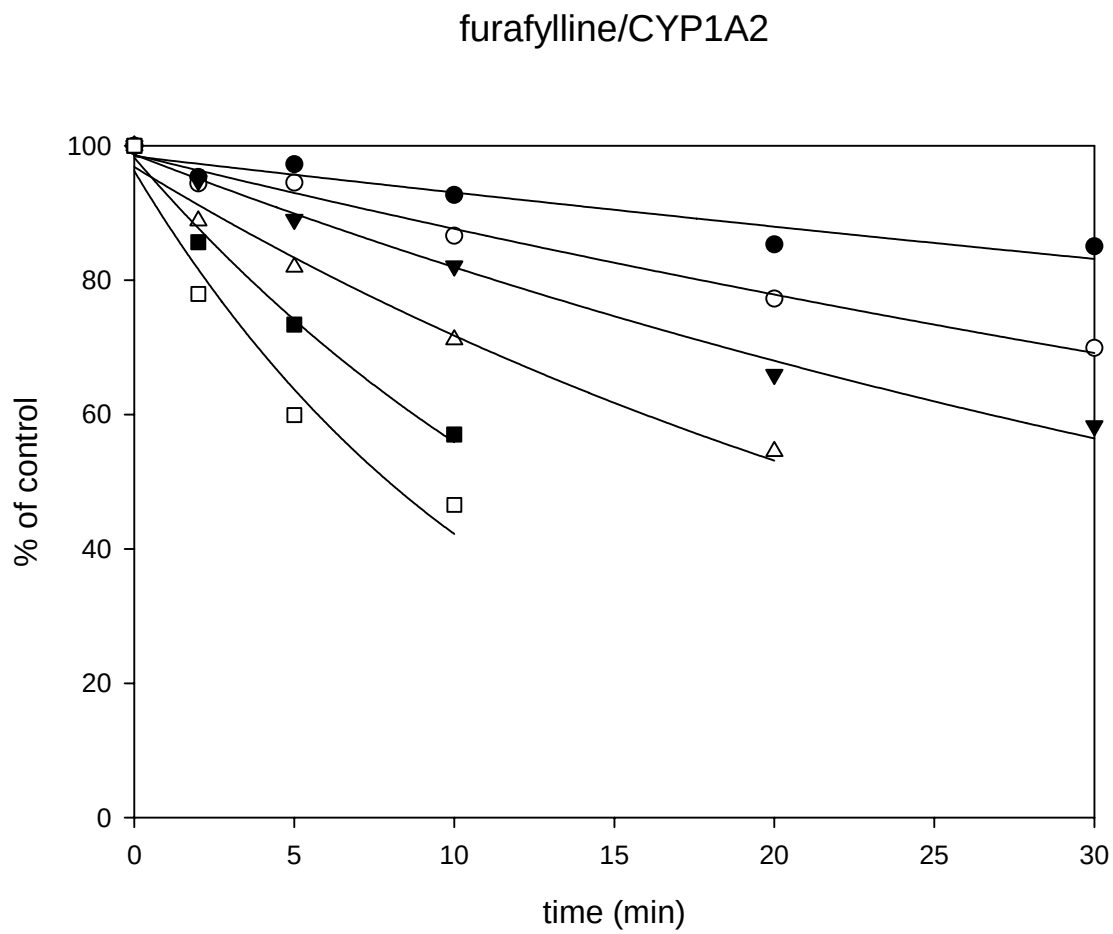
furafylline/CYP1A2
100
80
60
40
20
0
% of control
0
5
10
15
20
25
30
time (min)

CYP1A2 K_I/k_{inact}

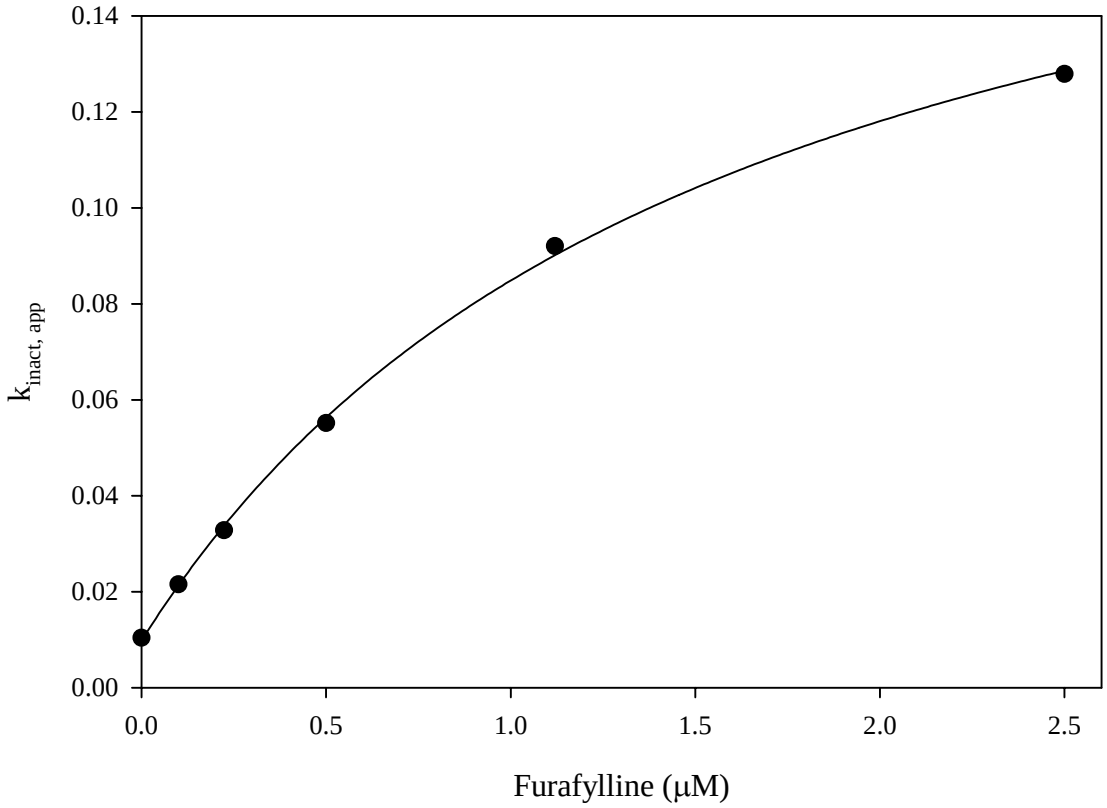

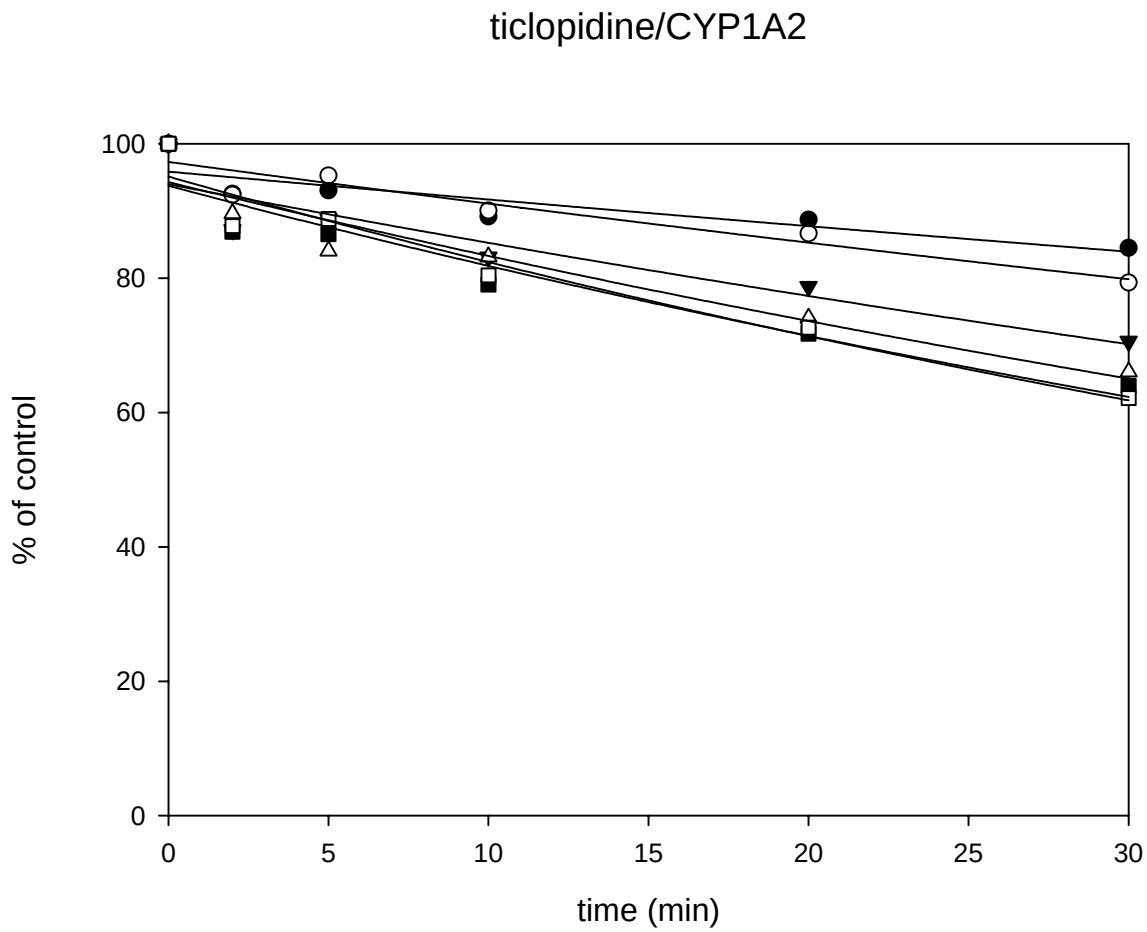
ticlopidine/CYP1A2
% of control
100
80
60
40
20
0
0
5
10
15
20
25
30
time (min)

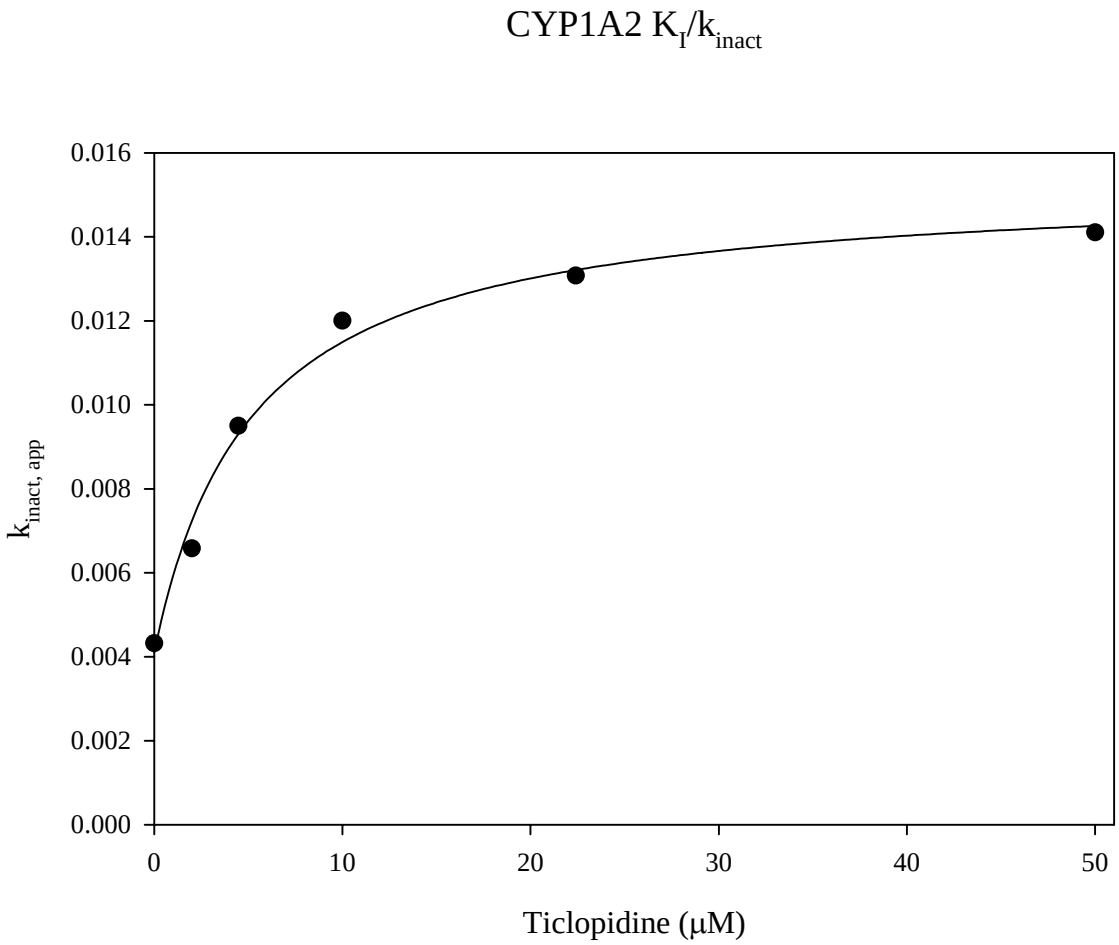
CYP1A2 K_I/k_{inact}
0.016
0.014
0.012
0.010
0.008
0.006
0.004
0.002
0.000
$k_{inact, app}$
0
10
20
30
40
50
Ticlopidine (μM)

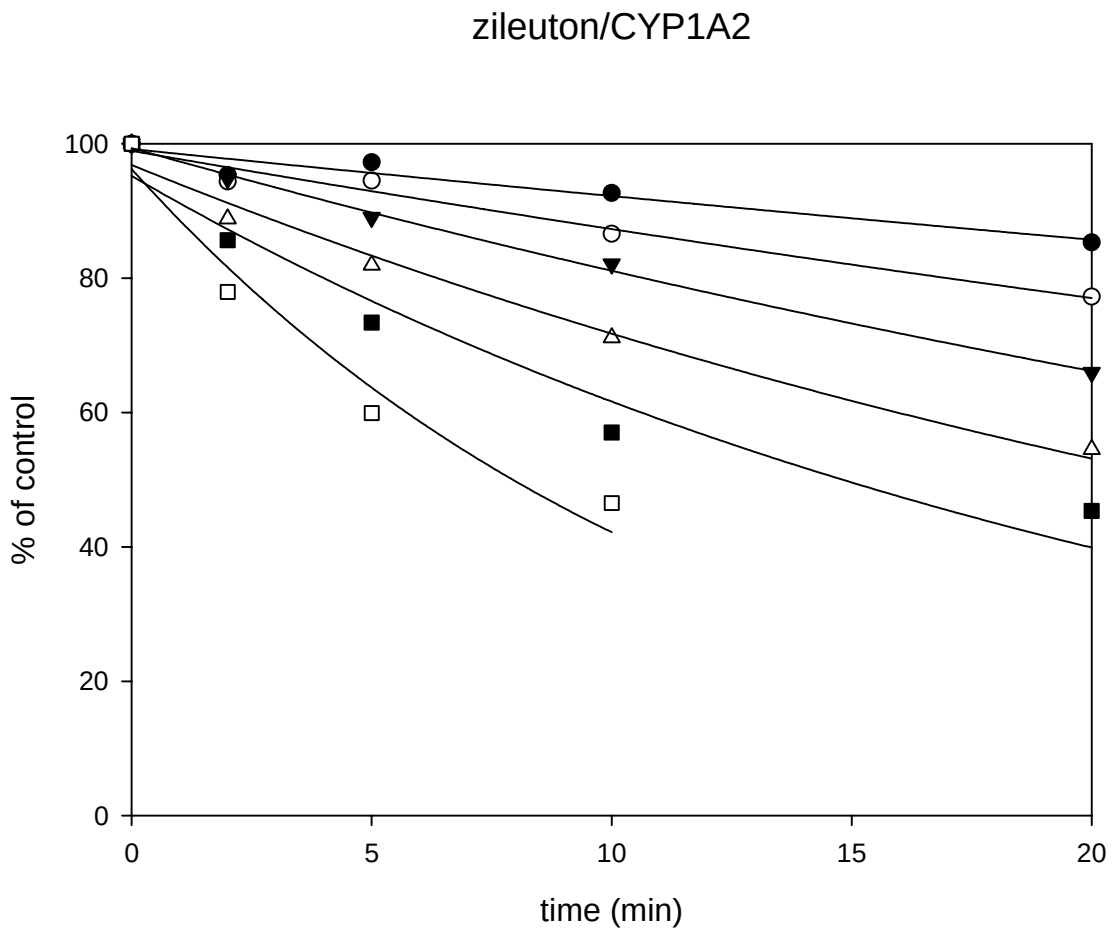
zileuton/CYP1A2
100
80
60
40
20
0
% of control
0
5
10
15
20
time (min)

CYP1A2 K_I/k_{inact}

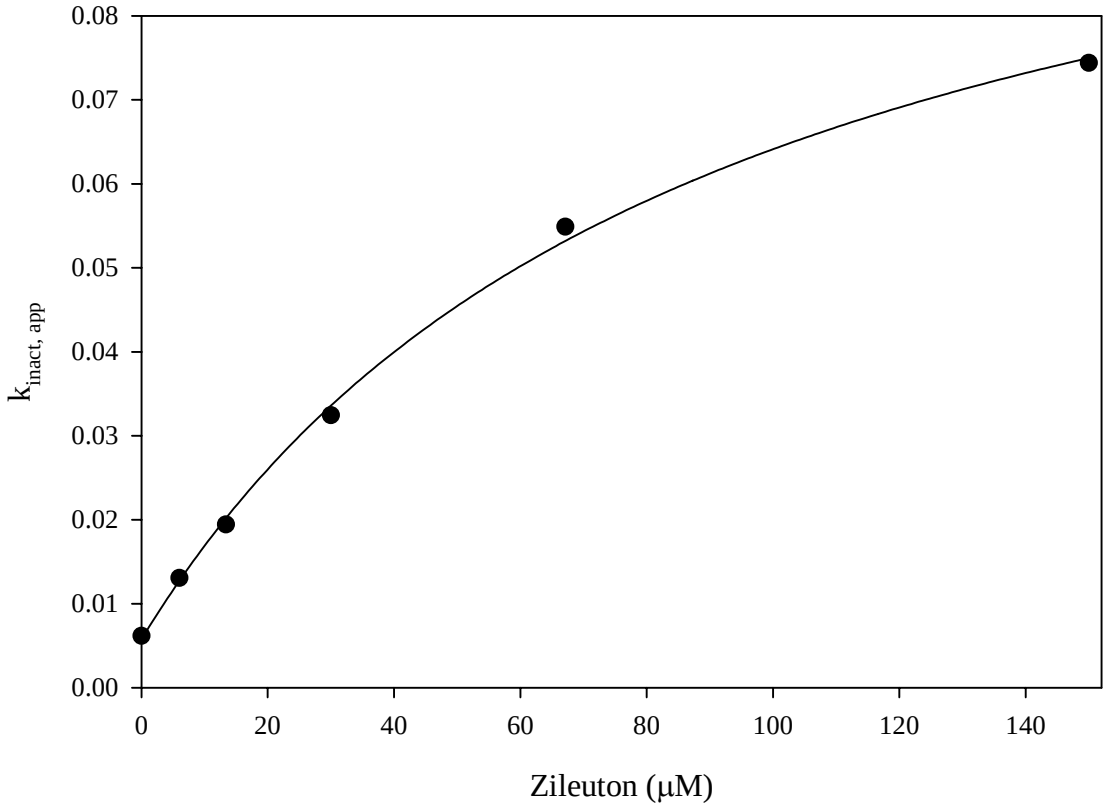

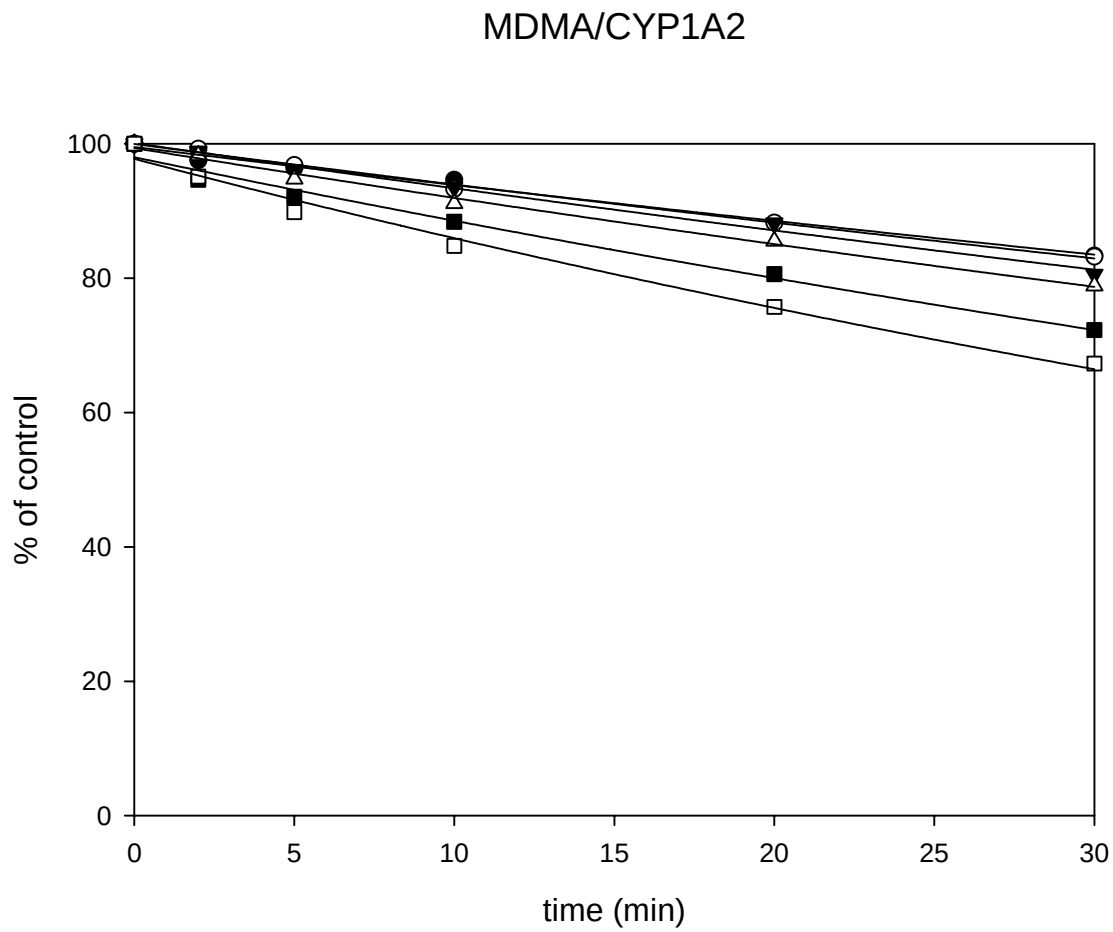
MDMA/CYP1A2
100
80
60
40
20
0
% of control
0
5
10
15
20
25
30
time (min)

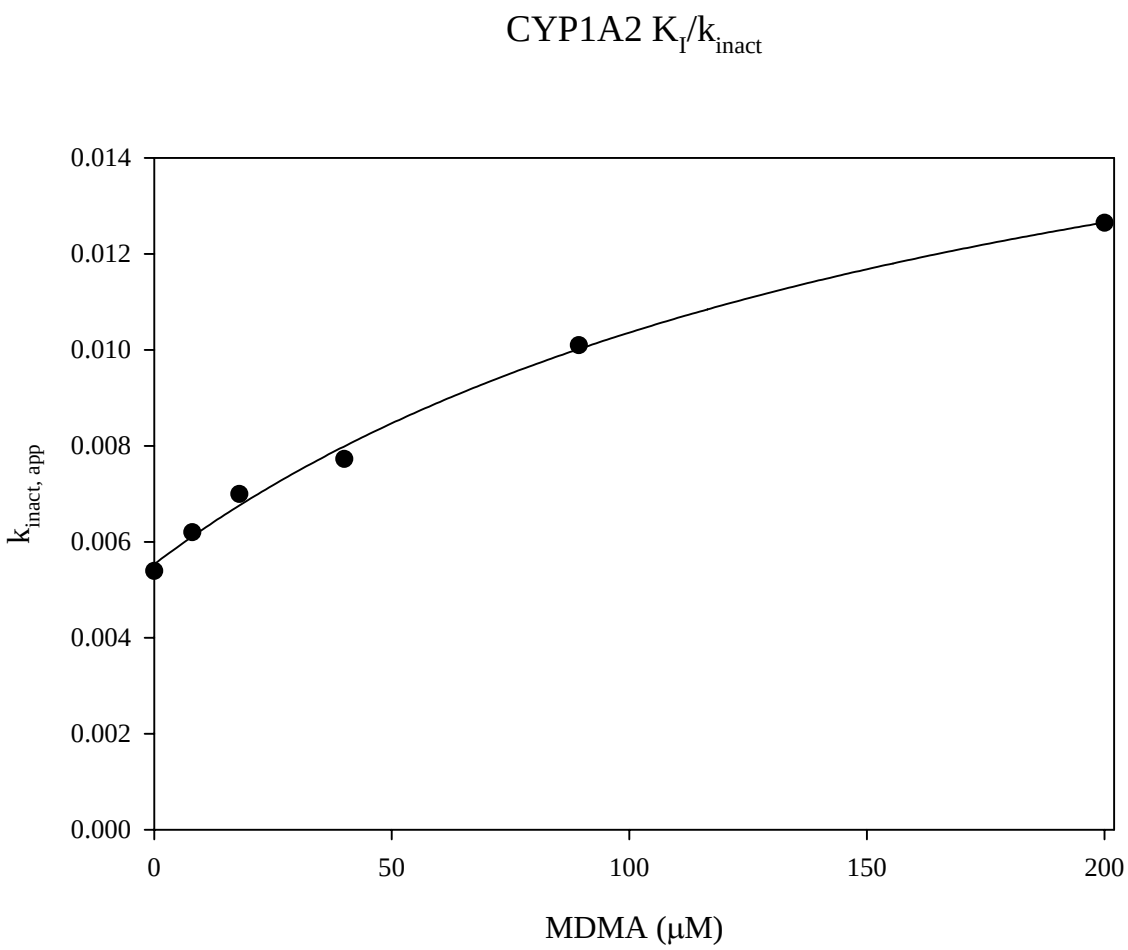
CYP1A2 K_I/k_{inact}
0.014
0.012
0.010
0.008
0.006
0.004
0.002
0.000
$k_{inact, app}$
0
50
100
150
200
MDMA (μM)

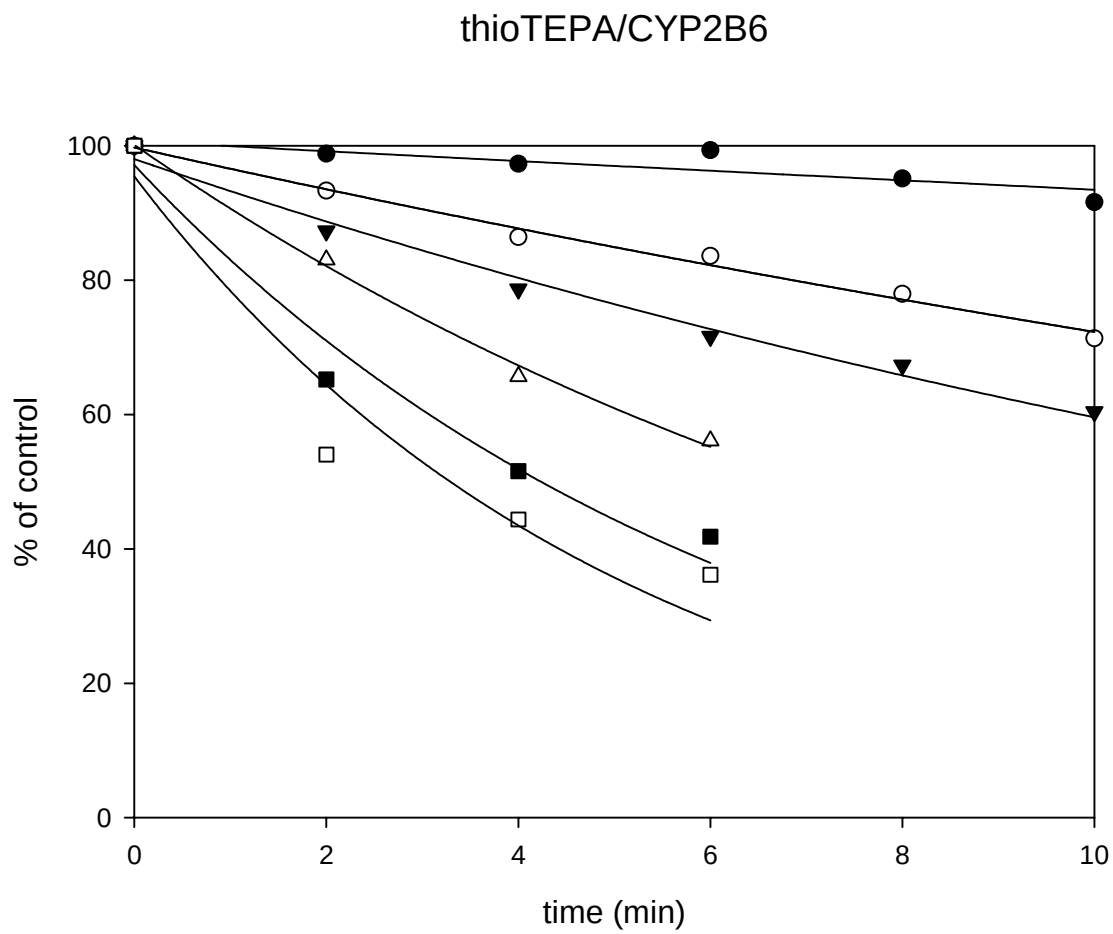
thioTEPA/CYP2B6
100
80
60
40
20
0
% of control
0
2
4
6
8
10
time (min)

CYP2B6 K_I/k_{inact}

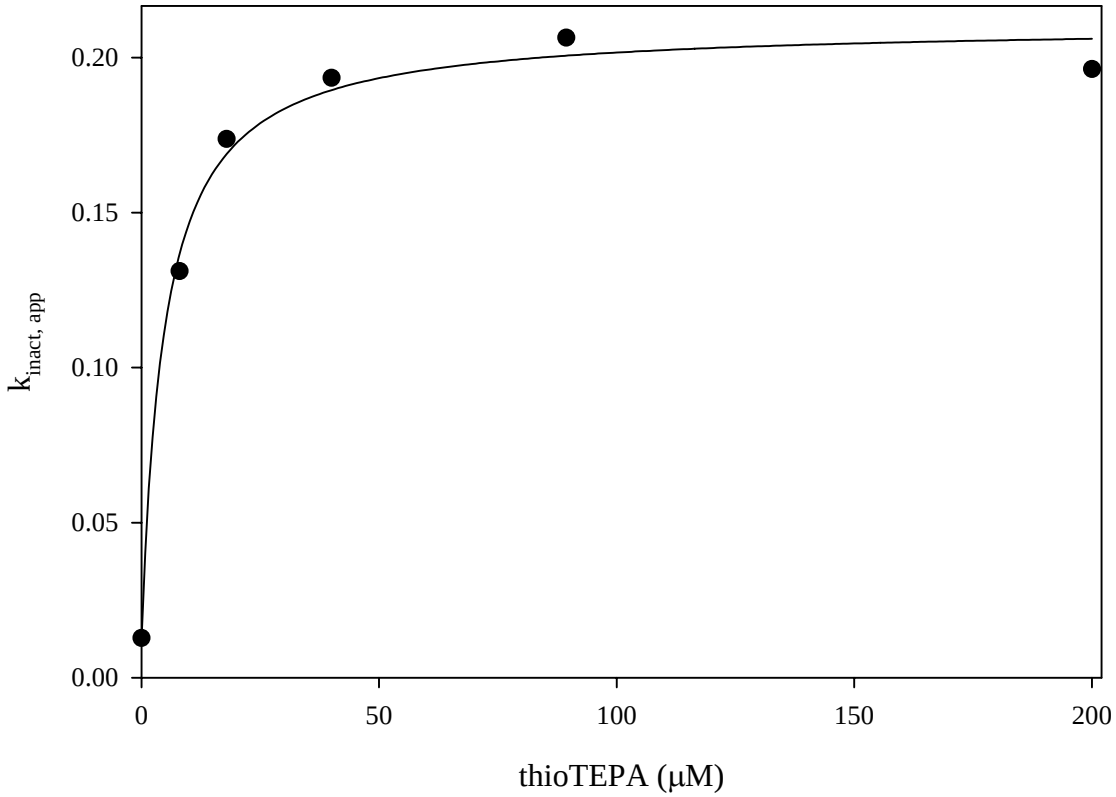

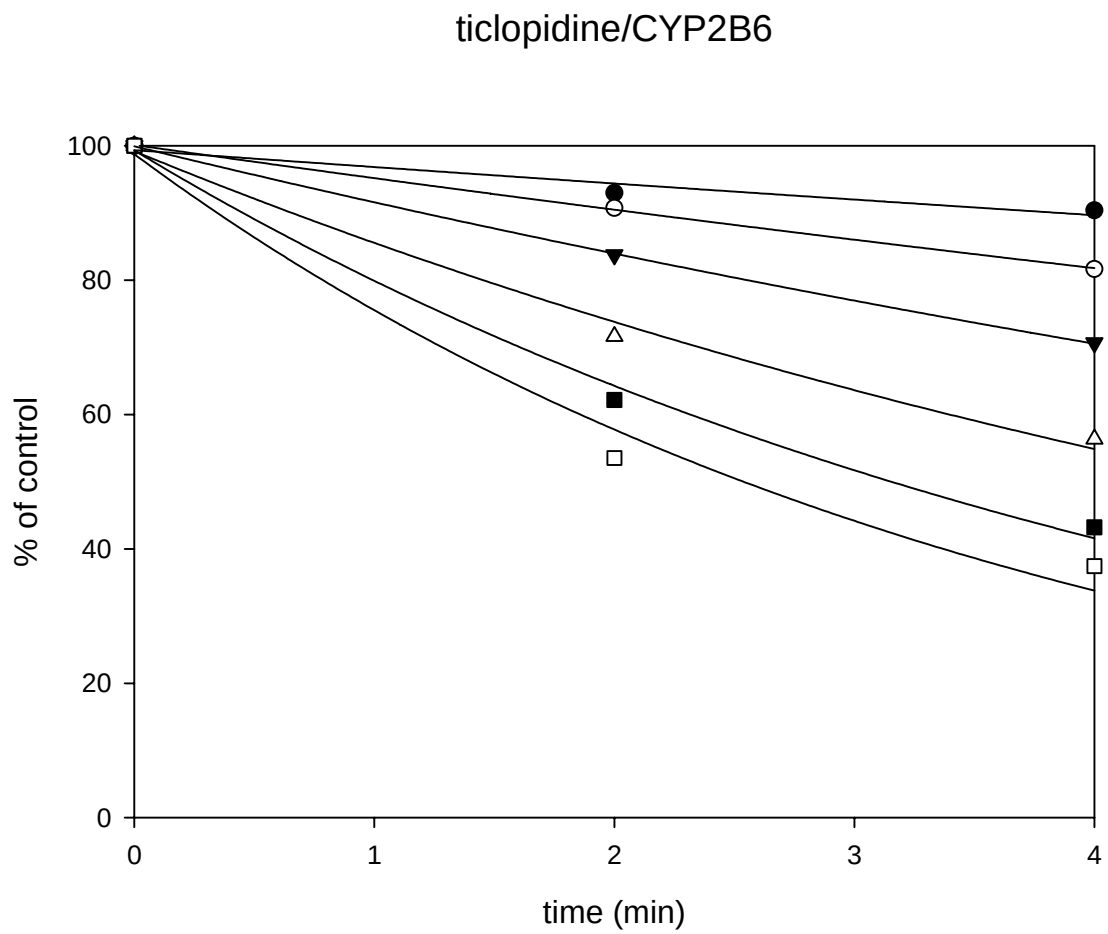
ticlopidine/CYP2B6
100
80
60
40
20
0
% of control
0
1
2
3
4
time (min)

CYP2B6 K_I/k_{inact}

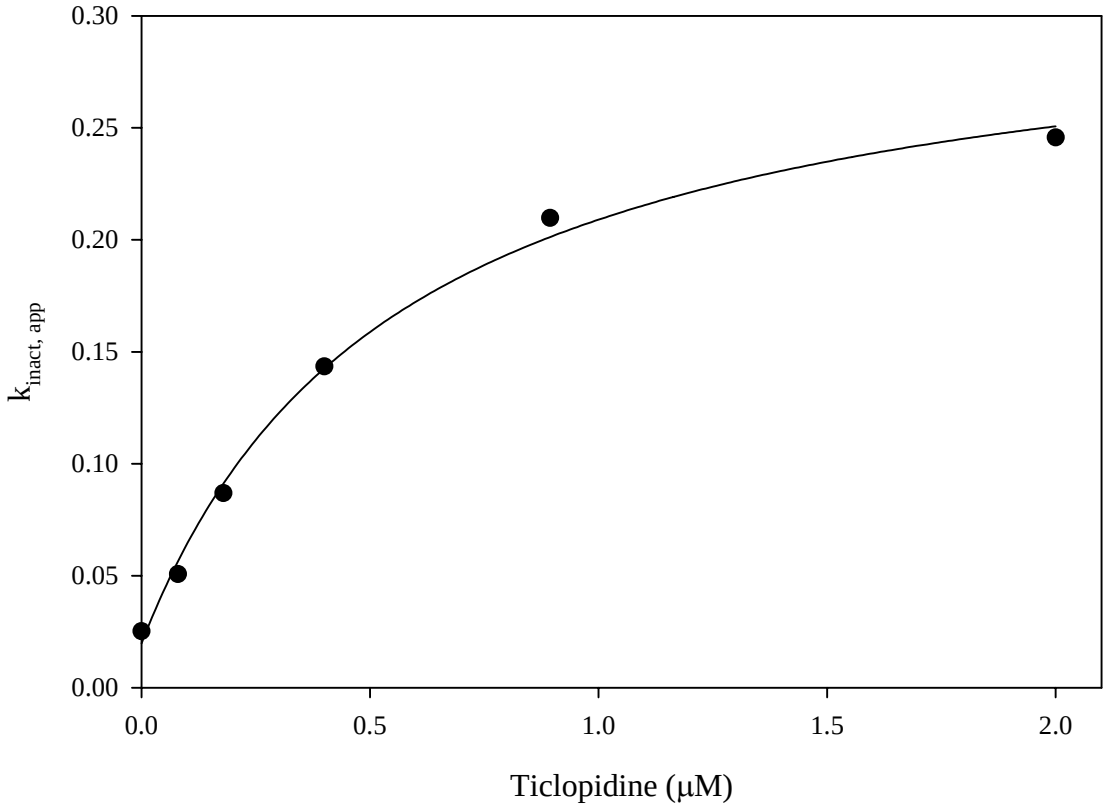

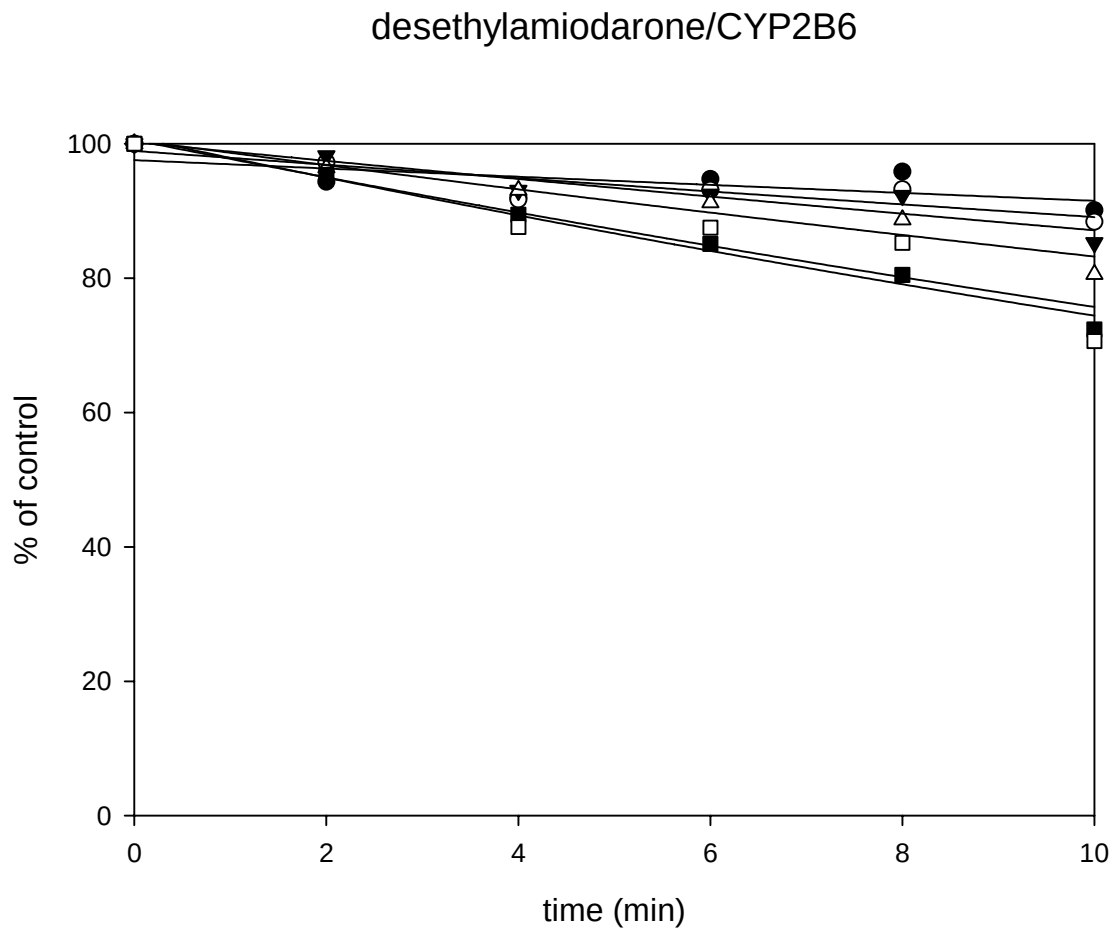
desethylamiodarone/CYP2B6
% of control
100
80
60
40
20
0
0
2
4
6
8
10
time (min)

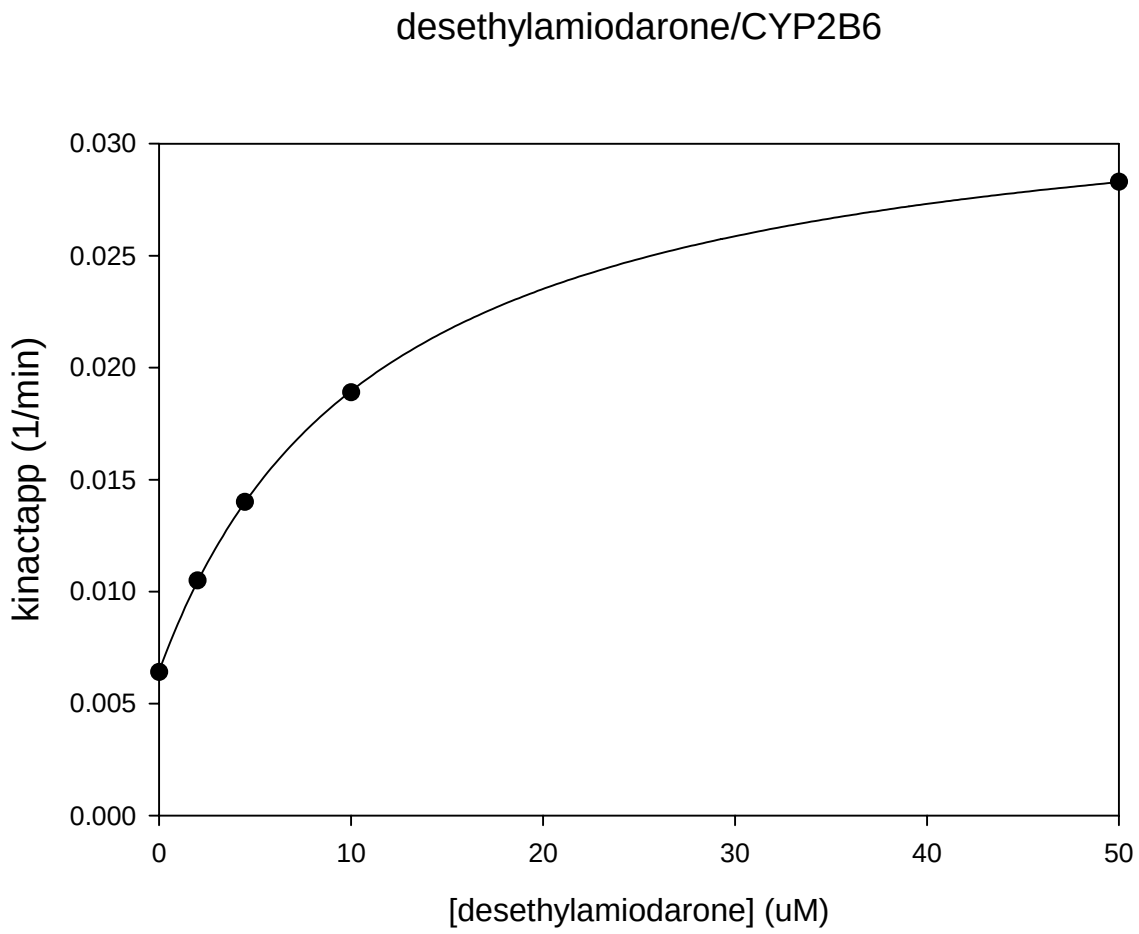
desethylamiodarone/CYP2B6
kinactapp (1/min)
0.030
0.025
0.020
0.015
0.010
0.005
0.000
0
10
20
30
40
50
[desethylamiodarone] (uM)

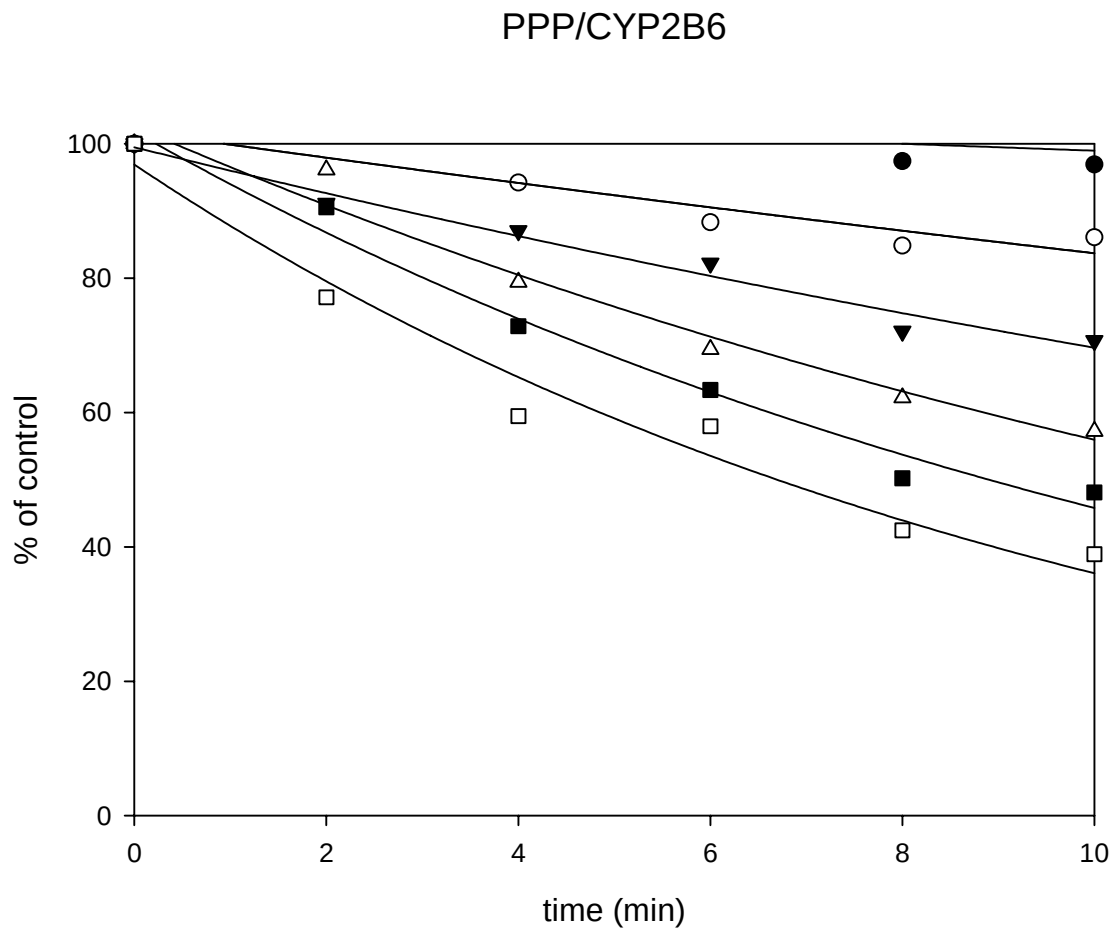
PPP/CYP2B6
% of control
100
80
60
40
20
0
0
2
4
6
8
10
time (min)

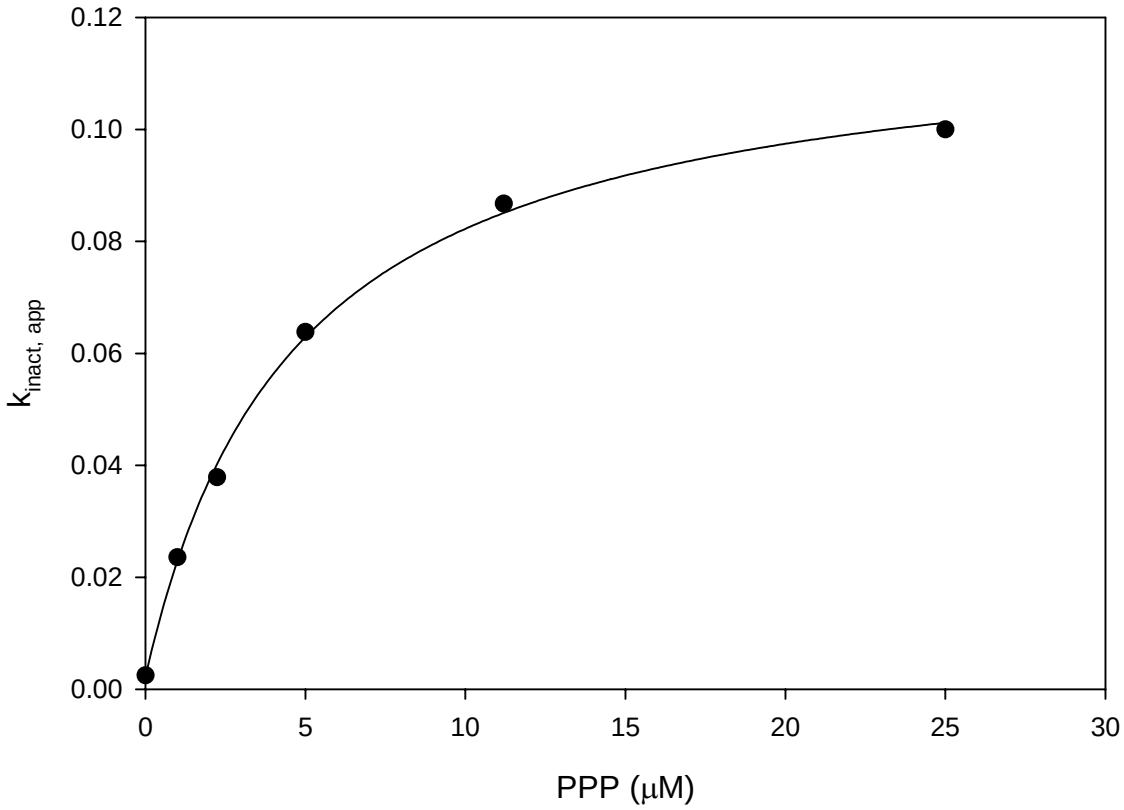
PPP/CYP2B6
0.12
0.10
0.08
0.06
0.04
0.02
0.00
$k_{inact, app}$
0
5
10
15
20
25
30
PPP (μM)

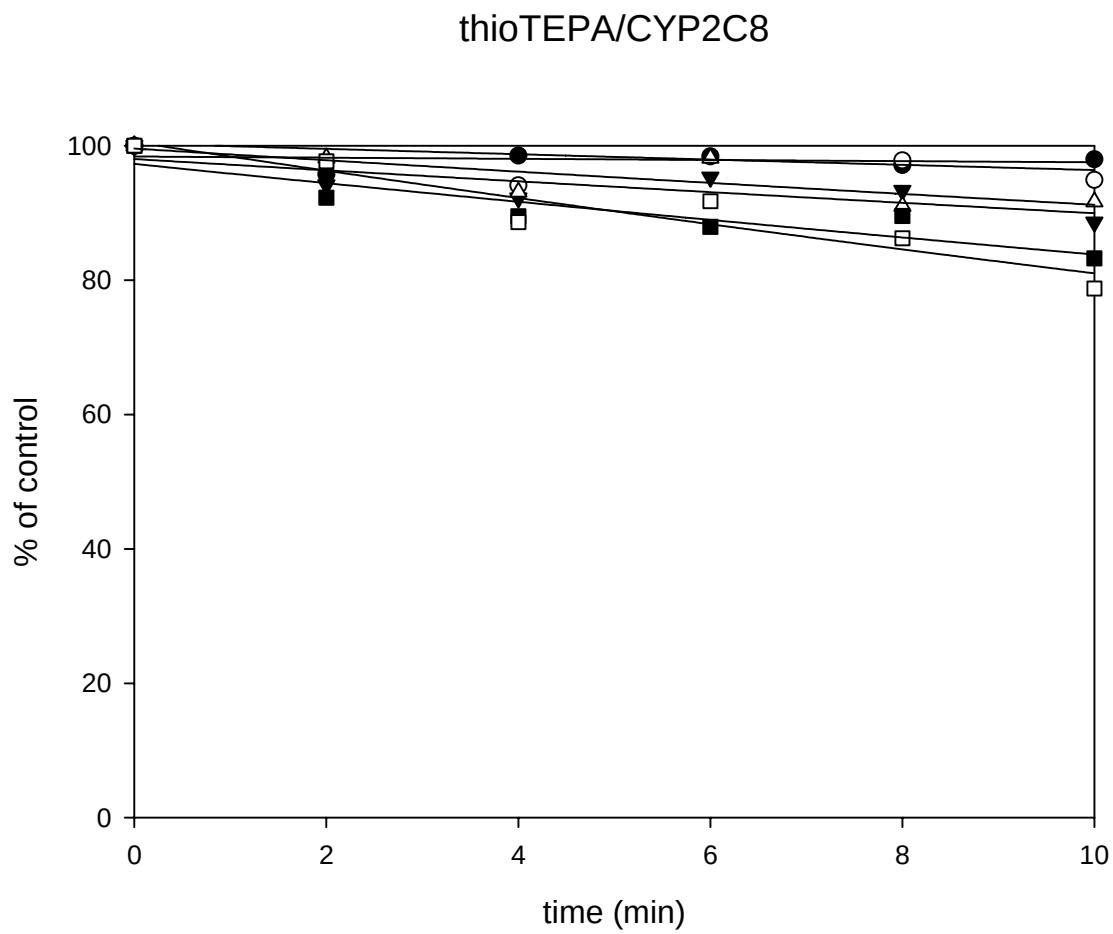
thioTEPA/CYP2C8
100
80
60
40
20
0
% of control
0
2
4
6
8
10
time (min)

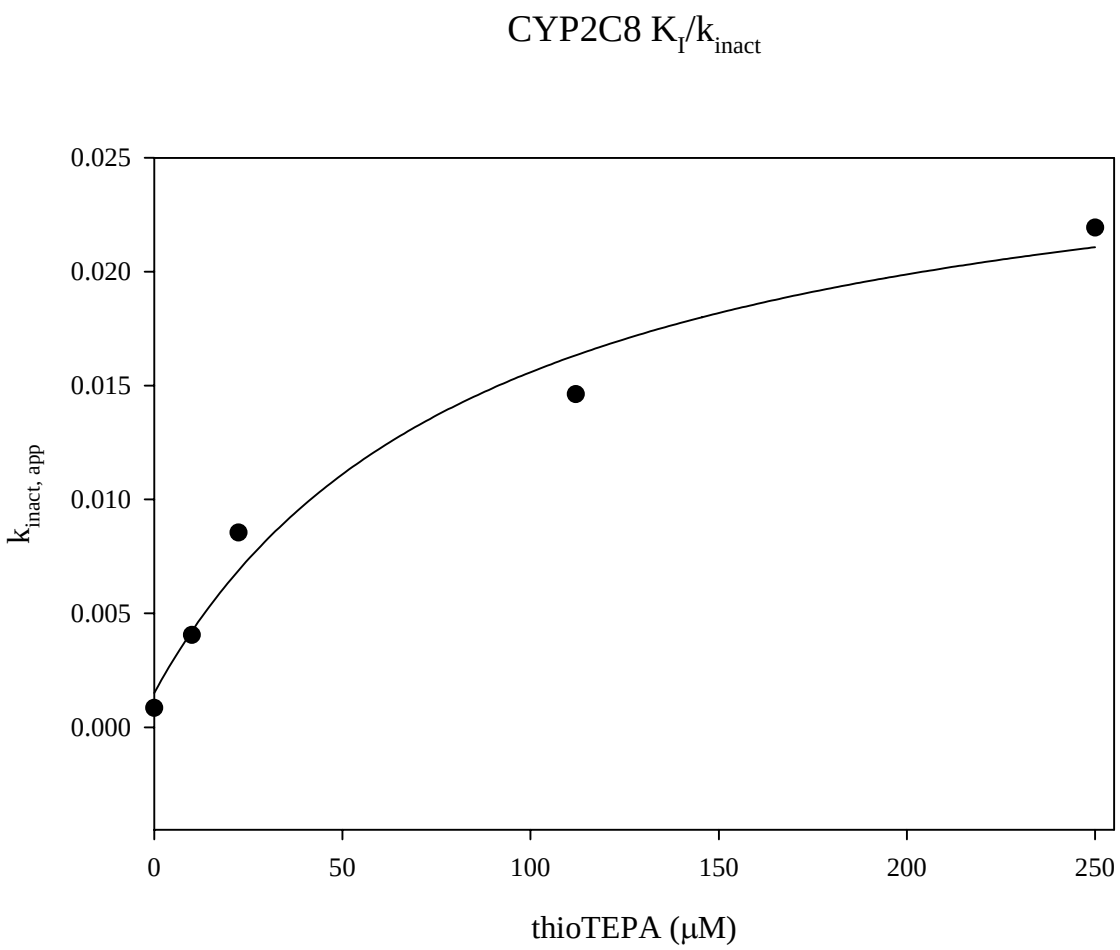
CYP2C8 K_I/k_{inact}
0.025
0.020
0.015
0.010
0.005
0.000
$k_{inact, app}$
0
50
100
150
200
250
thioTEPA (μM)

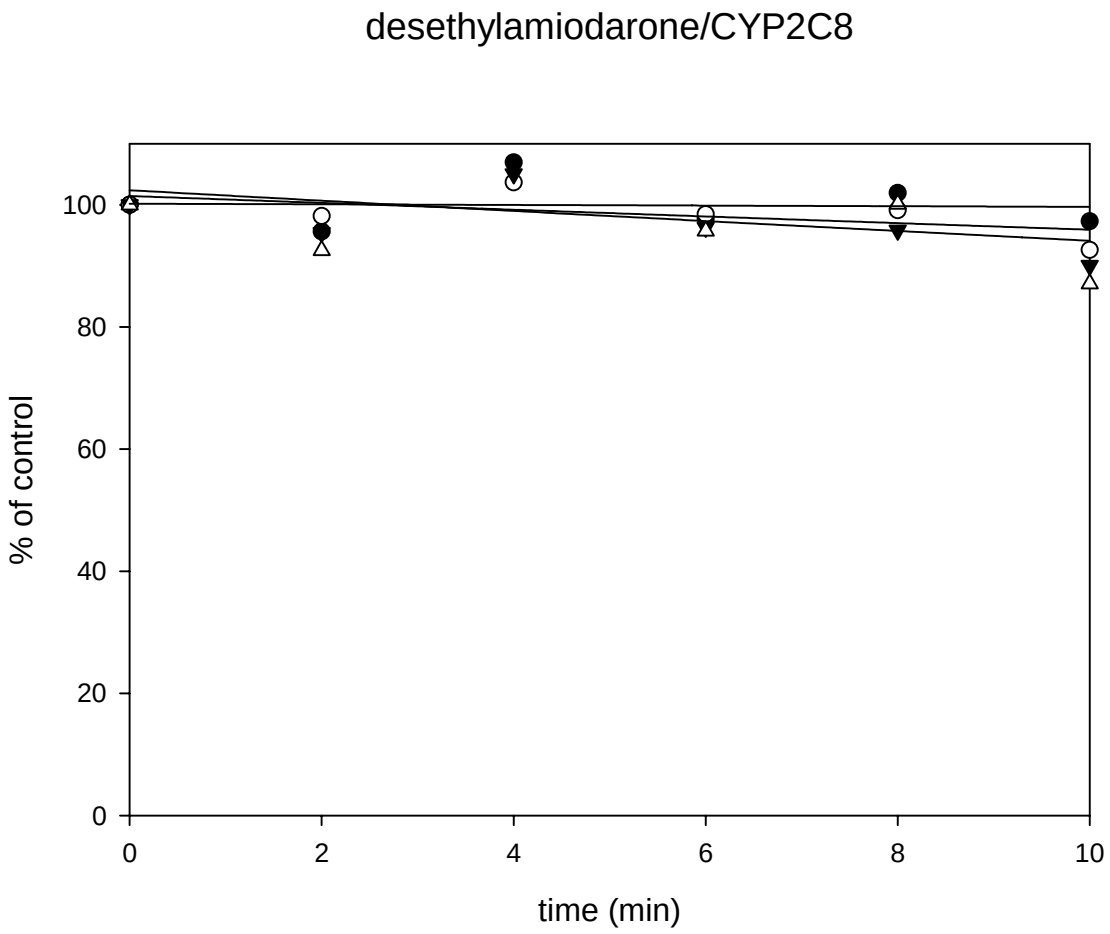
desethylamiodarone/CYP2C8
% of control
100
80
60
40
20
0
0
2
4
6
8
10
time (min)

CYP2C8 K_I/k_{inact}

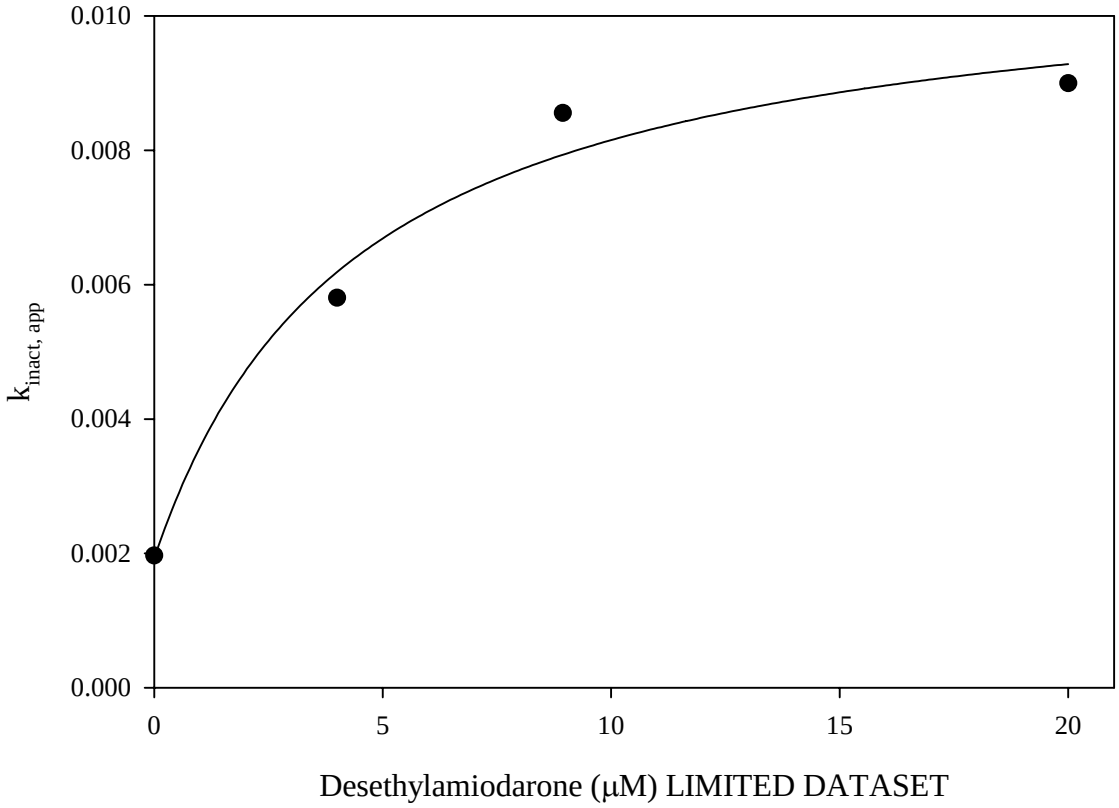

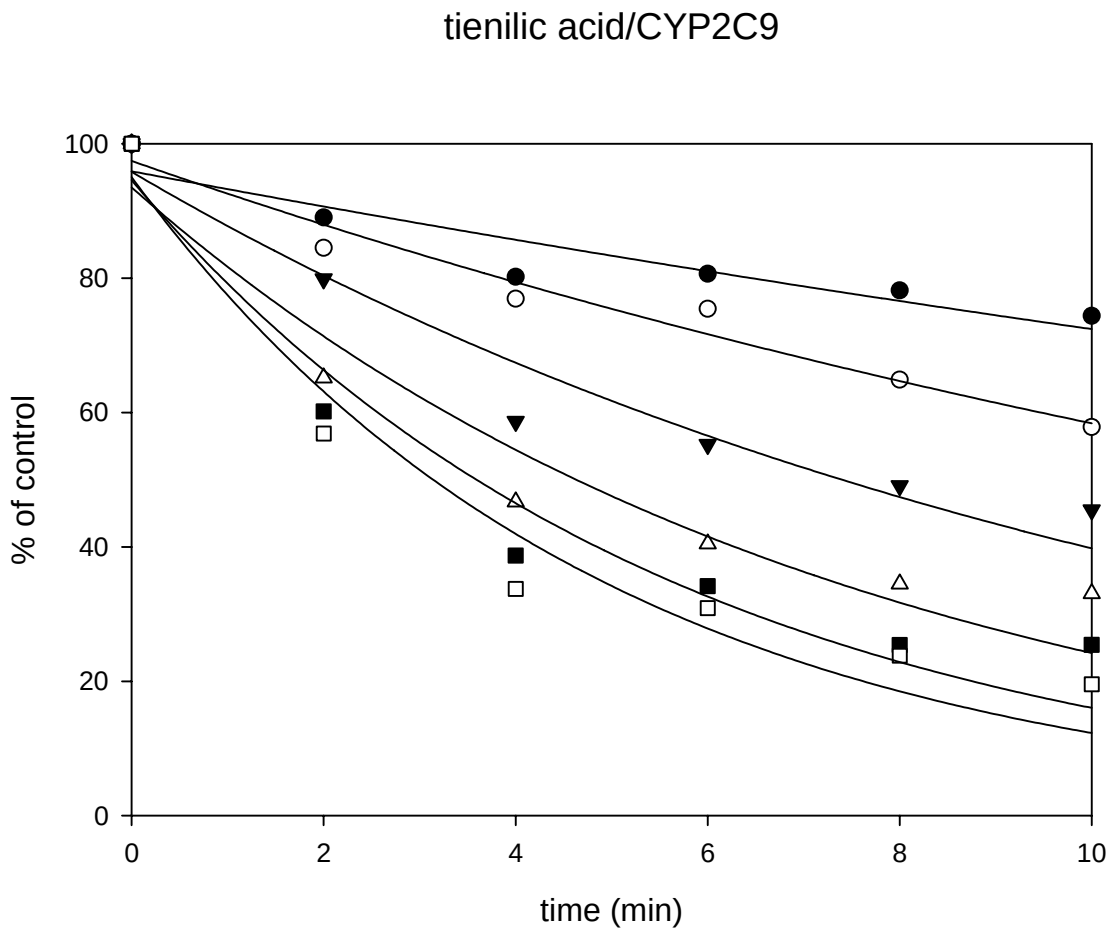
tienilic acid/CYP2C9
% of control
time (min)
0
20
40
60
80
100
0
2
4
6
8
10

CYP2C9 K_I/k_{inact}

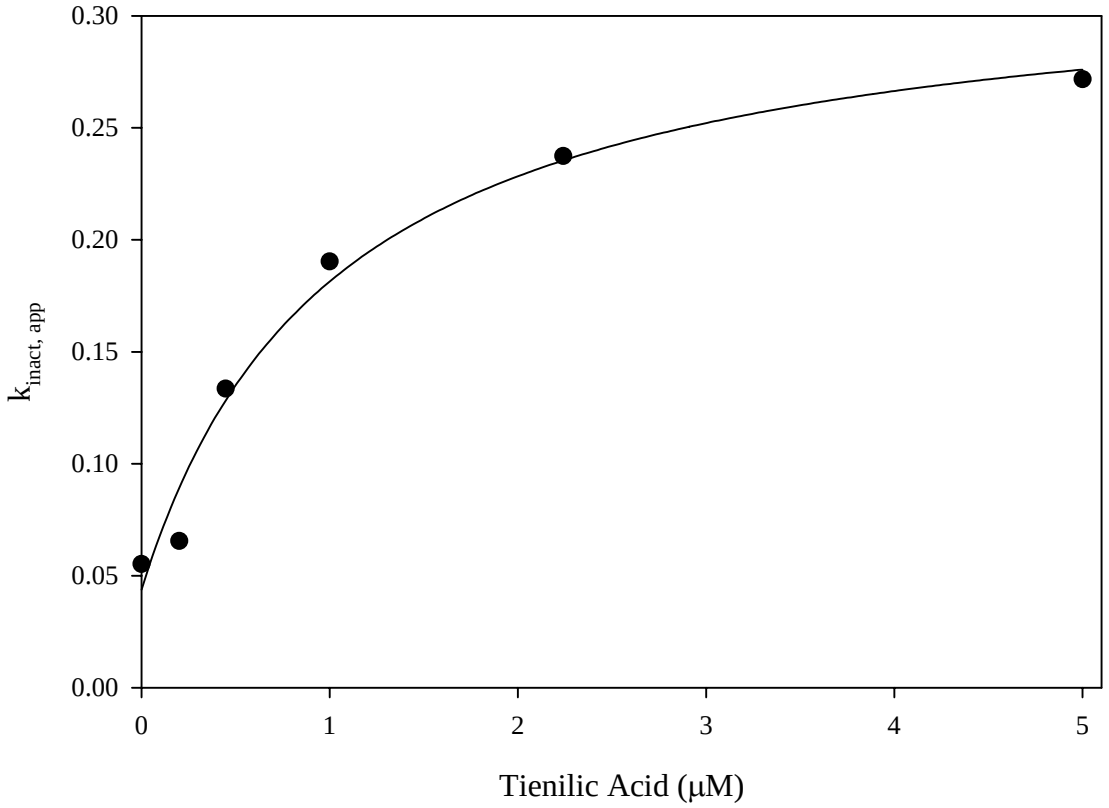

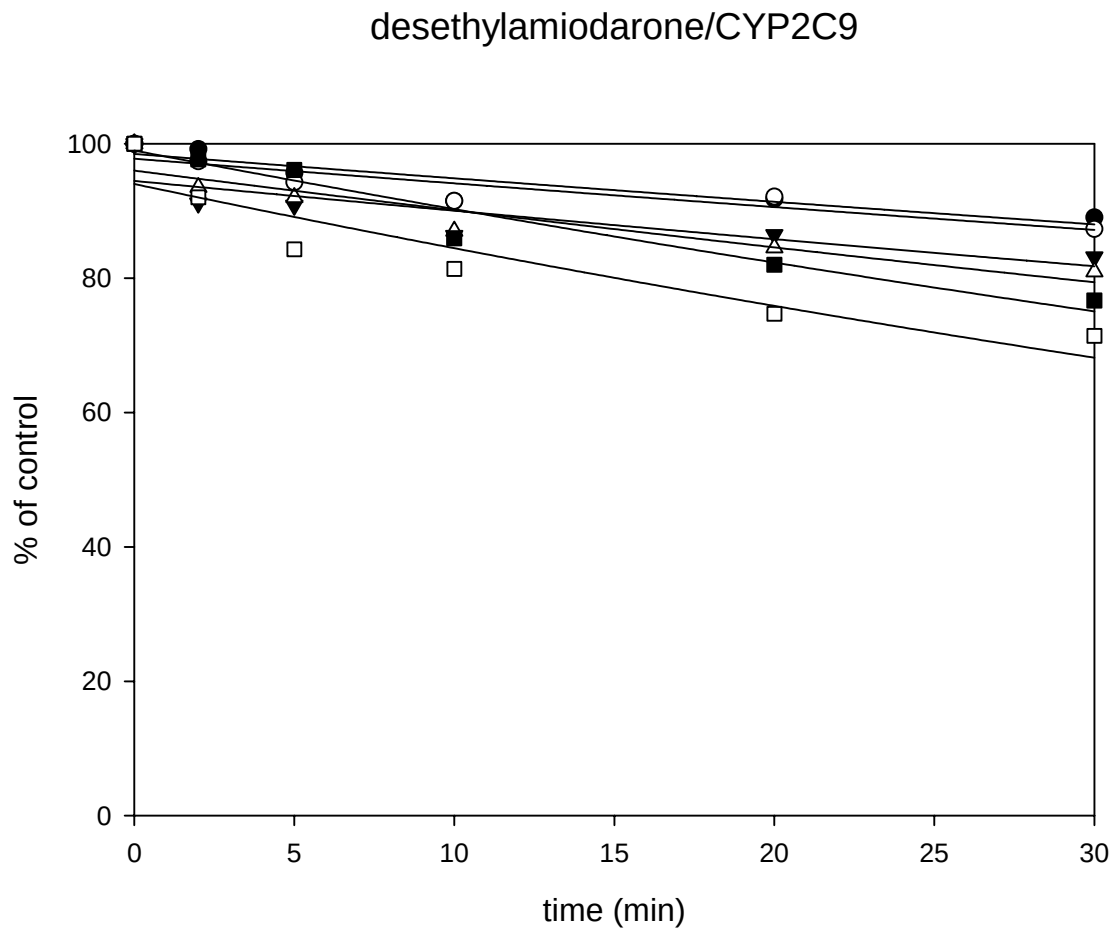
desethylamiodarone/CYP2C9
% of control
time (min)
100
80
60
40
20
0
0
5
10
15
20
25
30

CYP2C9 K_I/k_{inact}

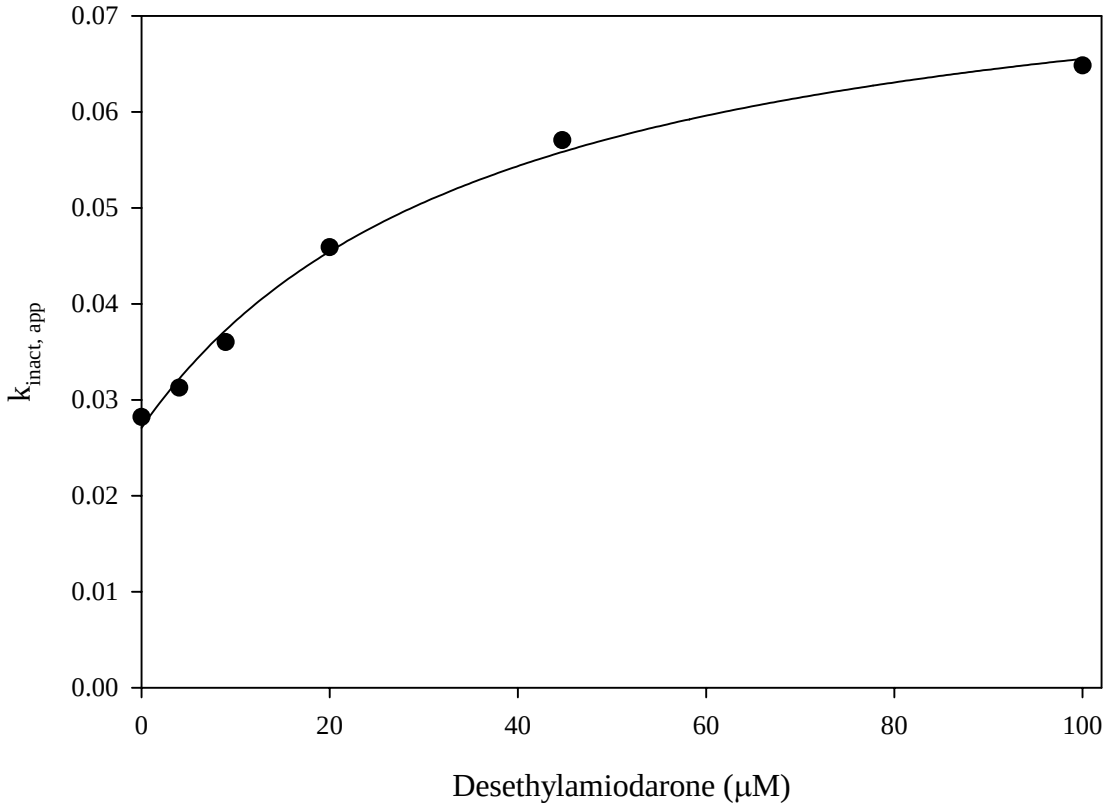

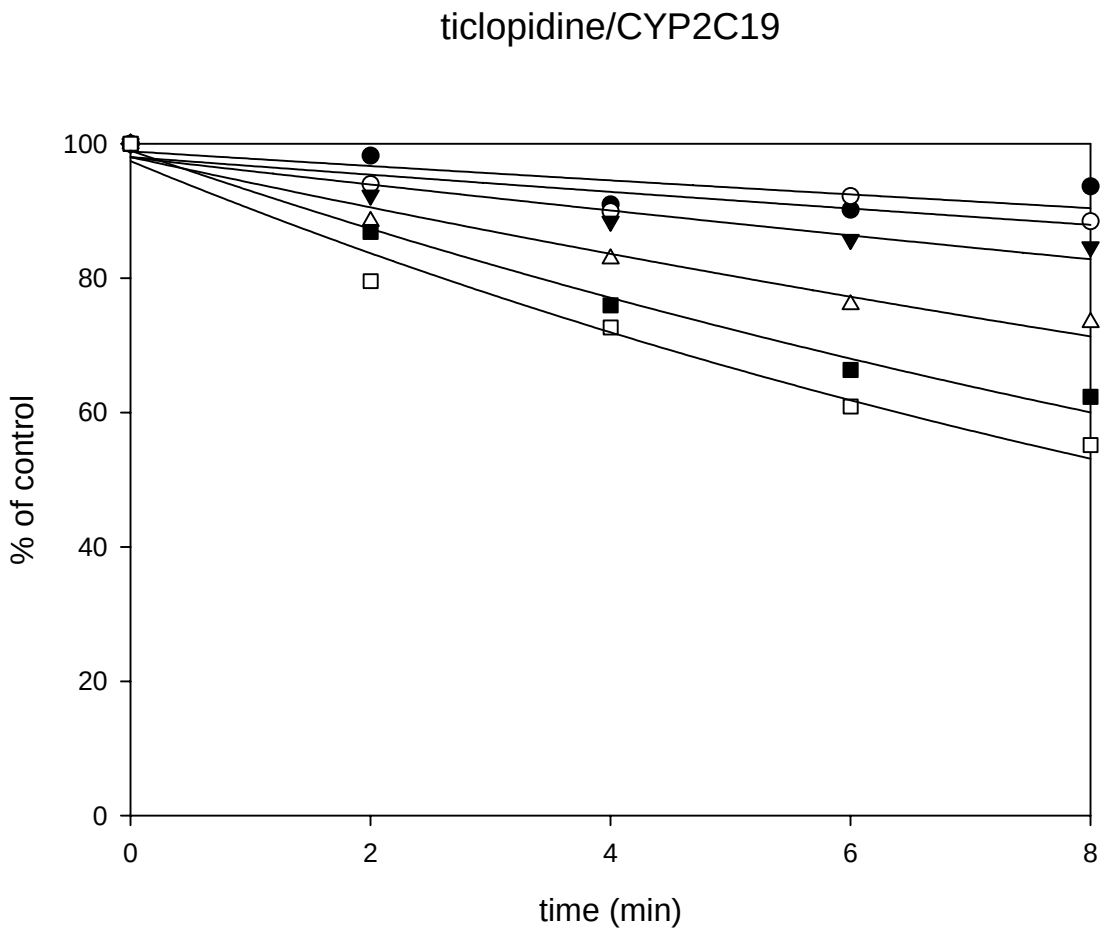
ticlopidine/CYP2C19
100
80
60
40
20
0
% of control
0
2
4
6
8
time (min)

CYP2C19 K_I/k_{inact}

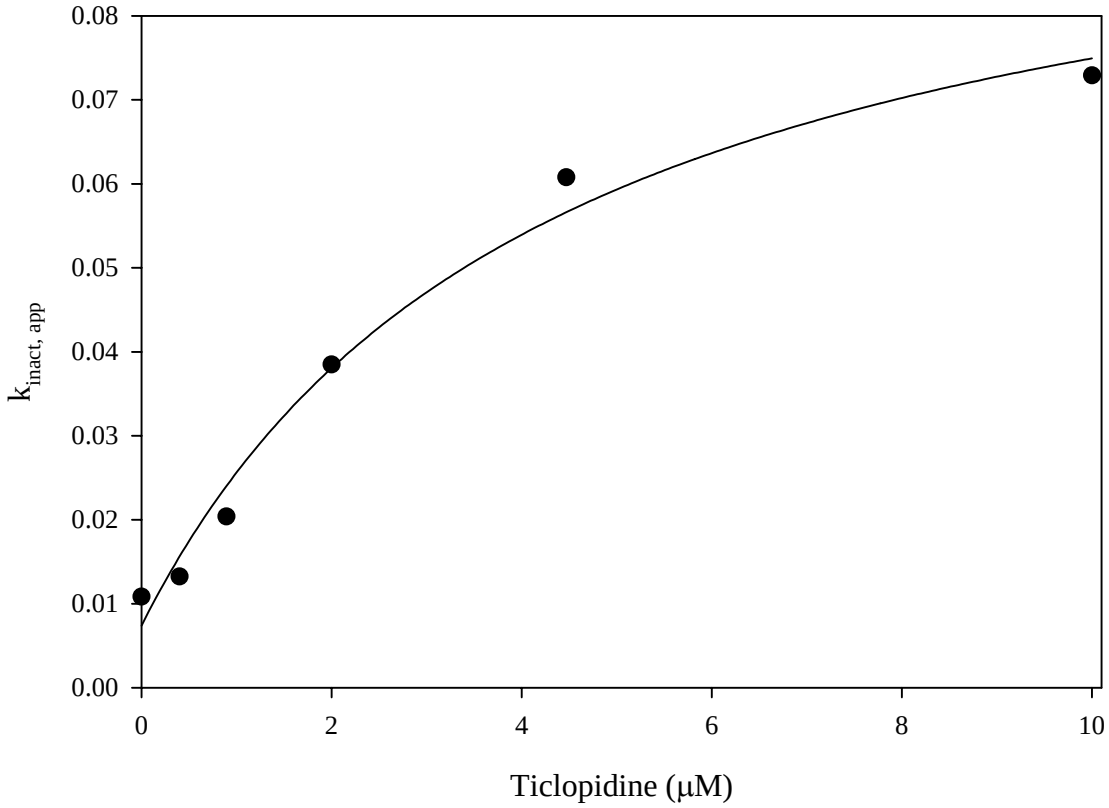

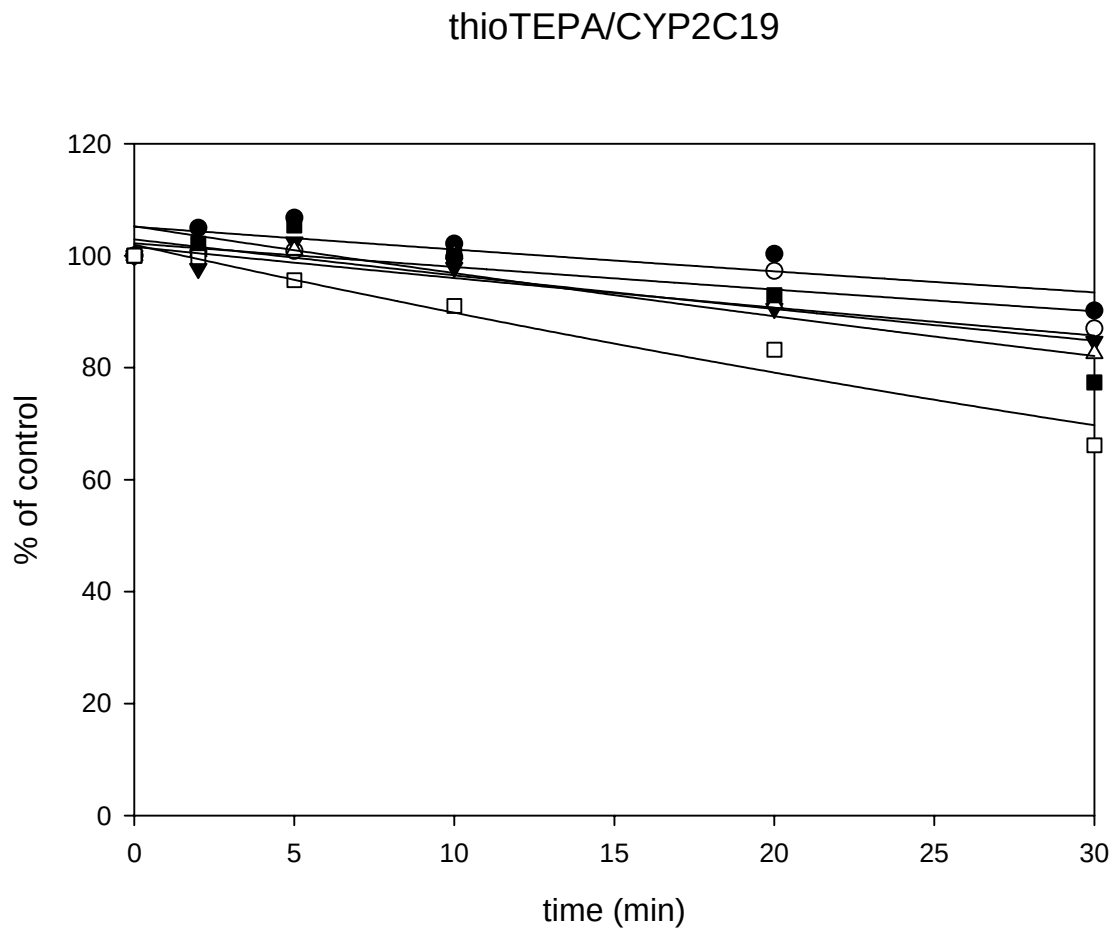
thioTEPA/CYP2C19
120
100
80
60
40
20
0
% of control
0
5
10
15
20
25
30
time (min)

CYP2C19 K_I/k_{inact}

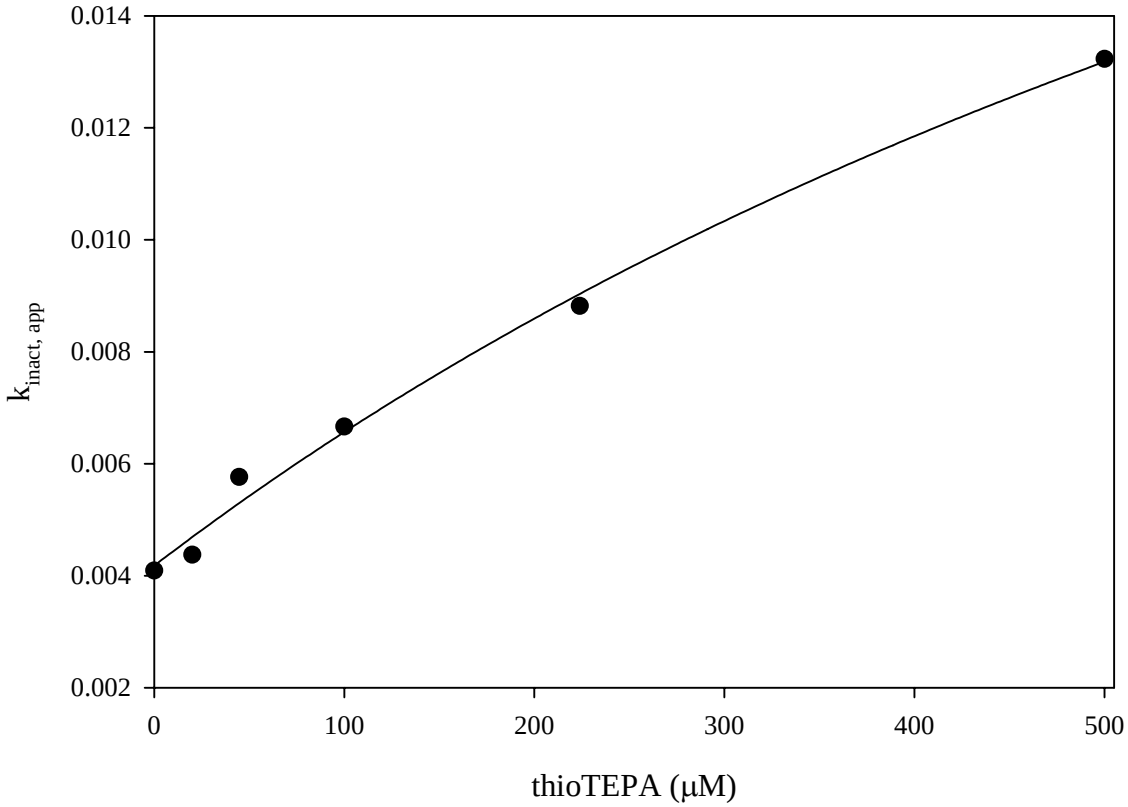

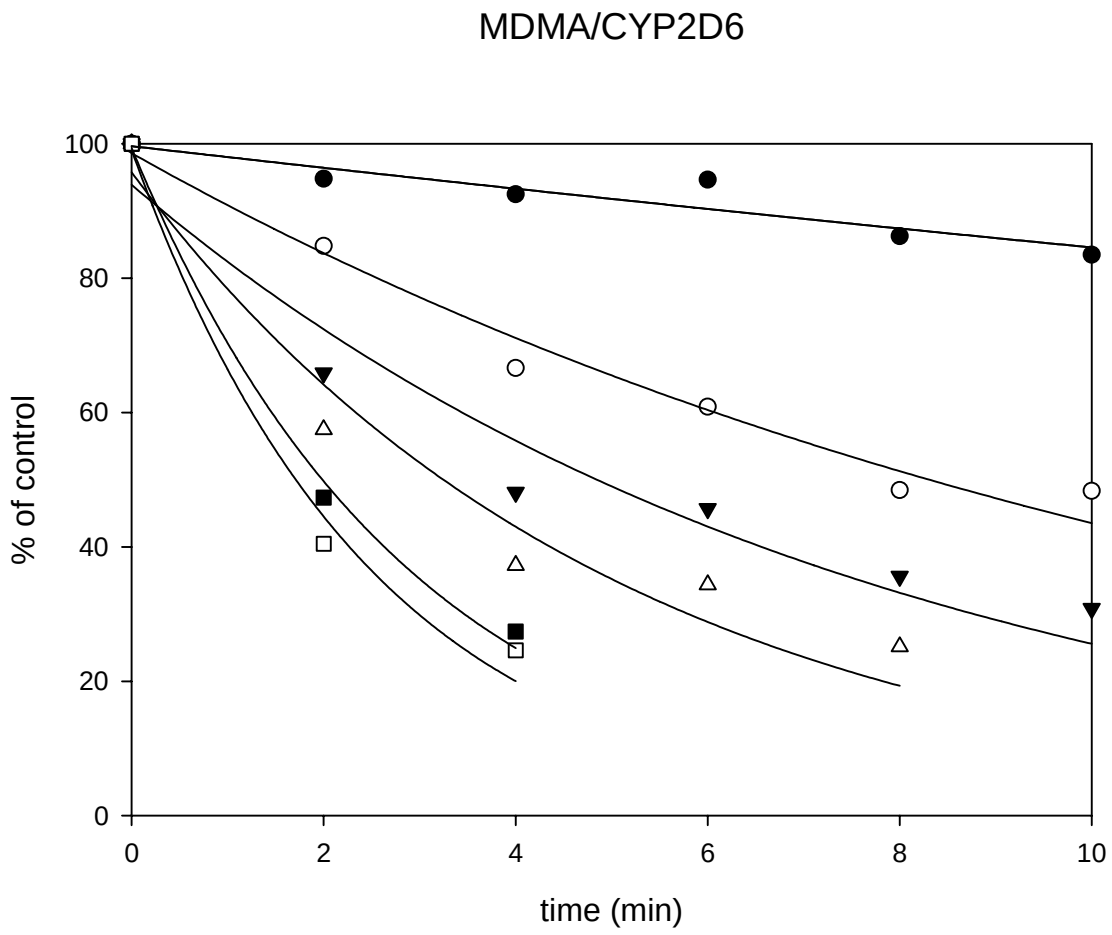
MDMA/CYP2D6
% of control
time (min)
0
20
40
60
80
100
0
2
4
6
8
10

CYP2D6 K_I/k_{inact}

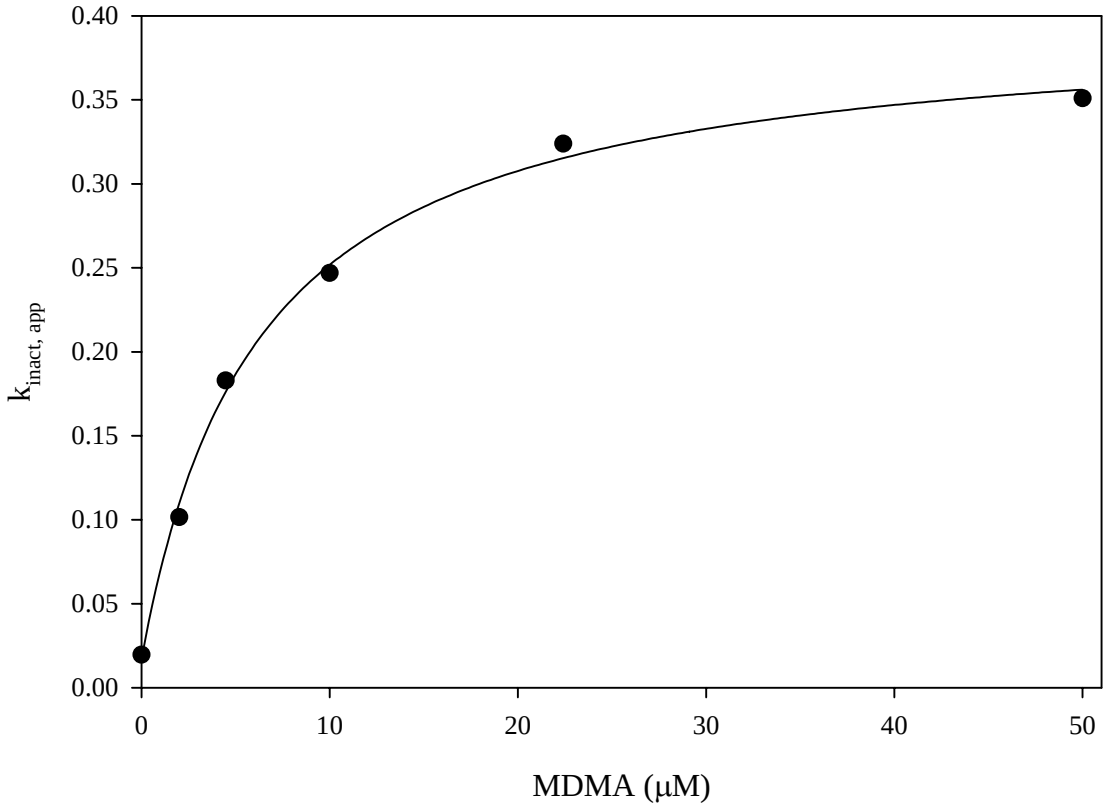

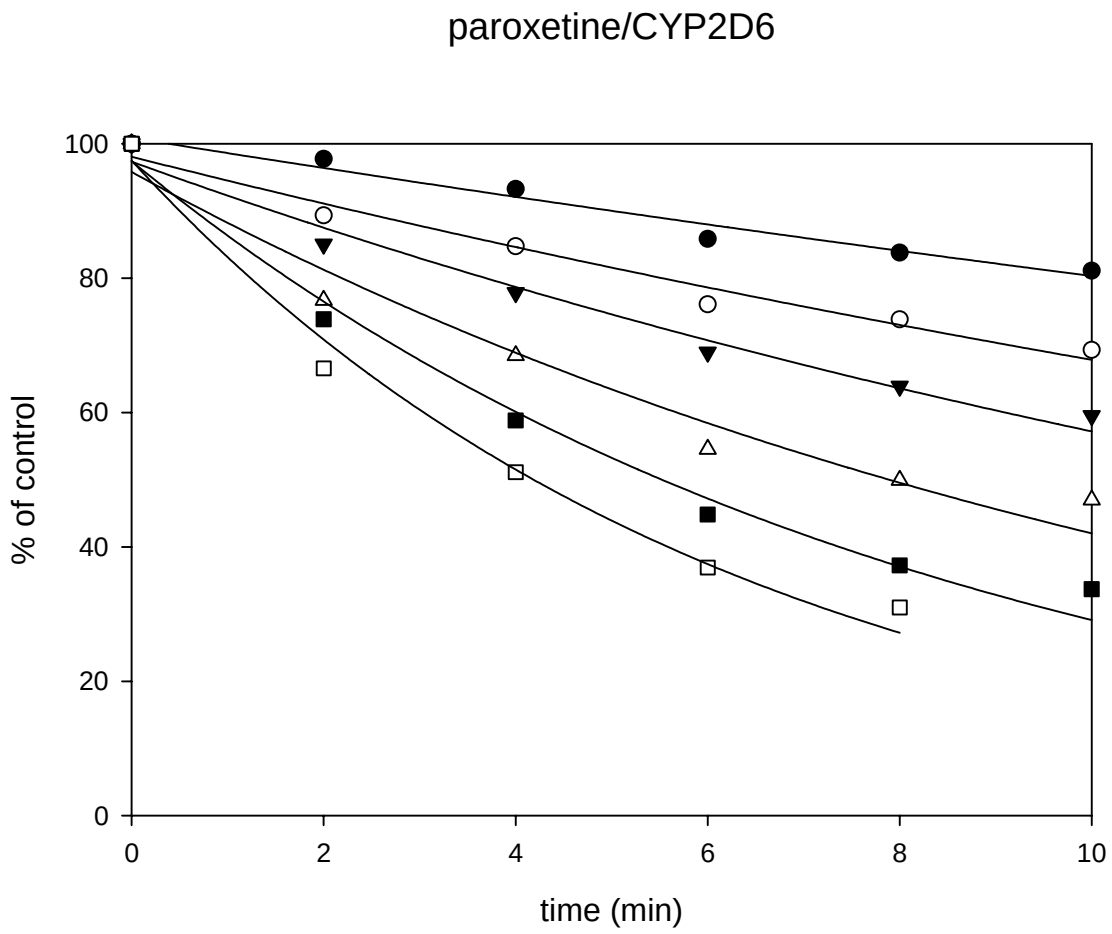
paroxetine/CYP2D6
% of control
100
80
60
40
20
0
0
2
4
6
8
10
time (min)

CYP2D6 K_I/k_{inact}

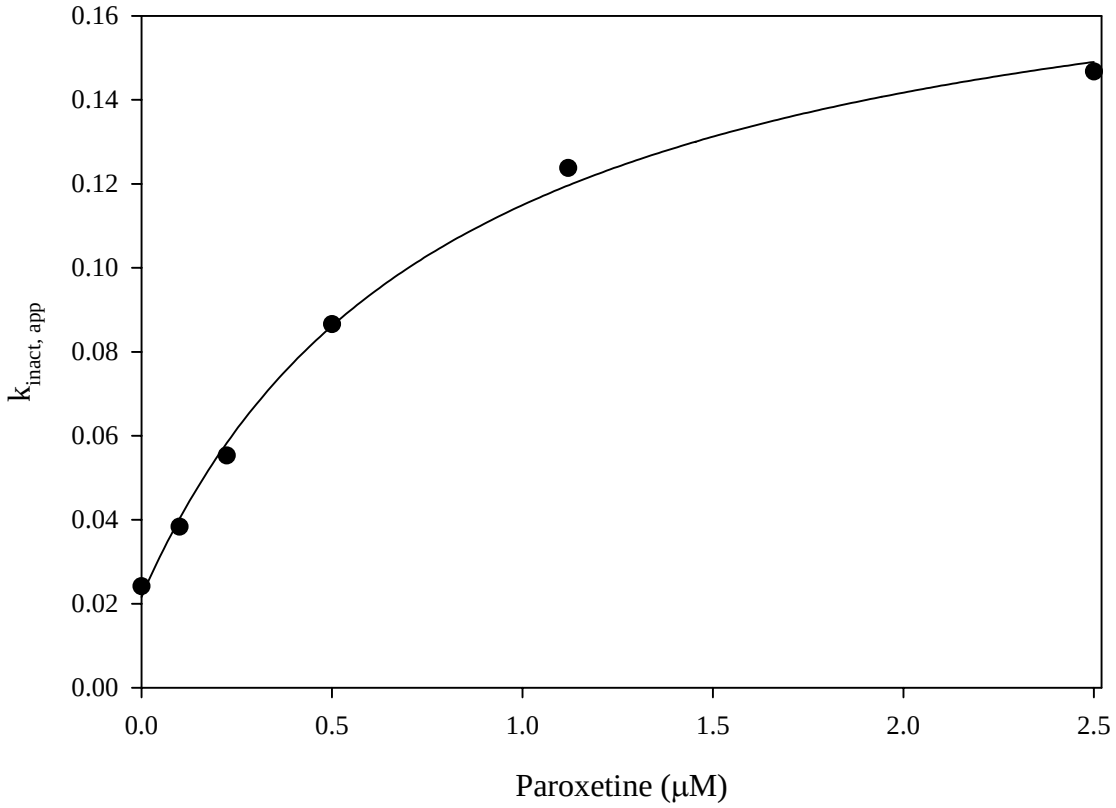

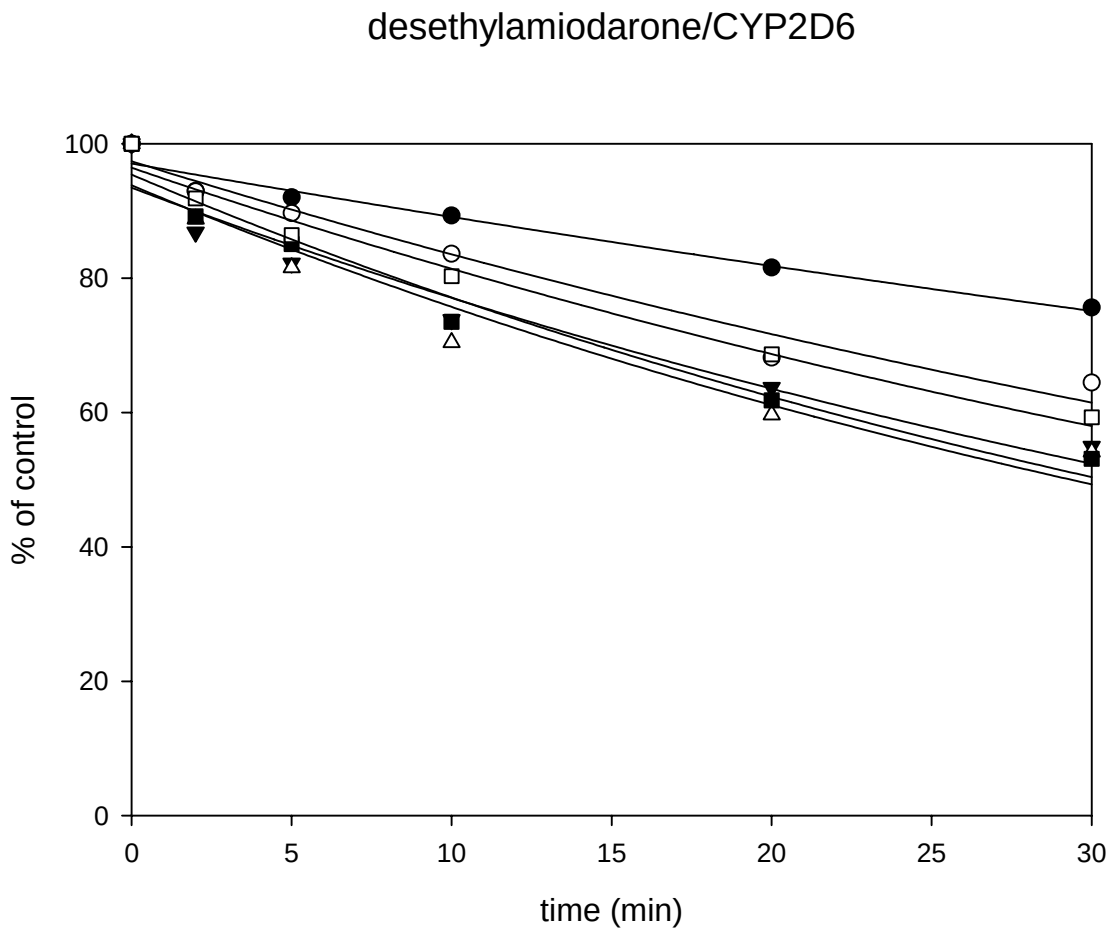
desethylamiodarone/CYP2D6
% of control
time (min)
100
80
60
40
20
0
0
5
10
15
20
25
30

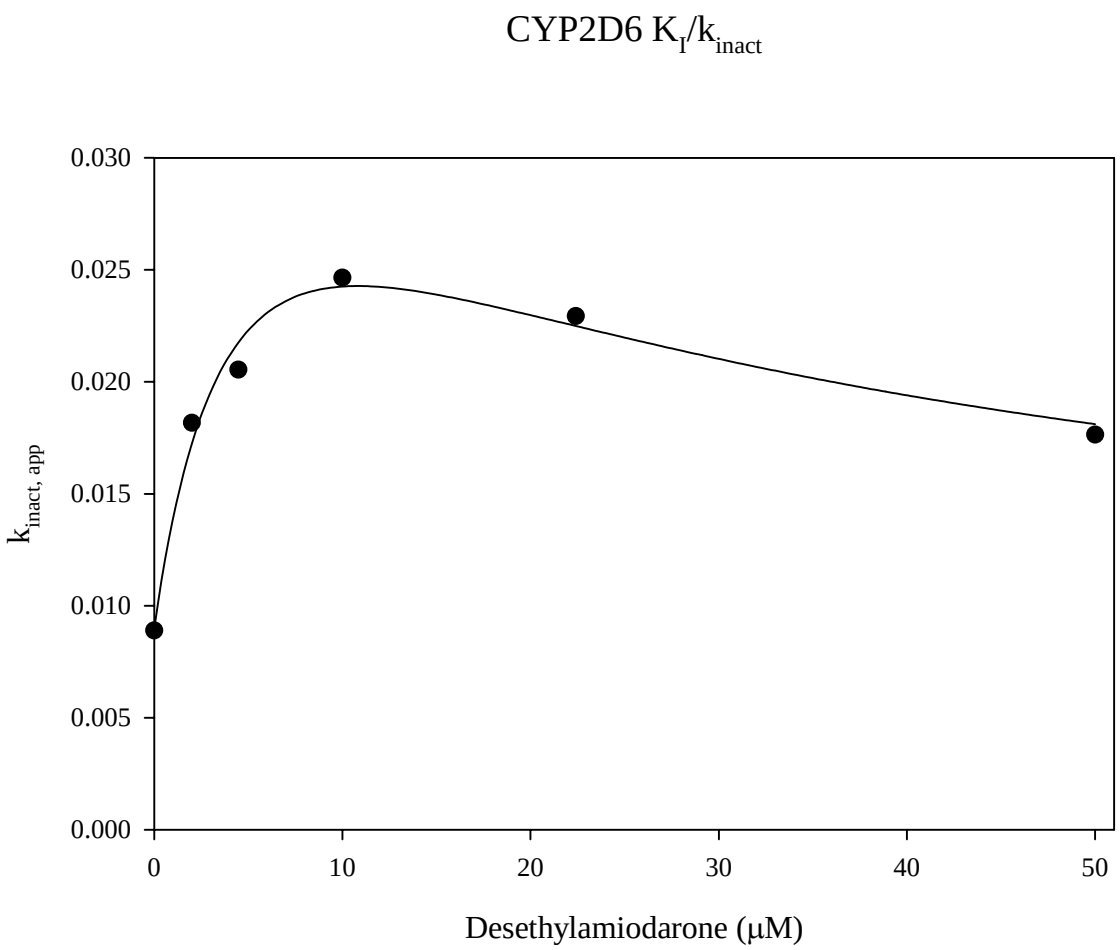
CYP2D6 K_I/k_{inact}
0.030
0.025
0.020
0.015
0.010
0.005
0.000
$k_{inact, app}$
0
10
20
30
40
50
Desethylamiodarone (μM)

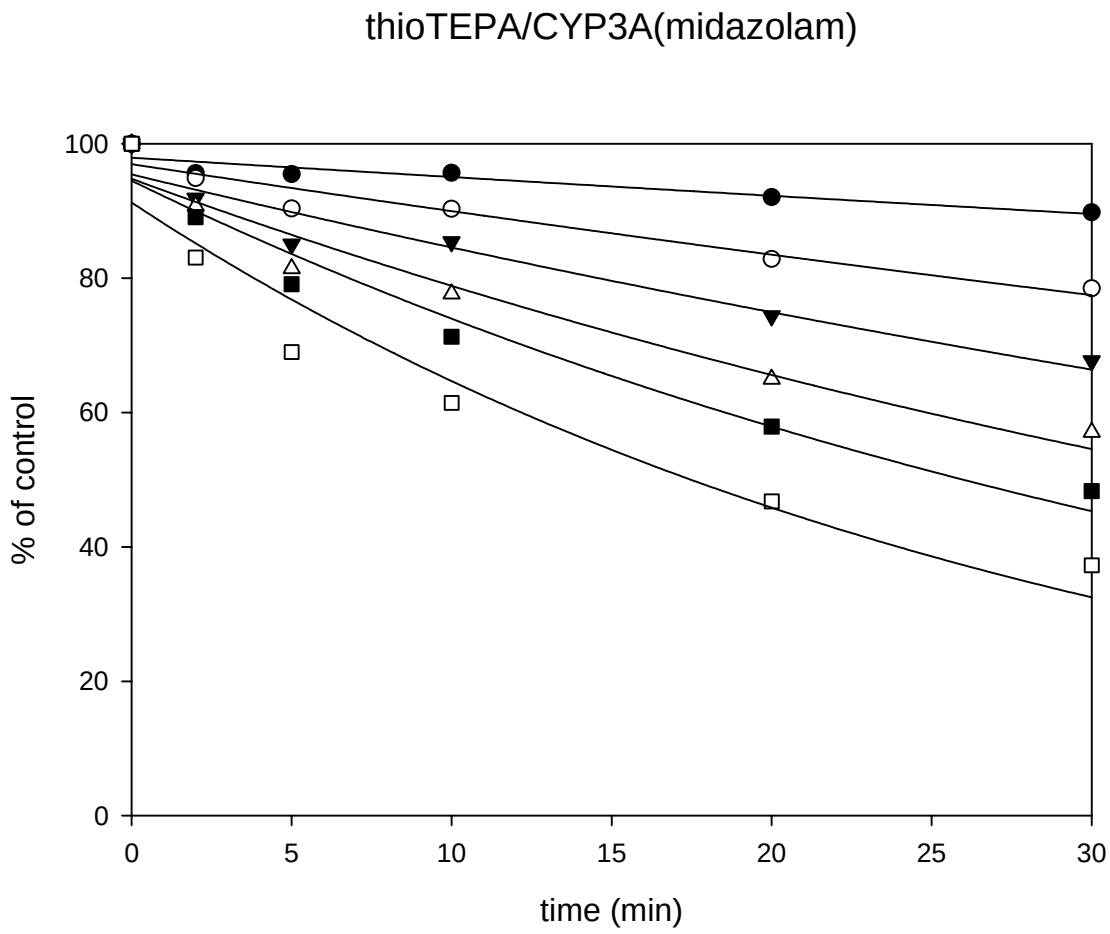
thioTEPA/CYP3A(midazolam)
% of control
time (min)
100
80
60
40
20
0
0
5
10
15
20
25
30

CYP3AM K_I/k_{inact}

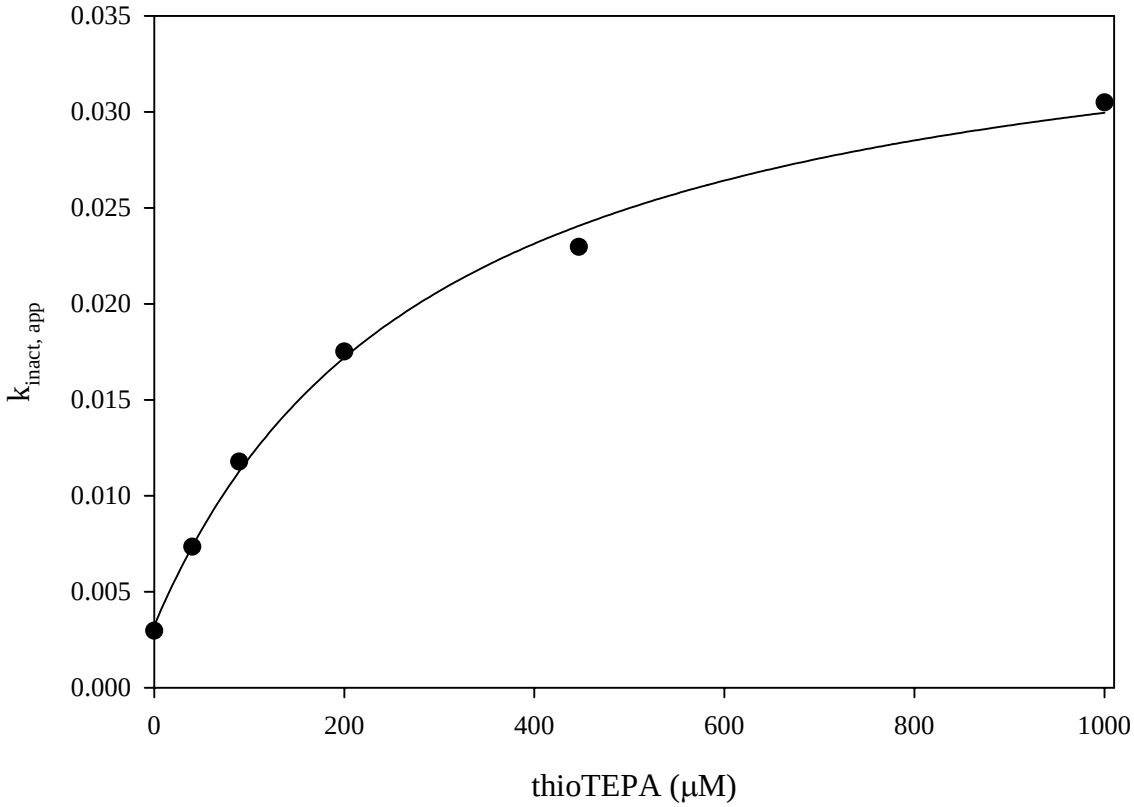

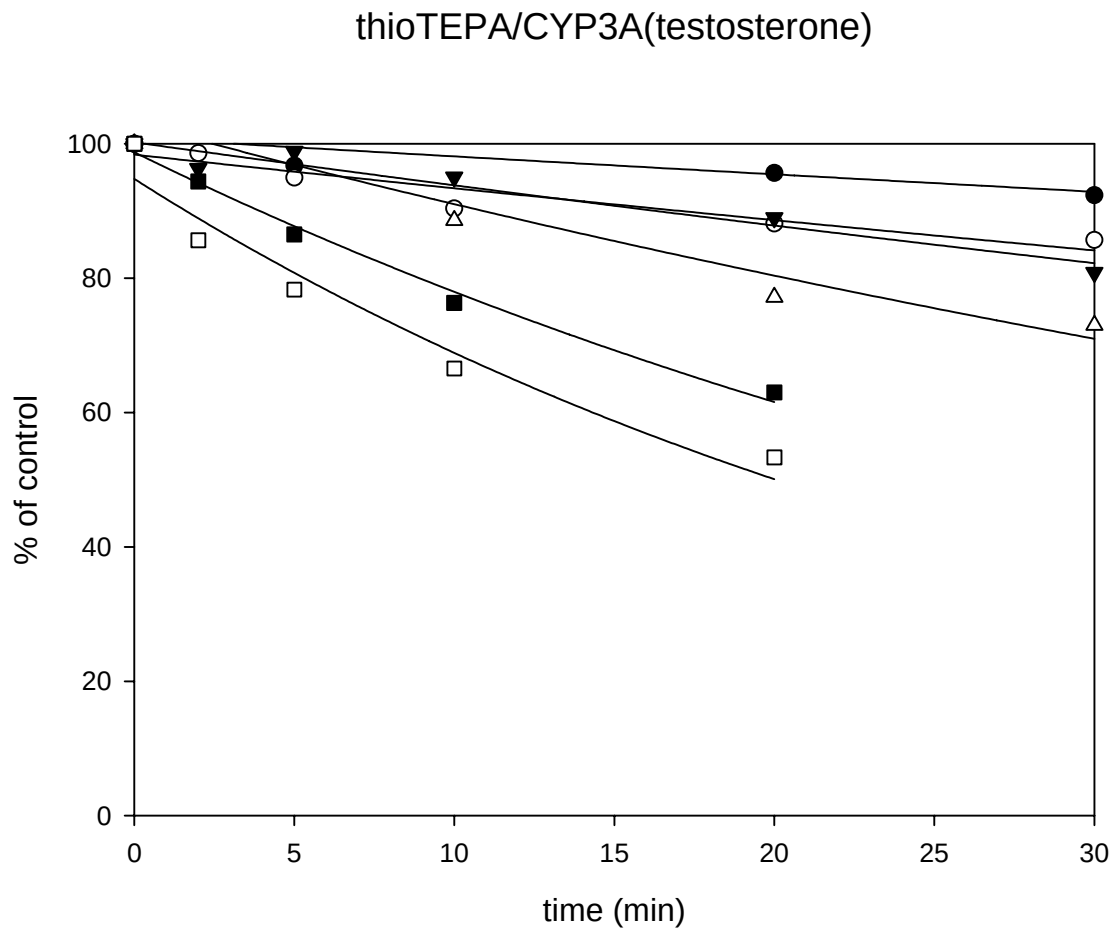
thioTEPA/CYP3A(testosterone)
100
80
60
40
20
0
% of control
0
5
10
15
20
25
30
time (min)

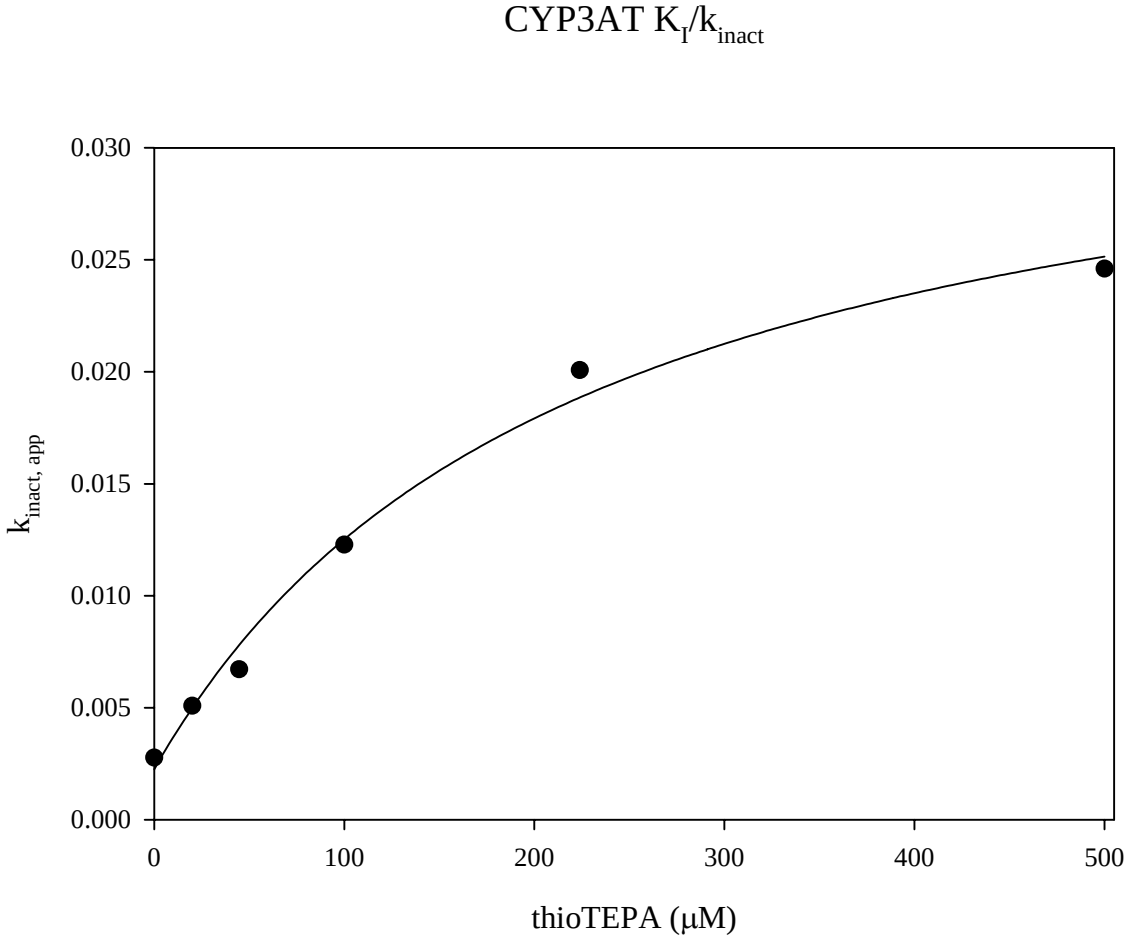
CYP3AT K_I/k_{inact}
0.030
0.025
0.020
0.015
0.010
0.005
0.000
$k_{inact, app}$
0
100
200
300
400
500
thioTEPA (μM)

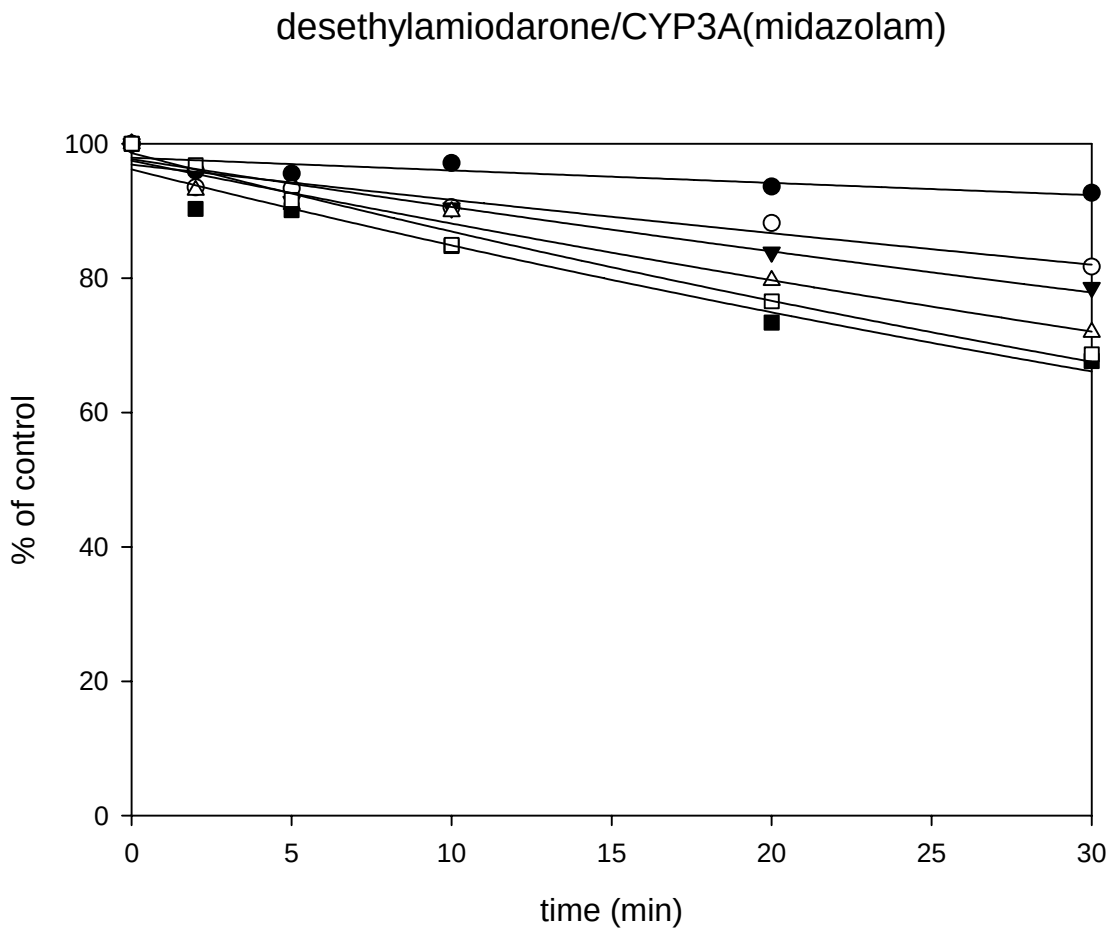
desethylamiodarone/CYP3A(midazolam)
% of control
time (min)
100
80
60
40
20
0
0
5
10
15
20
25
30

CYP3AM K_I/k_{inact}

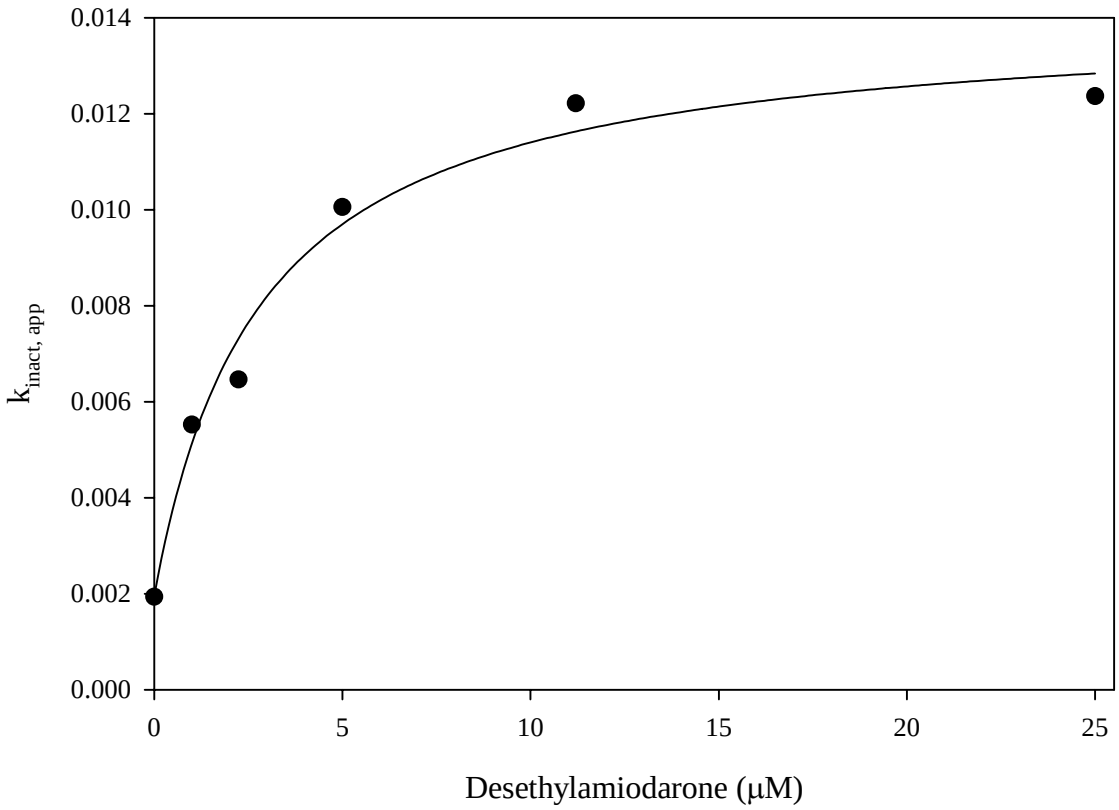

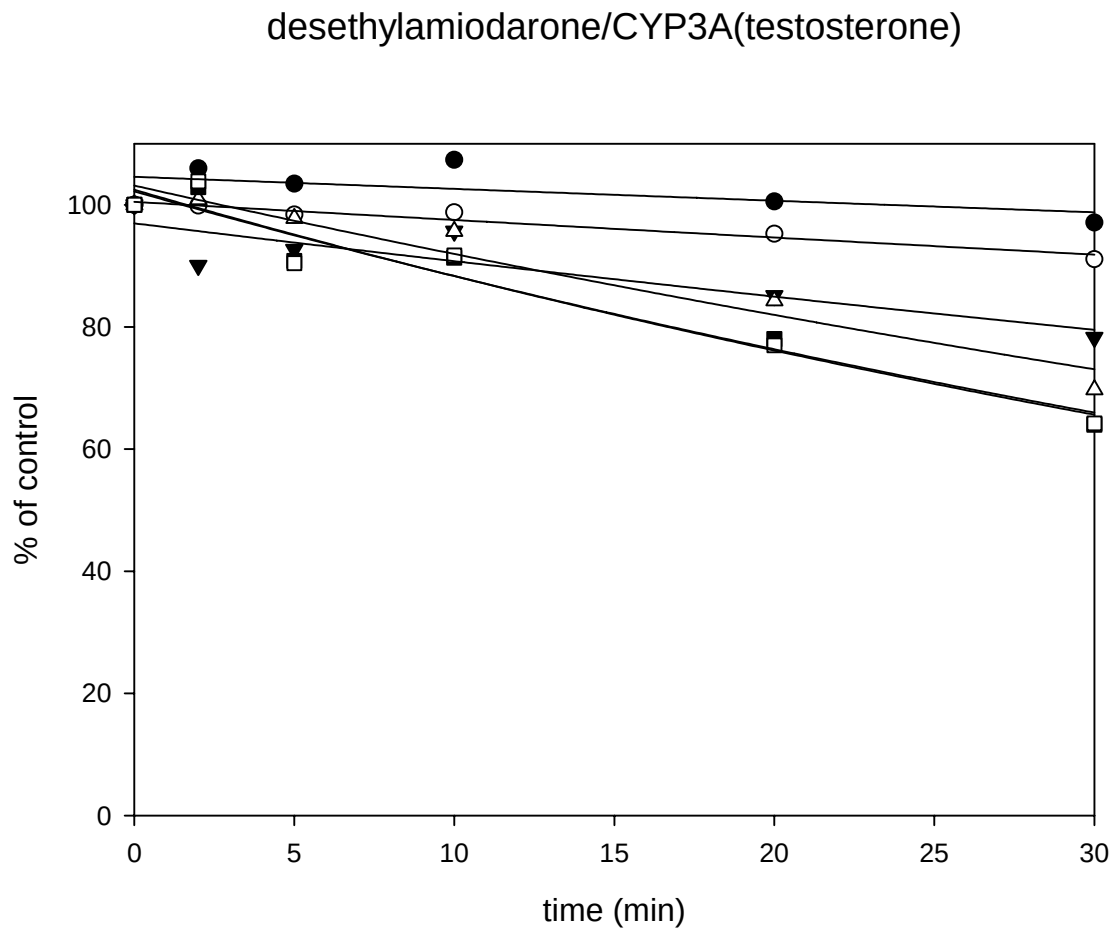
desethylamiodarone/CYP3A(testosterone)
% of control
100
80
60
40
20
0
0
5
10
15
20
25
30
time (min)

CYP3AT K_I/k_{inact}

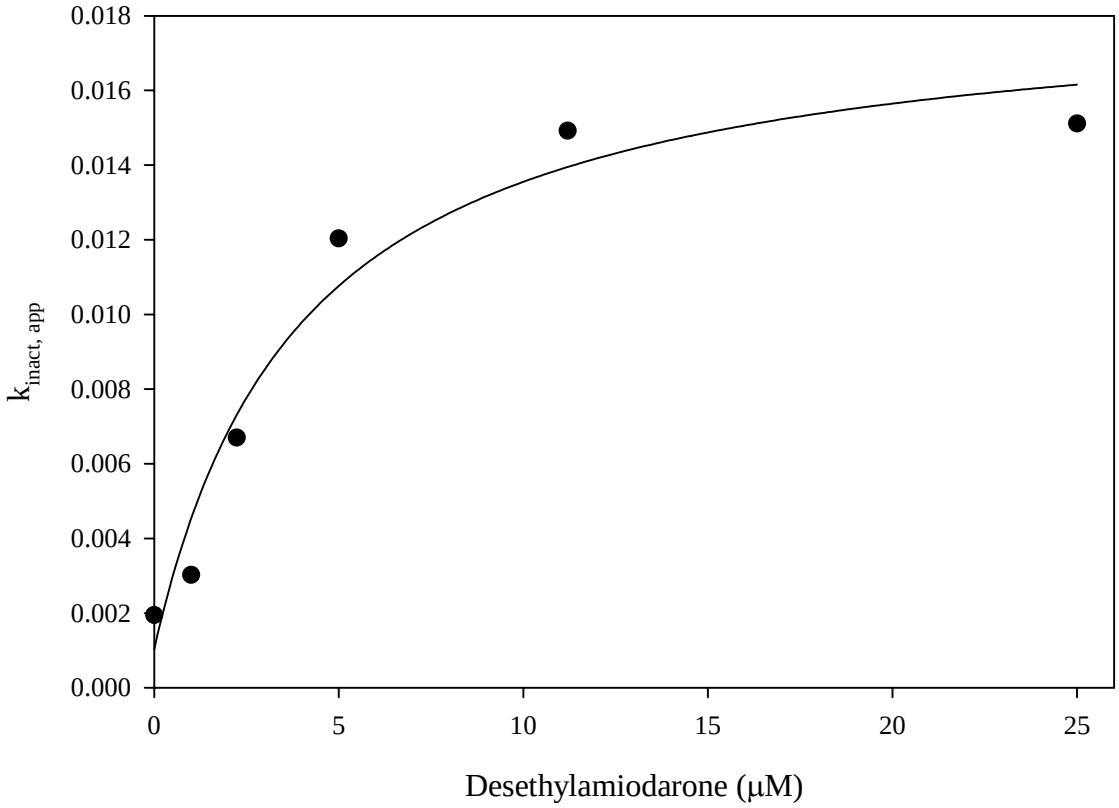

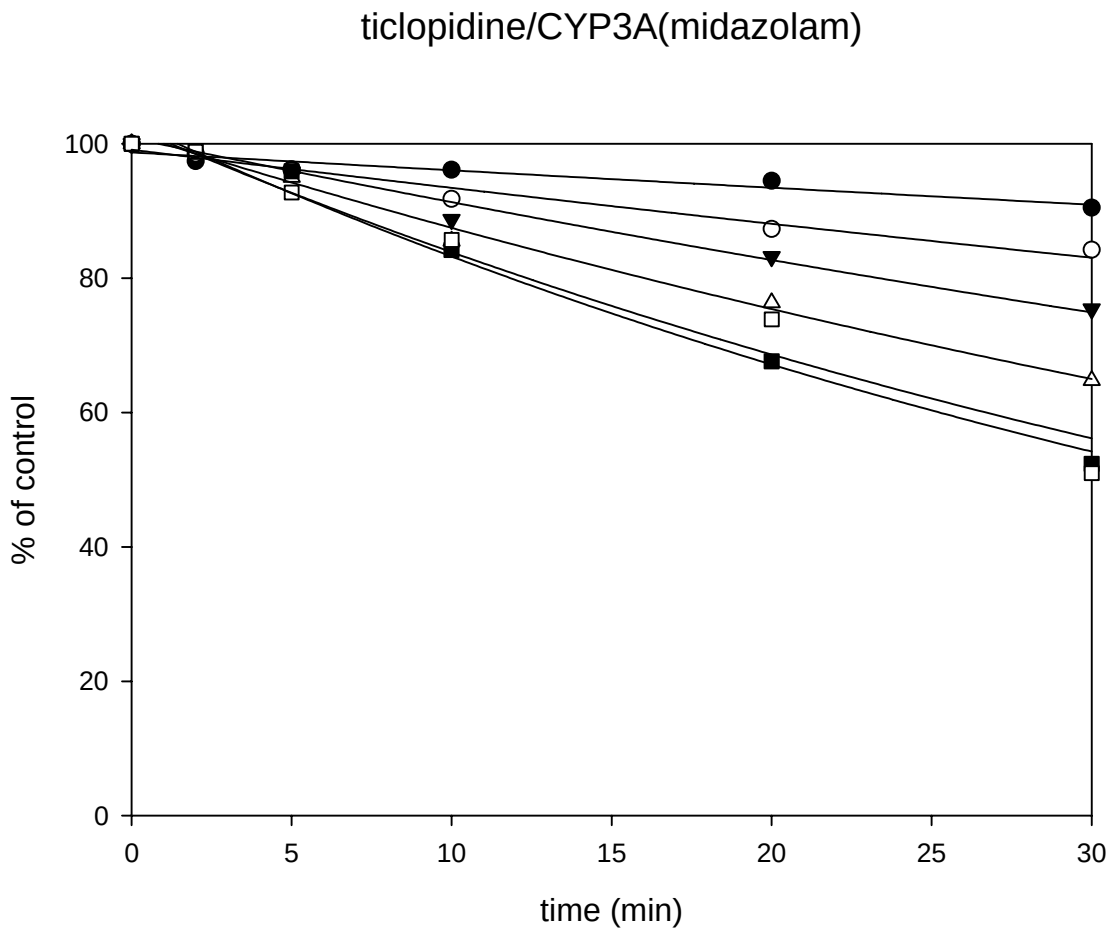
ticlopidine/CYP3A(midazolam)
% of control
100
80
60
40
20
0
0
5
10
15
20
25
30
time (min)

CYP3AM K_I/k_{inact}

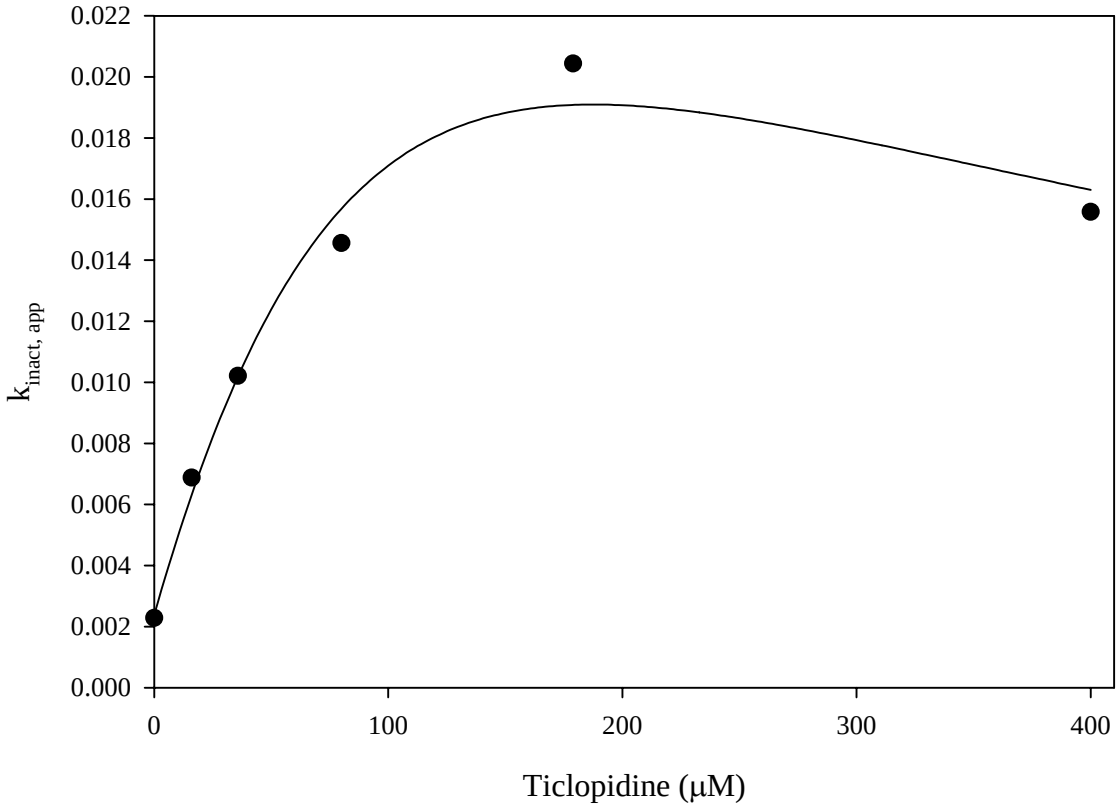

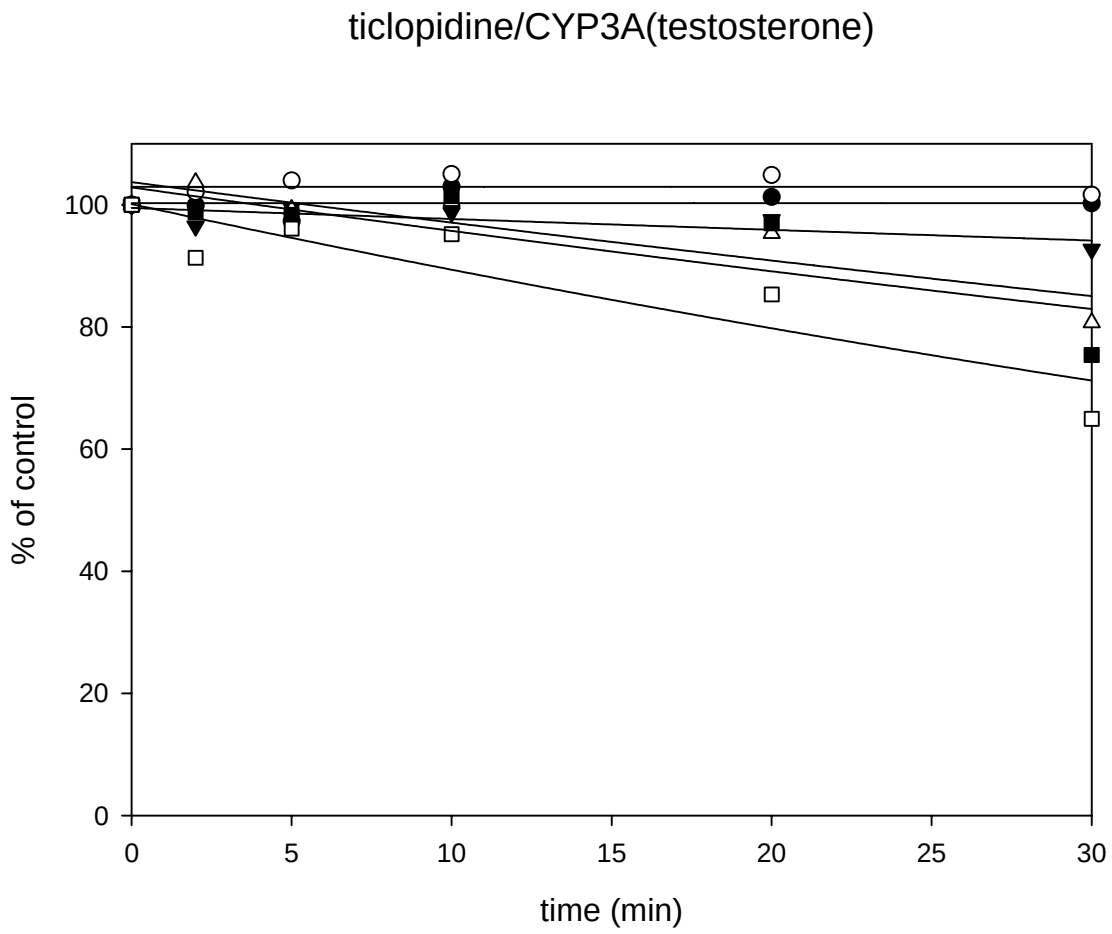
ticlopidine/CYP3A(testosterone)
% of control
100
80
60
40
20
0
0
5
10
15
20
25
30
time (min)

CYP3AT K_I/k_{inact}

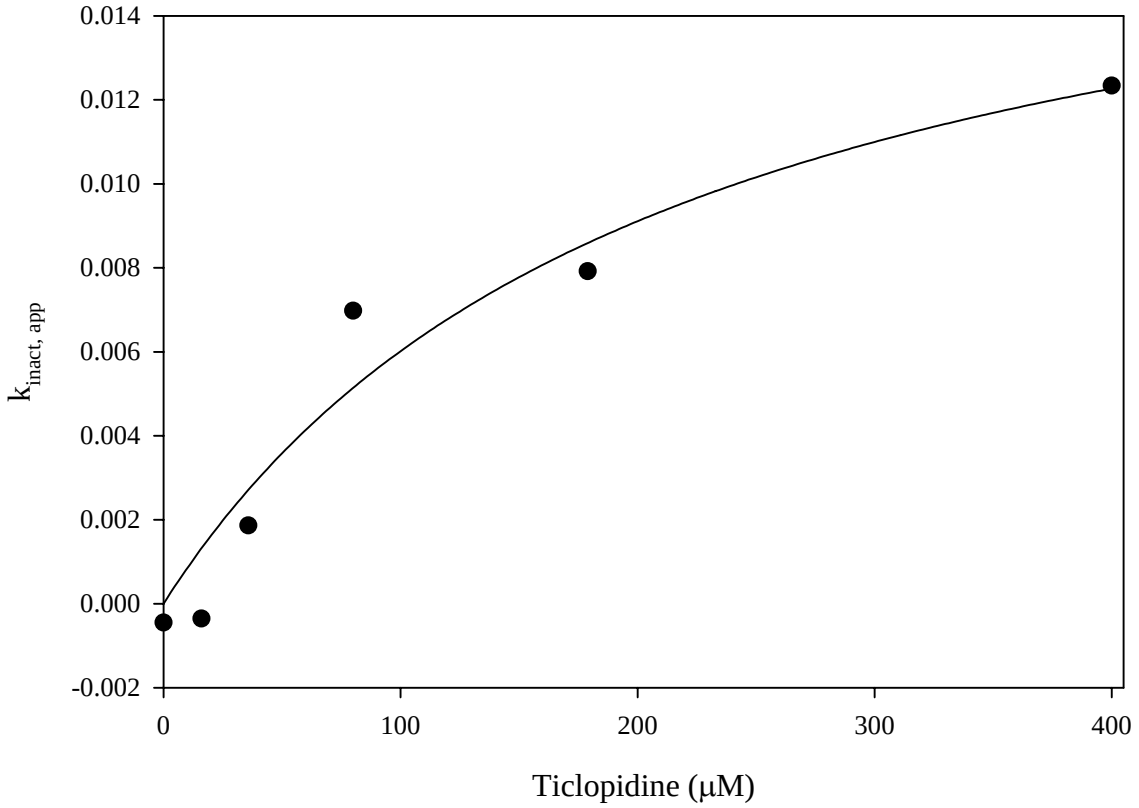

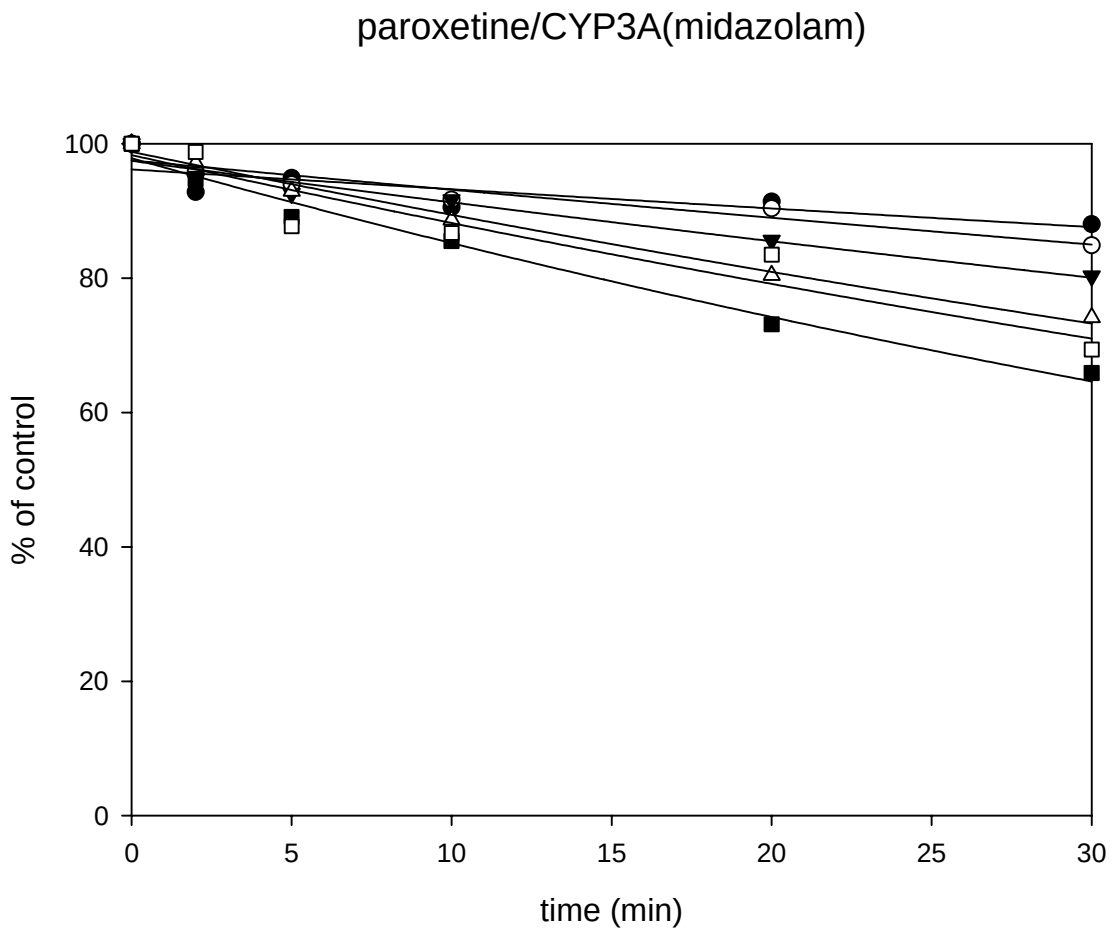
paroxetine/CYP3A(midazolam)
100
80
60
40
20
0
% of control
0
5
10
15
20
25
30
time (min)

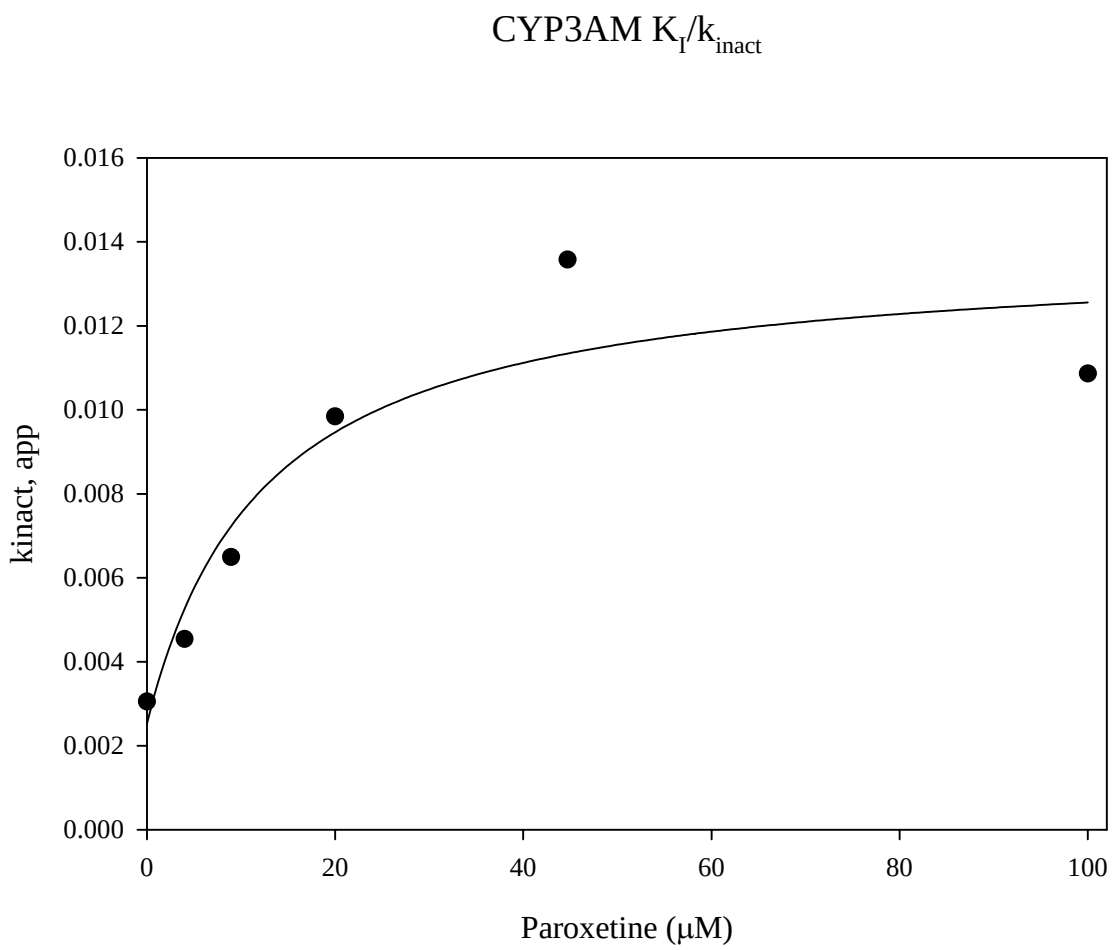
CYP3AM K_I/k_{inact}
kinact, app
0.016
0.014
0.012
0.010
0.008
0.006
0.004
0.002
0.000
0
20
40
60
80
100
Paroxetine (μM)

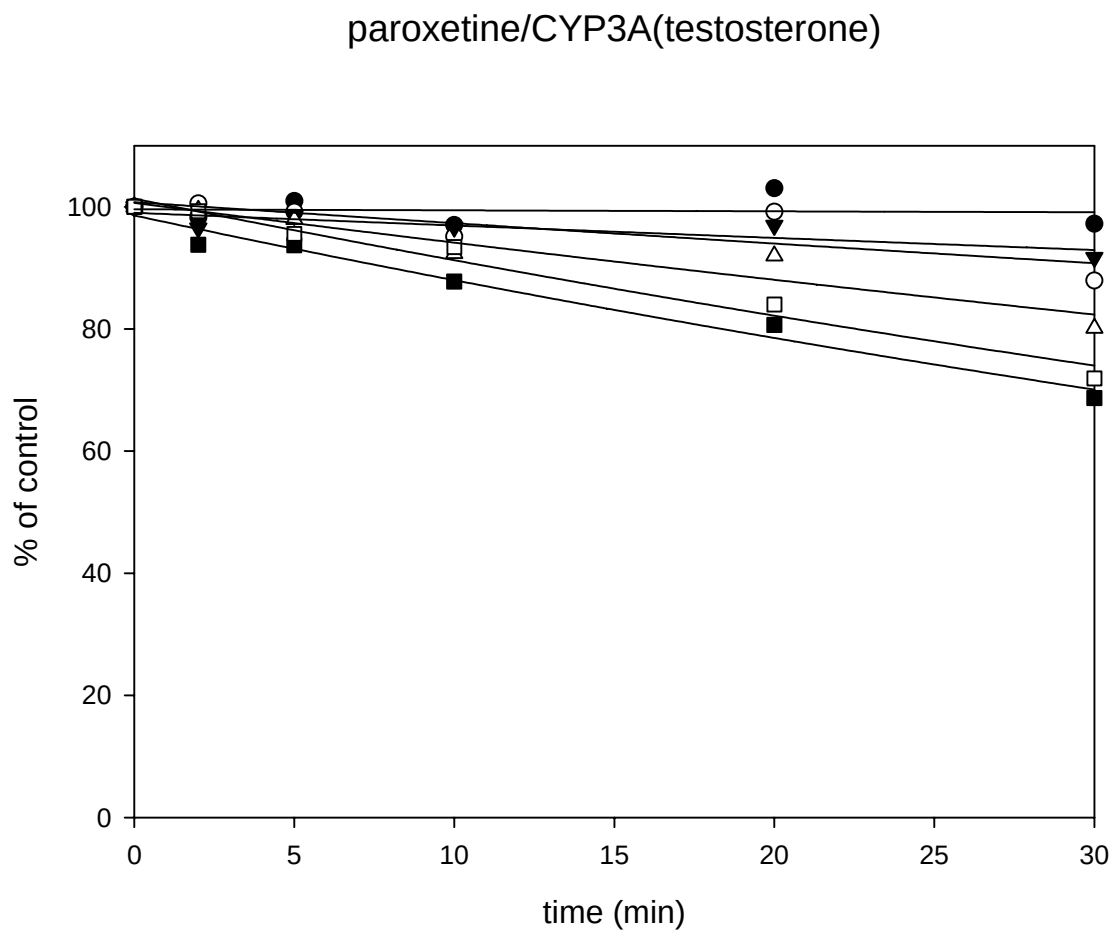
paroxetine/CYP3A(testosterone)
% of control
100
80
60
40
20
0
0
5
10
15
20
25
30
time (min)

CYP3AT K_I/k_{inact}

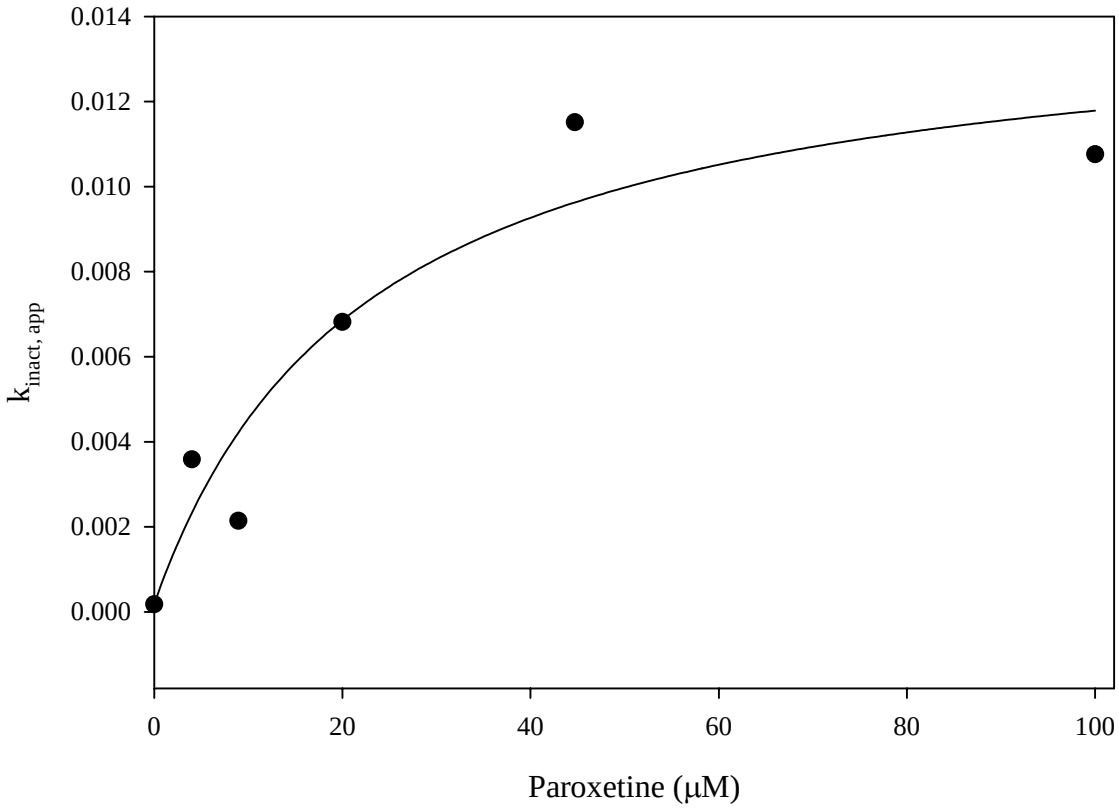

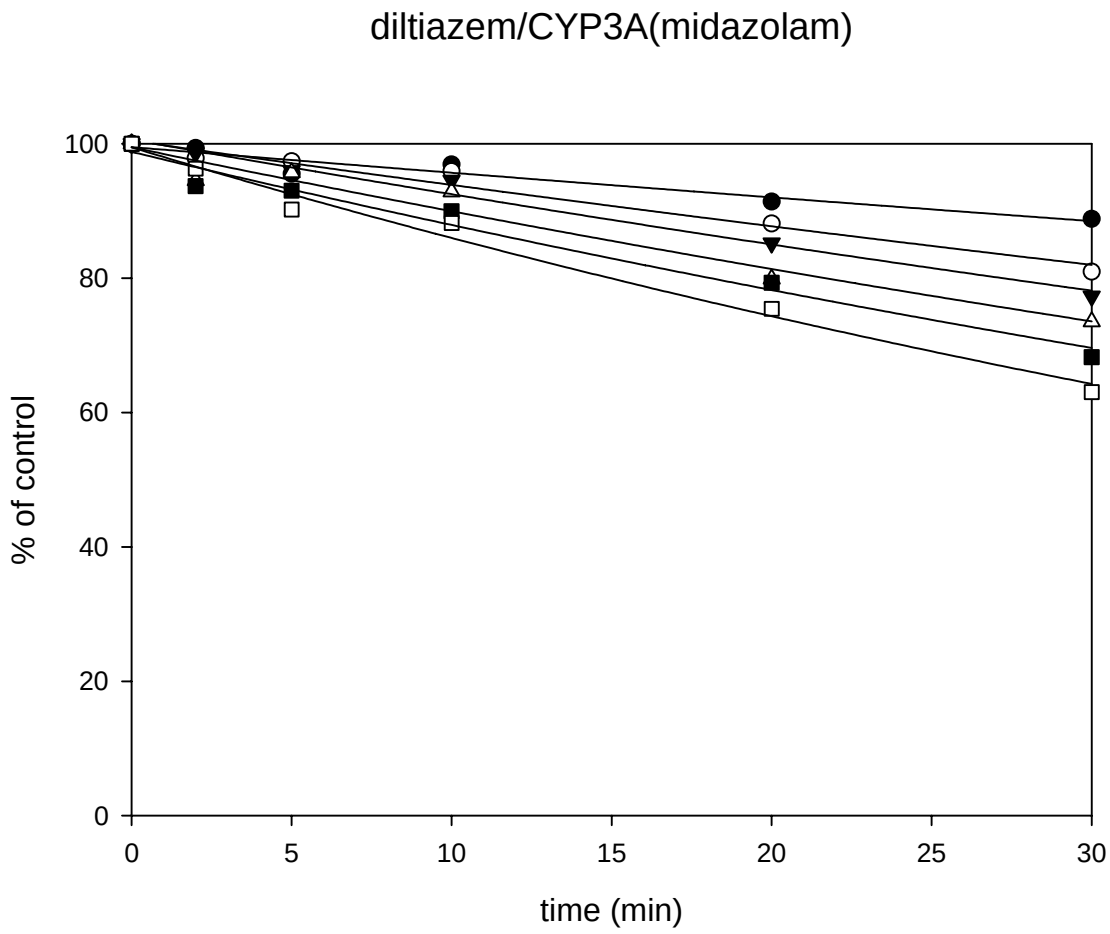
diltiazem/CYP3A(midazolam)
% of control
100
80
60
40
20
0
0
5
10
15
20
25
30
time (min)

CYP3AM KI/k_{inact}

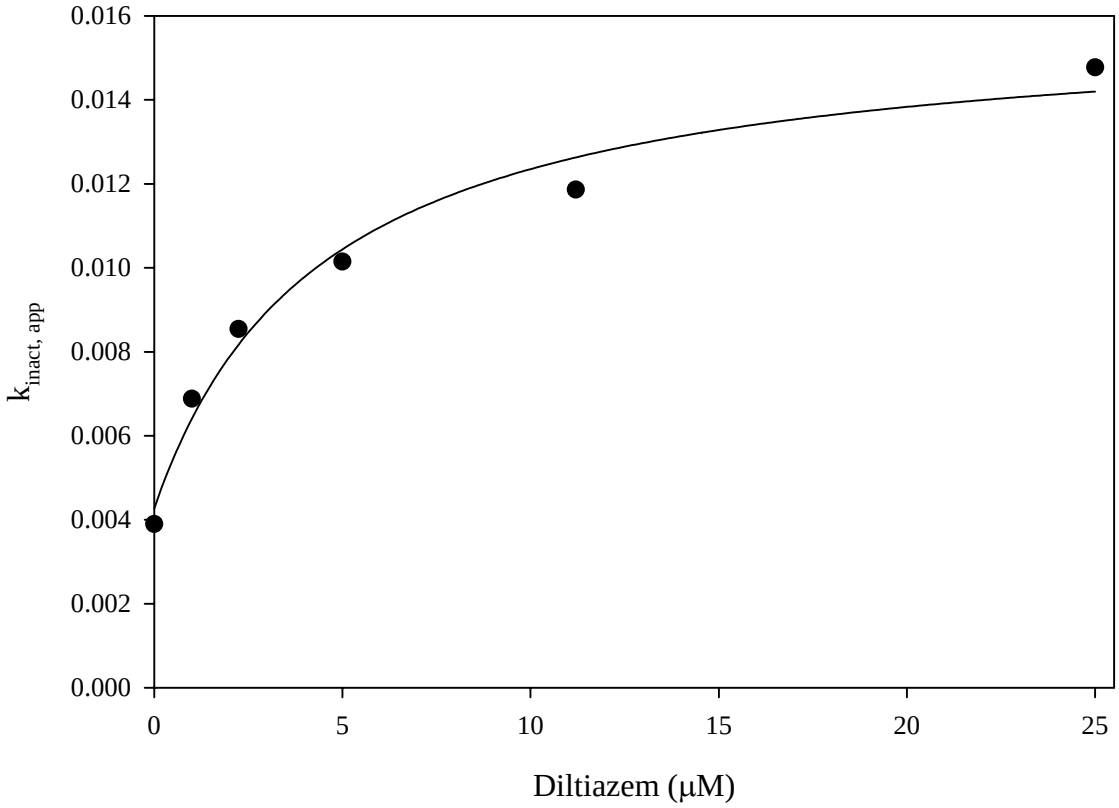

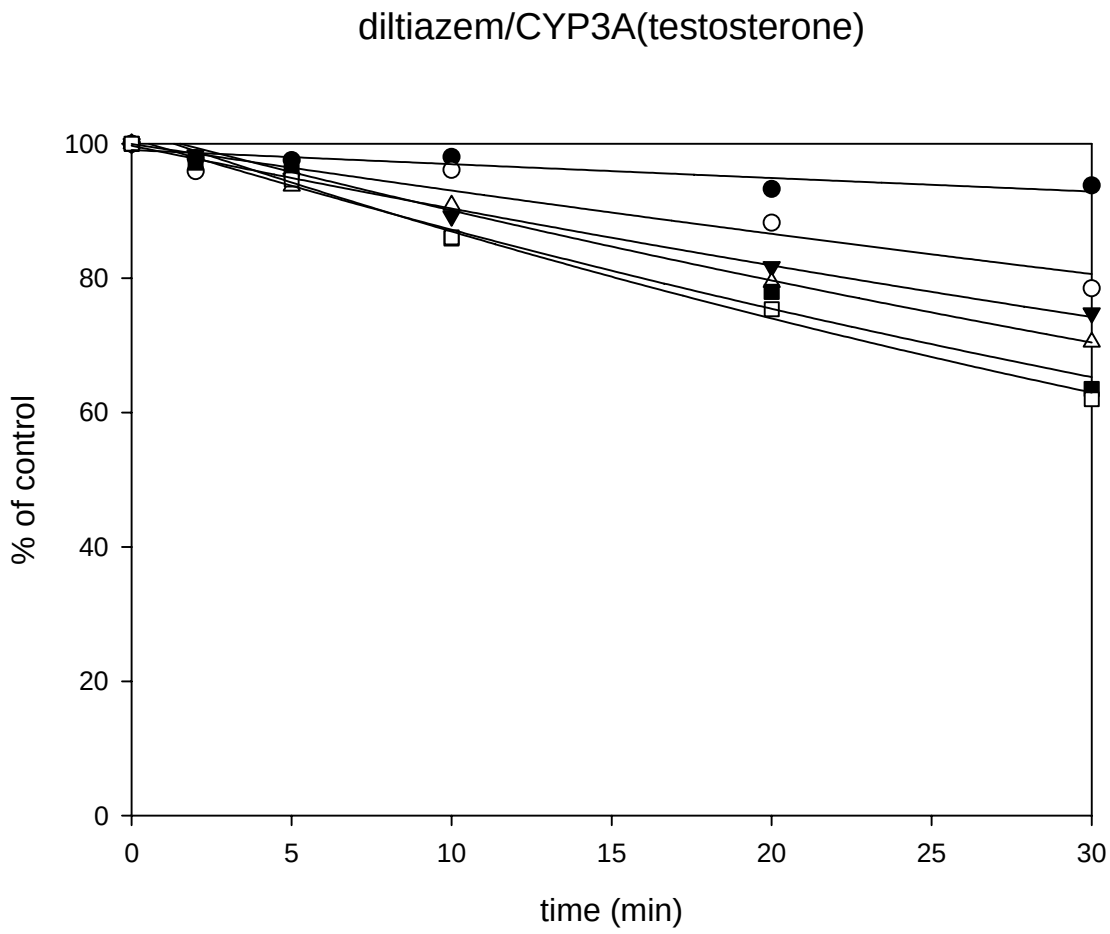
diltiazem/CYP3A(testosterone)
% of control
time (min)
100
80
60
40
20
0
0
5
10
15
20
25
30

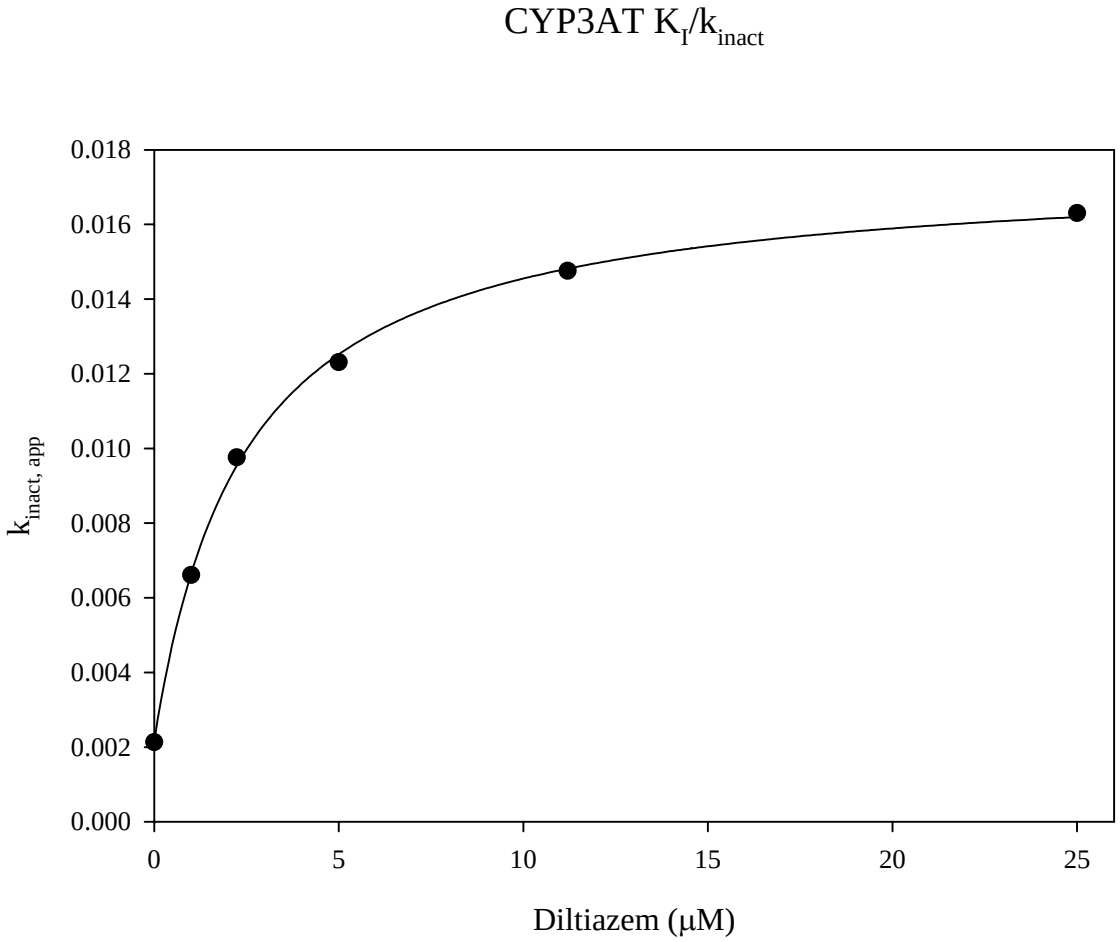
CYP3AT K_I/k_{inact}
0.018
0.016
0.014
0.012
0.010
0.008
0.006
0.004
0.002
0.000
$k_{inact, app}$
0
5
10
15
20
25
Diltiazem (μM)

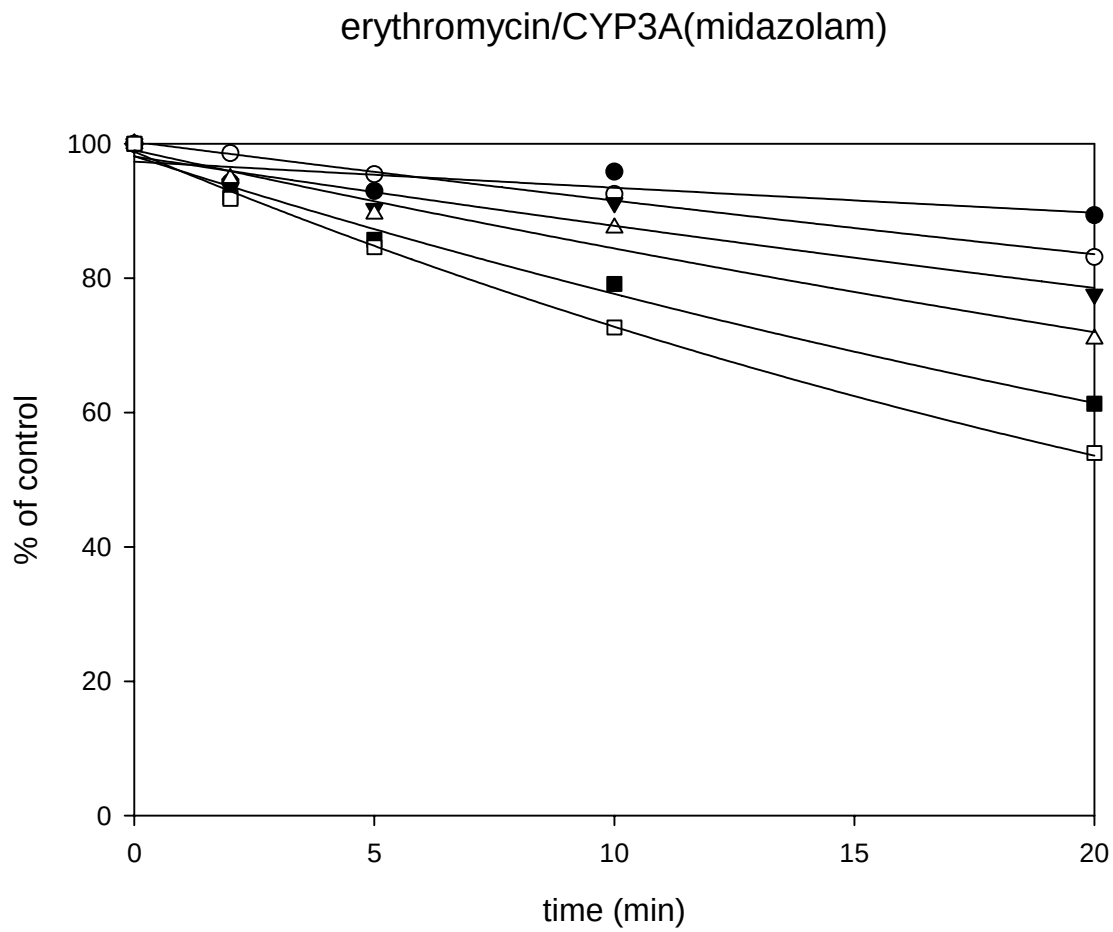
erythromycin/CYP3A(midazolam)
100
80
60
40
20
0
% of control
0
5
10
15
20
time (min)

CYP3AM K_I/k_{inact}

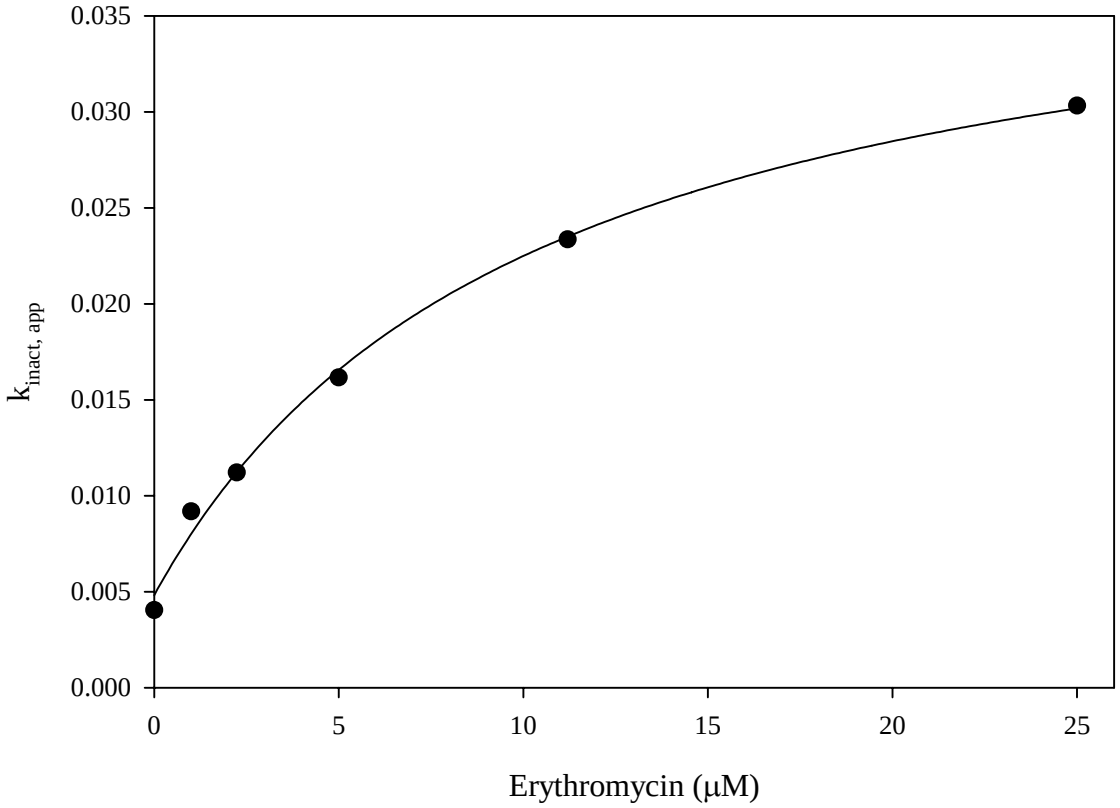

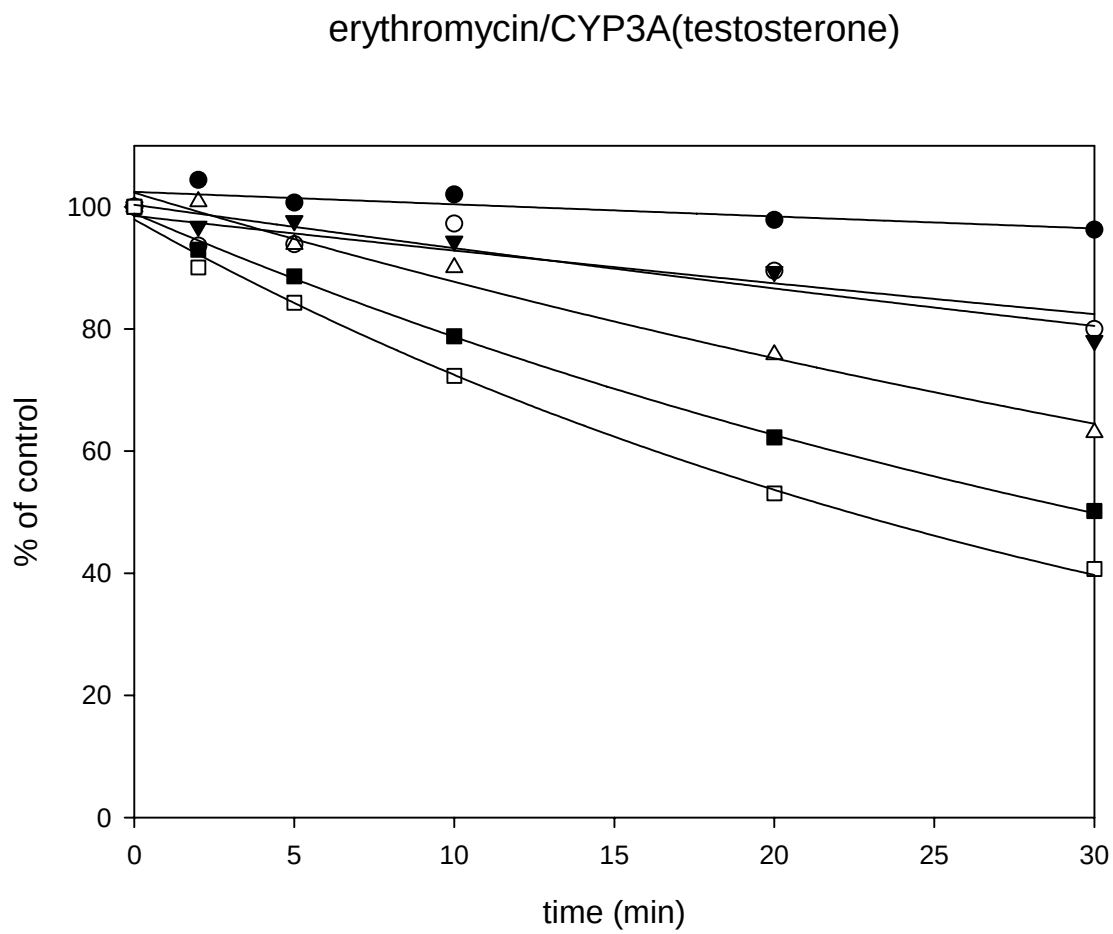
erythromycin/CYP3A(testosterone)
% of control
100
80
60
40
20
0
0
5
10
15
20
25
30
time (min)

CYP3AT K_I/k_{inact}

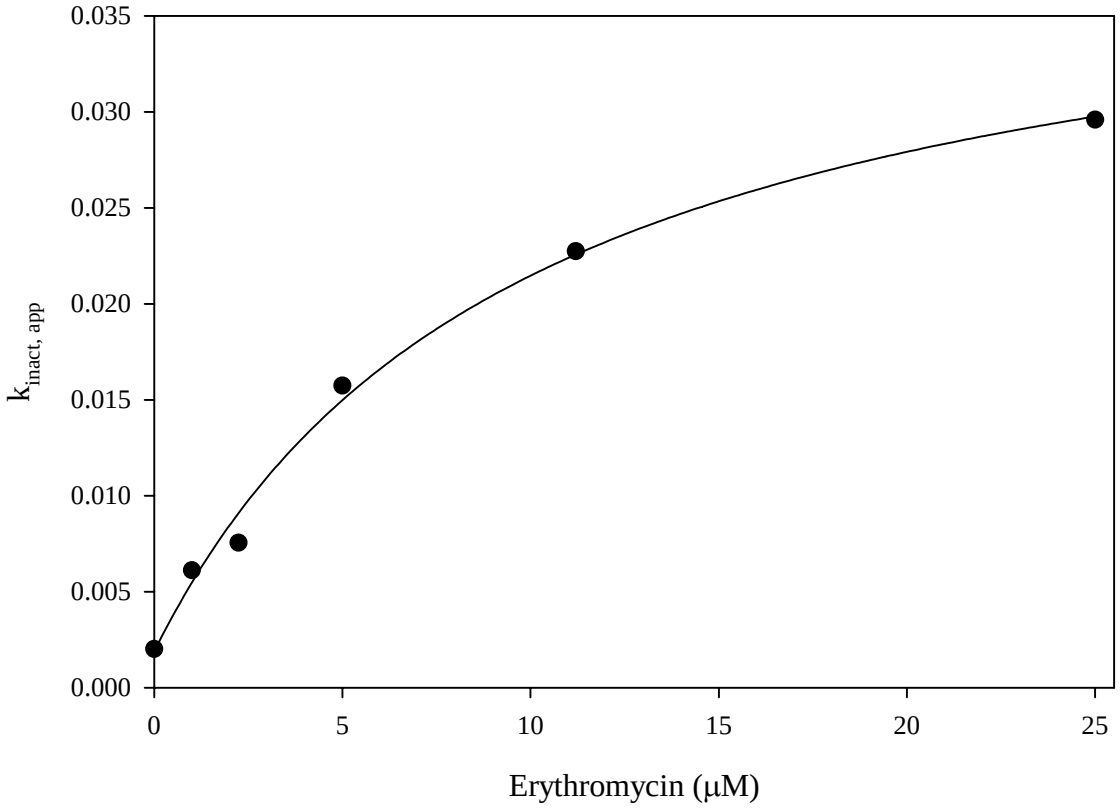

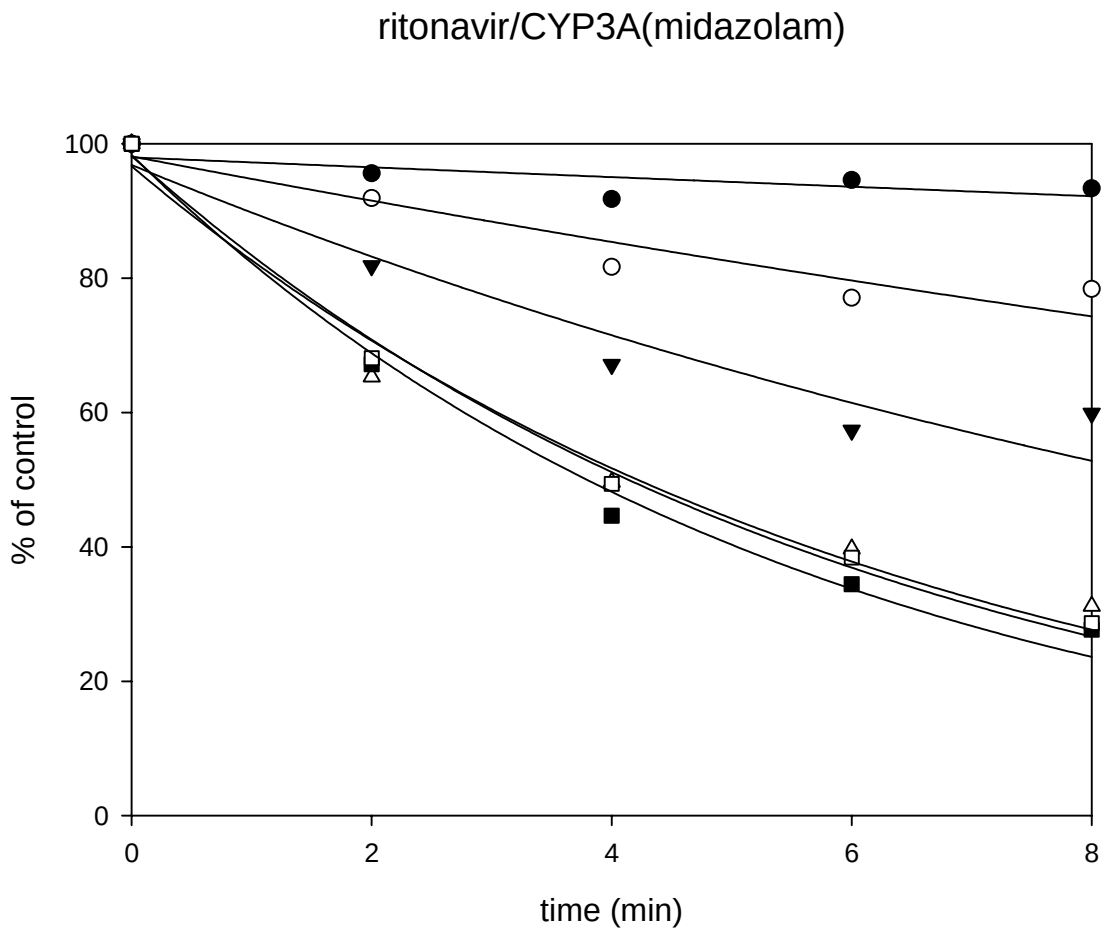
ritonavir/CYP3A(midazolam)
100
80
60
40
20
0
% of control
0
2
4
6
8
time (min)

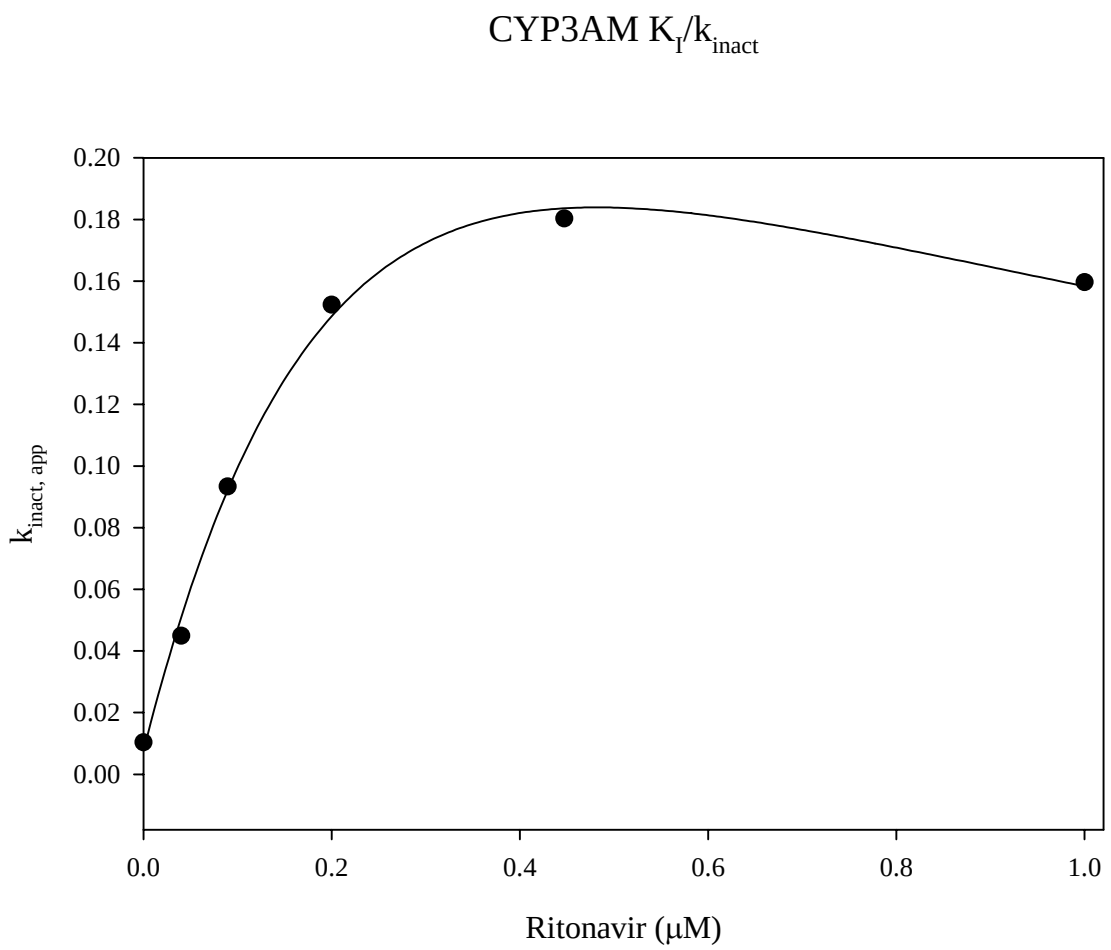
CYP3AM K_I/k_{inact}
0.20
0.18
0.16
0.14
0.12
0.10
0.08
0.06
0.04
0.02
0.00
$k_{inact, app}$
0.0
0.2
0.4
0.6
0.8
1.0
Ritonavir (μM)

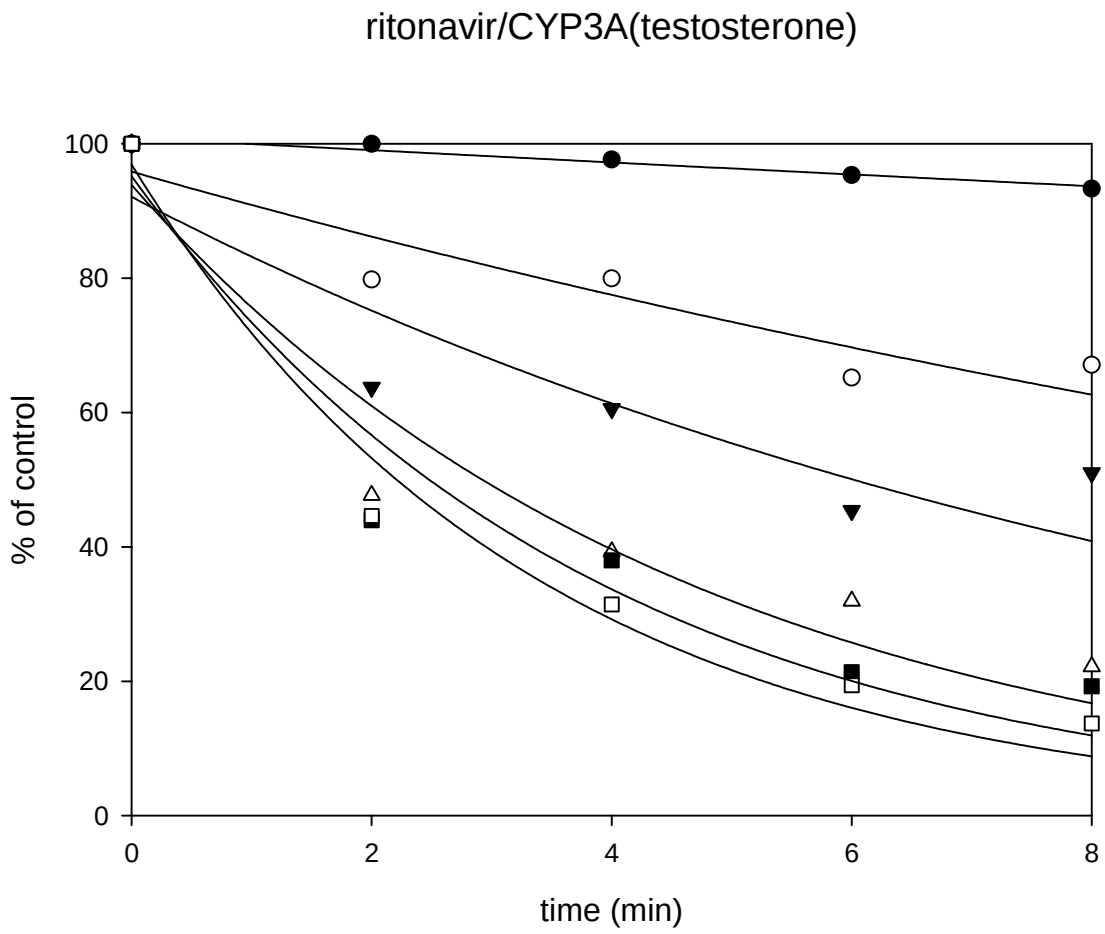
ritonavir/CYP3A(testosterone)
100
80
60
40
20
0
% of control
0
2
4
6
8
time (min)

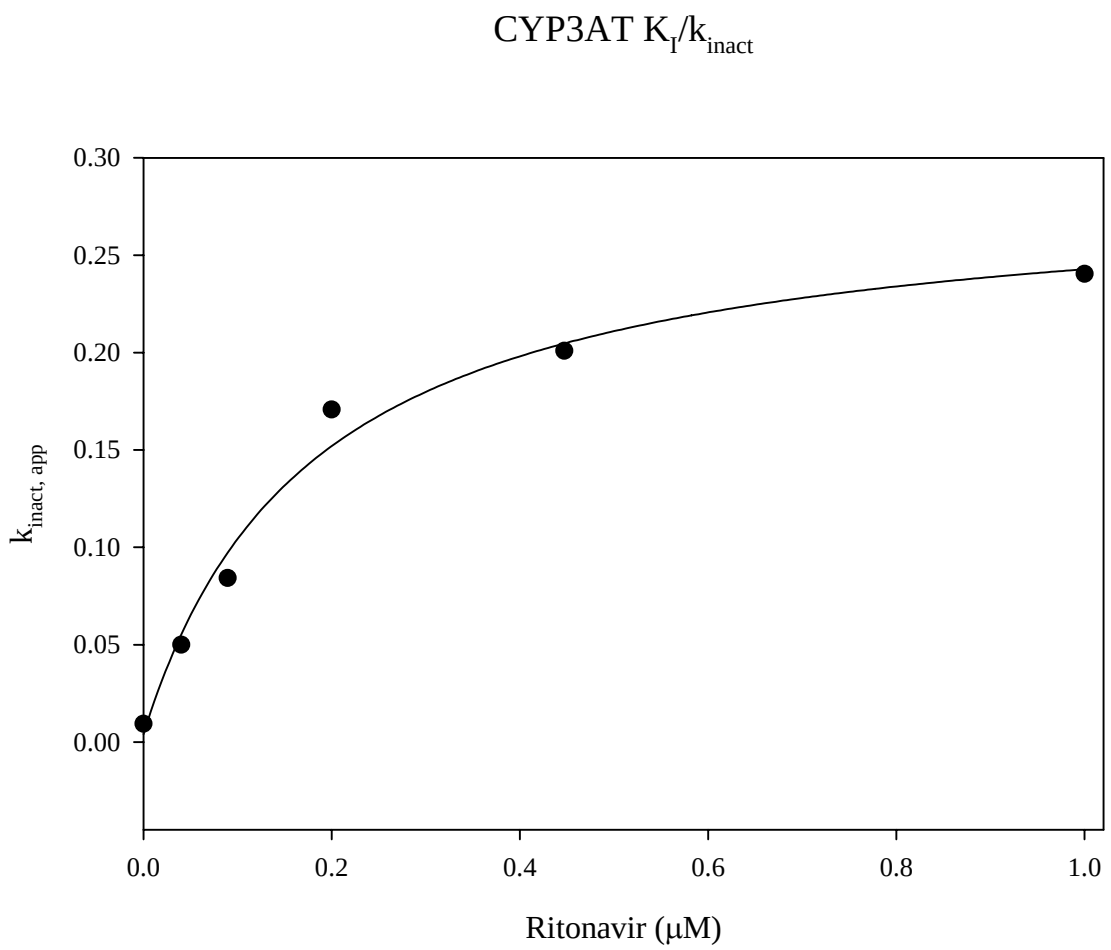
CYP3AT K_I/k_{inact}
0.30
0.25
0.20
0.15
0.10
0.05
0.00
$k_{inact, app}$
0.0
0.2
0.4
0.6
0.8
1.0
Ritonavir (μM)

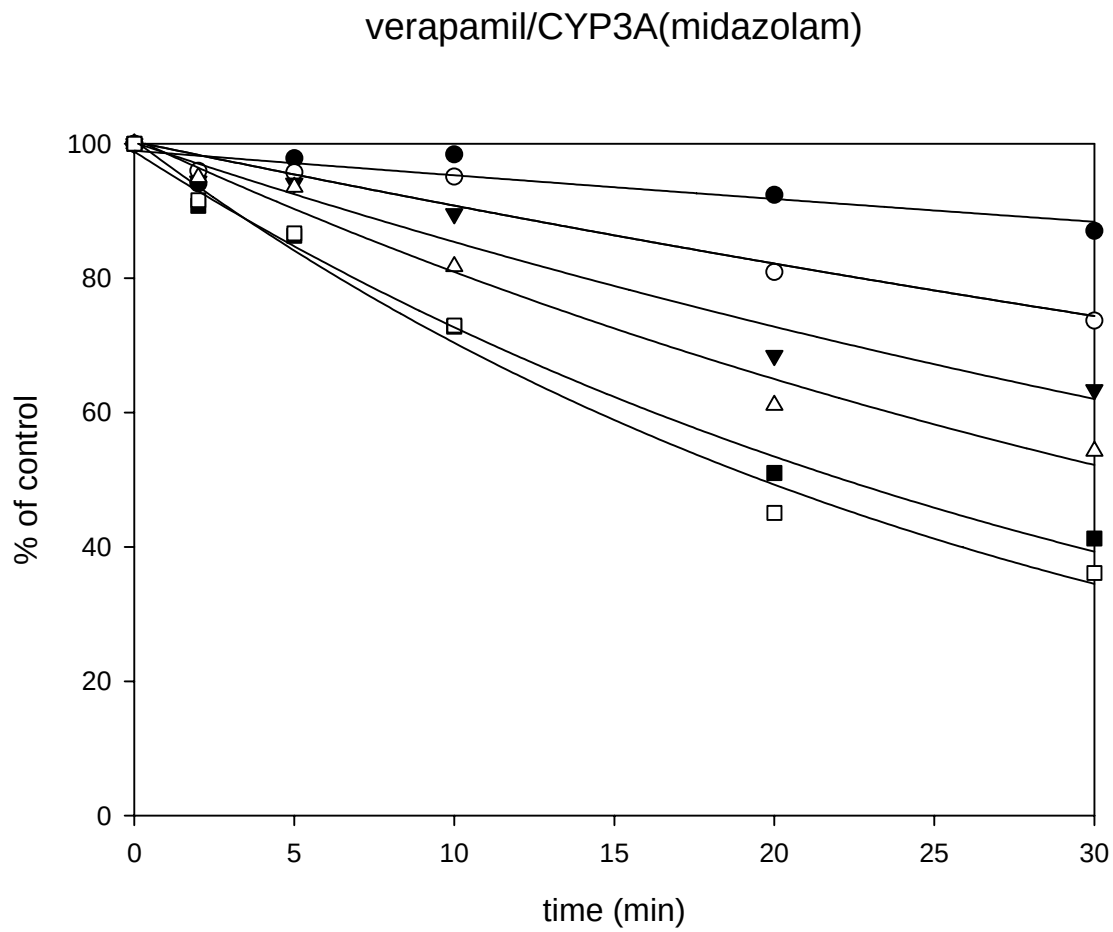
verapamil/CYP3A(midazolam)
% of control
time (min)
100
80
60
40
20
0
0
5
10
15
20
25
30

CYP3AM K_I/k_{inact}

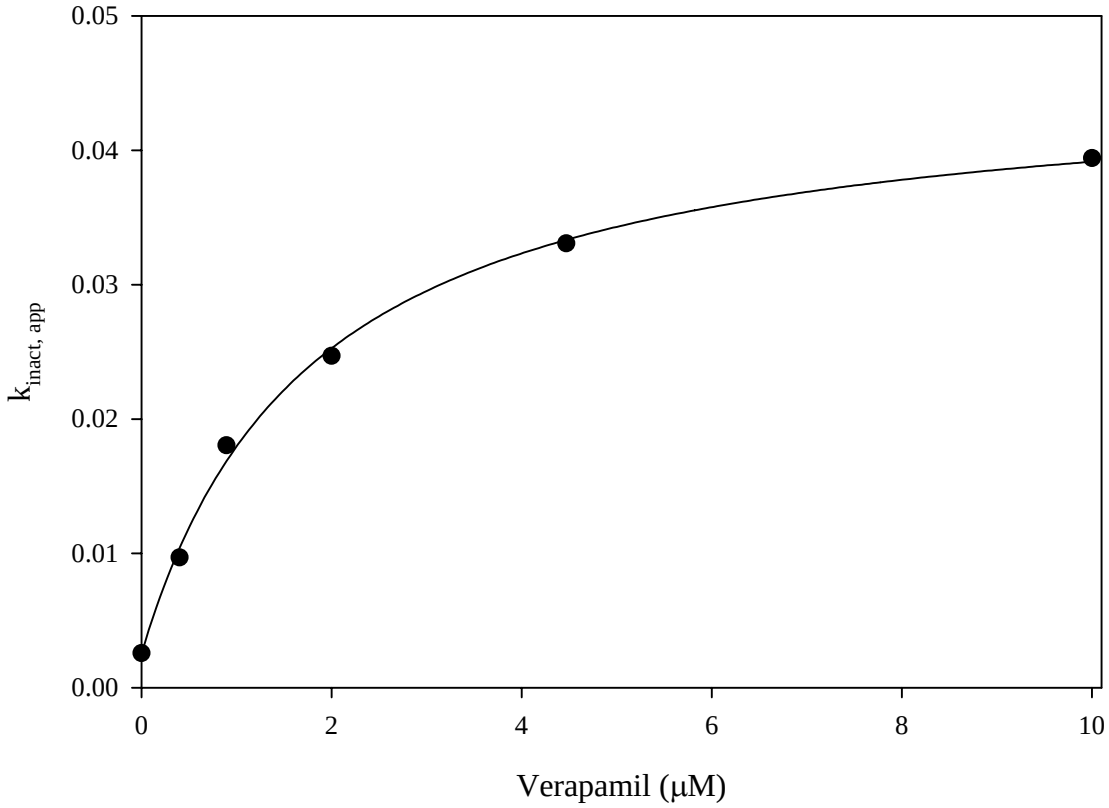

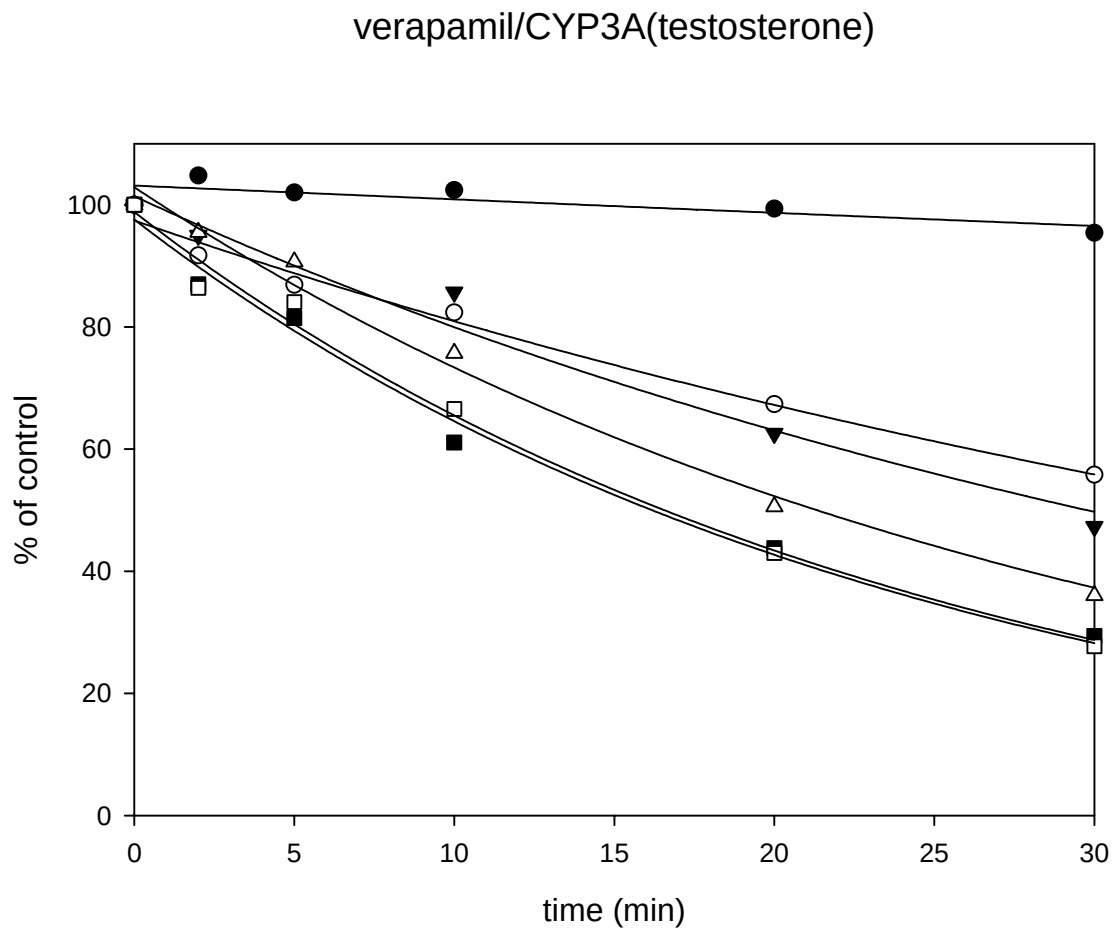
verapamil/CYP3A(testosterone)
% of control
100
80
60
40
20
0
0
5
10
15
20
25
30
time (min)

CYP3AT K_I/k_{inact}